

The Study of Bedforms and Equivalent Roughness Sizes in the Central Dithmarschen Bight

Dissertation
zur Erlangung des Doktorgrades
der Mathematisch-Naturwissenschaftlichen Fakultät
der Christian-Albrechts-Universität
Kiel

vorgelegt von
Gatot Haryo Pramono

Kiel
April 2005

Referent: Prof. Dr. Roberto Mayerle
Korreferent: Prof. Dr. Franciscus Colijn
Tag der mündlichen Prüfung: 25 June 2004
Zum Druck genehmigt Kiel, den ...

Der Dekan
gez.

...

This PhD thesis is dedicated to my father, my mother, Lelly, Salma and Salwa.

قُلْ لَوْ كَانَ الْبَحْرُ مِدَادًا لِكَلِمَاتِ رَبِّي لَنَفِدَ الْبَحْرُ
قَبْلَ أَنْ تَنْفَدَ كَلِمَاتُ رَبِّي وَلَوْ جِئْنَا بِمِثْلِهِ مَدَدًا

"Say: If the sea were ink for the words of my Lord, the sea would surely be consumed before the words of my Lord are exhausted, though We were to bring the like of that (sea) to add."

The Holy Quran 18:109

Acknowledgments

Praise be to God, the Cherisher and Sustainer of the worlds.

I will forever be grateful to the many people either directly or indirectly for the completion of this thesis. I have benefited enormously from their advice, support and patient.

This thesis would never have been concluded without the supervision and nurturing of my advisor, Prof. Dr. Roberto Mayerle. He contributed tremendously to my scientific development. He showed a great patient when trying to make me understand about the research. He always challenged me to produce my best. He monitored my progress and advised me with valuable insights of coping the problems. Thanks a lot Roberto!

I also appreciate Prof. Dr. Franciscus Colijn for accepting to be the *Korreferent* of my dissertation.

I feel very fortunate to receive scholarship from German Academic Exchange Service or Deutsche Akademische Austauschdienst (DAAD). The financial support is provided not only for my research but also for the living expense, my family needs, insurance and renting of apartment.

I would like to thank my colleagues in the Coastal Research Laboratory. The friendship and support are always shown to me during my work in the office. In particular, I am grateful to Poerbandono, Jort Wilkens, Fernando Toro, Piyamarn Leangruxa, Talal Etri, Dirk Schulz, Markus Diesing, Marcus Reckermann, Wiwin Windupranata, Adam Kubicki and Christian Winter for being informative and good humoured.

I would like to express my thanks to colleagues in Research and Technology Centre Westcoast or Forschungs- und Technologiezentrum Westküste (FTZ) in Buesum. Klaus Ricklefs helped me in the preparation of field measurements. He also taught me on how to work with acoustic devices and suggested on the handling of data. I also thank Uwe Becker and Burkhard Meier for their help during the measurement campaign.

Finally, the unconditional love and support of my family is undoubtedly as the major part for the success of my works. Lelly Indriasari, you lift my soul and give me courage to face the research each day. I may have started this journey on my own, but you gave me the strength to finish it. Delicious Indonesian foods, tidy rooms and

cute children are few things which make me smile when returning home. Salma Syahidah and Salwa Salsabila, my beloved kids, also make me realize the significance of my research for their future.

For my father who has passed away when I was a child, I pray that God accepts your good deeds. The enormous encouragement is also given by my lovely mother. I know that we are thousands kilometer away, but our single emotion to be together stimulates me to hasten my works. Great thanks also to my father-in-law Taryono, my mother-in-law Zubaidah, my brother Seno Pudjisardjono and my sister Retno Satyadahaningtyas for their support to my Doctorate study.

Abstract

The bedforms and equivalent roughness sizes in tidal channels of the Central Dithmarschen Bight on the basis of field measurements and numerical modeling are studied. Side scan sonar and echo sounder were employed to acquire bedform dimensions, while acoustic profilers were used to measure current velocities. Well-defined current profiles were obtained from an acoustic profiler moored to a bottom platform. For the coherence of field measurements, it is recommended that bedforms and current profiles should be measured simultaneously. Echo sounder and side scan sonar should be used to obtain respectively dimensions and orientation of bedforms. The upward and downward looking acoustic profilers should be moored to a bottom platform for recording velocities in the near bed and up to surface. Both devices should be configured to record profiles in small bin sizes for short time intervals.

Megaripples and subaqueous dunes were found in a few locations in tidal channels. The bedform heights range from 0.10m to 0.50m and the bedform lengths vary from 4m to 22m. According to transect measurements of echo sounder in the inner Piep channel, the bedform dimensions did not vary significantly during a tidal cycle. In addition, bedform migration between 2m and 5m were found per tidal phase, following the directions of flood and ebb currents.

The equivalent roughness size is estimated on the basis of best fit line of velocities in the bottom boundary layer. Factors relevant for selection of valid velocity profiles are depth integrated velocity, velocity direction and correlation coefficient of best fit line. Although reasonable estimations are obtained, the equivalent roughness sizes cannot be predicted during low and high water levels. In addition, fluctuations of equivalent roughness sizes are observed due to the change of velocity magnitude.

The obtained bedform dimensions and flow conditions are used to check existing equations for estimation of bedform dimensions and equivalent roughness sizes. The current data fit well with the existing equations. Only minor changes were applied on the coefficient of formulas to estimate bedform dimensions and equivalent roughness sizes. Numerical model simulations are carried out in conjunction with modified equations to develop maps of bedforms and equivalent roughness sizes in the study area. The availability and type of sediments are taken into account. The produced maps show reasonable agreements with conditions in tidal channels. In general, the empirical equations are able to predict bedform dimensions and equivalent

roughness sizes in shallow areas. The predicted values are usually overestimated in the deeper parts of tidal channels.

Kurzfassung

Die Sohlformen und äquivalenten Sohlrauigkeiten in den Tide-Rinnen der inneren Dithmarscher Bucht sind erforscht worden. Seitensicht-Sonar und Echolot sind eingesetzt worden, um die Sohlformen zu identifizieren und ADCPs (Acoustic Doppler Current Profiler), um Strömungsgeschwindigkeiten zu messen. Mit einem auf einer Bodenplattform befestigten ADCP konnten eindeutige Geschwindigkeitsprofile erfasst werden. Für exakte Feldmessungen ist es wichtig, dass die Sohlformen und Geschwindigkeitsprofile gleichzeitig gemessen werden. Echolot und Seitensicht-Sonar sollten eingesetzt werden, um einerseits die Dimensionen und andererseits die Ausrichtung der Sohlformen zu bestimmen. Die nach oben und nach unten gerichteten ADCPs sollten an einer Bodenplattform befestigt sein, um die Geschwindigkeiten am Boden und oberhalb der Plattform aufzuzeichnen. Beide Geräte sollten so konfiguriert sein, dass sie die Geschwindigkeitsprofile sowohl in kleinen vertikalen Abständen als auch in kleinen zeitlichen Schritten aufzeichnen.

Megarrippeln und subaquatische Dünen wurden nur in wenigen Bereichen der Tide-Rinnen gefunden. Die Höhe der Sohlformen liegt im Bereich von 0.10m bis 0.50m und deren Länge variiert von 4m bis 22m. Auf der Basis von Profilmessungen mit dem Echolot in der Piep-Rinne konnte festgestellt werden, dass die Dimensionen der Sohlformen sich über einen Tide-Zyklus nicht signifikant ändern. Weiterhin wurde eine Wanderung der Sohlformen zwischen 2m und 5m pro Ebb- bzw. Flutphase ermittelt, wobei die Wanderungsrichtung der Strömungsrichtung entsprach.

Die äquivalente Bodenrauigkeit wurde auf Basis der „best fit“-Linie der Geschwindigkeitsprofile in der sohlnahen Schicht abgeschätzt. Die relevanten Faktoren in der Auswahl der Profile sind die tiefengemittelte Geschwindigkeit, die Geschwindigkeitsrichtung und die Korrelationskoeffizient der „best fit“-Linie. Obwohl plausible Abschätzungen erzielt werden, kann die äquivalente Bodenrauigkeit nicht während Hochwasser und Niedrigwasser bestimmt werden. Weiterhin wurden Schwankungen der äquivalenten Rauigkeiten durch Größenänderungen der Strömungsgeschwindigkeit registriert.

Die ermittelten Dimensionen der Sohlformen und Strömungsbedingungen wurden benutzt, um die in der Literatur existierenden Gleichungen zu überprüfen. Relativ geringe Anpassungen der Koeffizienten in den angewandten Formeln

wurden gemacht, um die Dimensionen der Sohlformen und die äquivalenten Rauigkeiten abzuschätzen. Die Simulationen mit einem numerischen Modell sind in Zusammenhang mit den angepassten Formeln durchgeführt worden, um Karten der Sohlformen und äquivalenten Rauigkeiten des Untersuchungsgebietes zu generieren. Verfügbarkeit und Typen der Sedimente wurden berücksichtigt. Die erzeugte Karten zeigen eine vernünftige Übereinstimmung mit den Bedingungen in den Tide-Rinnen. Im Allgemeinen sind die empirischen Gleichungen in der Lage, die Dimensionen der Sohlformen und der äquivalenten Rauigkeiten in flachen Bereichen zu prognostizieren. Die prognostizierten Größen für die tieferen Bereiche der Priele sind in der Regel zu groß.

Abstrak

Bedform dan kekasaran ekuivalen pada kanal pasang surut di bagian tengah teluk Dithmarschen dipelajari dalam penelitian ini. *Side scan sonar* dan *echo sounder* digunakan untuk memperoleh *bedform*, sedangkan alat-alat pendeteksi profil akustik digunakan untuk mengukur kecepatan arus. Profil arus yang terdefinisi baik diperoleh dari alat yang terpasang pada anjungan di dasar. Untuk pengukuran yang tepat, pengukuran *bedform* dan kecepatan arus dianjurkan untuk dilakukan secara bersamaan. *Echo sounder* dan *side scan sonar* sebaiknya digunakan untuk mendapatkan dimensi dan orientasi dari *bedform*. Alat pendeteksi profil yang diarahkan ke atas dan ke bawah sebaiknya dipasang pada anjungan di dasar untuk merekam arus di sekitar dasar dan arus sampai ke permukaan. Kedua alat tersebut sebaiknya dikonfigurasi untuk merekam profil kecepatan dengan resolusi yang tinggi pada interval yang pendek.

Megaripple dan *dune* ditemukan pada beberapa lokasi di kanal pasang surut. Tinggi *bedform* berkisar dari 0.10m sampai 0.50m dan panjang *bedform* bervariasi antara 4m dan 22m. Berdasarkan pengukuran melintang dengan menggunakan *echo sounder* di kanal *inner Piep*, dimensi dari *bedform* tidak banyak berubah selama suatu siklus pasang surut. Selanjutnya, migrasi *bedform* antara 2m dan 5m ditemukan per fase pasang surut, mengikuti arah dari arus pasang surut.

Perkiraan dari kekasaran ekuivalen didapatkan berdasarkan garis berkesesuaian dari kecepatan arus di bawah dasar laut. Faktor-faktor yang digunakan untuk menyeleksi profil kecepatan adalah *depth-integrated* kecepatan, arah kecepatan arus dan koefisien korelasi dari garis berkesesuaian. Meskipun estimasi yang sesuai didapatkan, kekasaran ekuivalen tidak dapat diprediksi ketika permukaan air rendah dan tinggi. Selanjutnya, fluktuasi dari kekasaran juga ekuivalen terlihat yang dikarenakan perubahan dari kecepatan arus.

Dimensi *bedform* dan kondisi aliran yang didapatkan dari pengukuran diterapkan pada persamaan yang sudah ada. Hanya sedikit perubahan dilakukan pada koefisien persamaan untuk memperkirakan dimensi *bedform* dan kekasaran ekuivalen. Simulasi dari model numerik dan persamaan yang telah dirubah digunakan untuk membuat peta *bedform* dan kekasaran ekuivalen di lokasi studi. Keberadaan dan jenis endapan turut diperhatikan dalam pembuatan peta. Peta yang dihasilkan menunjukkan beberapa kecocokan dengan kondisi di kanal pasang surut. Secara

umum, persamaan-persamaan empirik dapat digunakan untuk memperkirakan dimensi *bedform* dan kekasaran ekuivalen di kanal yang dangkal. Nilai-nilai yang terlalu besar diprediksi di bagian kanal yang dalam.

Contents

Acknowledgments	i
Abstract	iii
Kurzfassung	v
Abstrak	vii
Contents	ix
List of Figures	xiii
List of Tables	xvii
Notations	xix
1 Introduction	1
1.1 Significance and statement of the problem.....	1
1.2 Background	1
1.3 Objectives.....	2
1.4 Outline	2
2 Literature review	5
2.1 Introduction.....	5
2.2 Bedforms.....	5
2.2.1 Development of bedforms.....	6
2.2.2 Classification of bedforms	8
2.2.3 Estimation of bedform dimensions	13
2.3 Equivalent roughness sizes	17
2.3.1 Grain roughness.....	17
2.3.2 Form roughness	19
2.3.3 Estimation of equivalent roughness sizes	22
2.4 Discussion.....	26

3	Study area and field measurements	29
3.1	Introduction.....	29
3.2	Description of study area	29
3.2.1	Meteorology	29
3.2.2	Geology	30
3.2.3	Morphology.....	32
3.2.4	Hydrodynamic conditions	32
3.3	Measurements of bedforms.....	33
3.3.1	Side scan sonar	34
3.3.2	Echo sounder	34
3.4	Measurements of current velocities	34
3.4.1	Acoustic profiling with 50cm bin resolution	36
3.4.2	Acoustic profiling with 25cm bin resolution	39
3.4.3	Acoustic profiling with 5cm bin resolution	40
3.5	Simultaneous measurements of bedforms and current velocities.....	42
3.5.1	Echo sounder	42
3.5.2	Acoustic profiling with 15cm bin resolution	43
3.6	Discussion.....	46
4	Bedform dimensions	49
4.1	Introduction.....	49
4.2	Bedform lengths throughout the tidal channels	49
4.3	Bedform dimensions at defined locations.....	51
4.3.1	Piep channel	51
4.3.2	Norderpiep and Suederpiep channels.....	52
4.3.3	Inner Piep channel	52
4.4	Development of bedform dimensions	57
4.5	Comparison with existing bedform classifications.....	60
4.6	Comparison with empirical equations to estimate bedform dimensions....	64
4.6.1	Height of bedforms.....	64
4.6.2	Length of bedforms	66
4.7	Discussion.....	66
5	Equivalent roughness sizes	69
5.1	Introduction.....	69
5.2	Criteria for selection of valid velocity profiles	69
5.2.1	Number of bins	69
5.2.2	Correlation coefficient.....	70
5.2.3	Velocity magnitude	73
5.2.4	Velocity direction.....	74
5.2.5	Displacement height.....	75

5.2.6	Average of ensembles	77
5.3	Estimation of equivalent roughness sizes	81
5.3.1	Measurements with acoustic profiler with 5cm bin size.....	82
5.3.2	Measurements with acoustic profiler with 15cm bin size.....	84
5.3.3	Measurements with acoustic profiler with 50cm bin size.....	87
5.4	Estimation of equivalent roughness sizes from depth integrated velocities	95
5.4.1	Measurements with acoustic profiler with 15cm bin size.....	95
5.4.2	Measurements with acoustic profiler with 50cm bin size.....	97
5.5	Verification of the effectiveness of formulas for evaluation of form roughness.....	101
5.5.1	Ripples.....	103
5.5.2	Dunes.....	104
5.6	Discussion.....	105
6	Estimation of bedforms and roughness using empirical equations.....	107
6.1	Introduction.....	107
6.2	Numerical model setup for the study area	107
6.2.1	Model grid	108
6.2.2	Open Boundary condition.....	108
6.2.3	Bathymetry	108
6.3	Spatial distribution of bedforms and roughness.....	108
6.3.1	Transport stage parameters.....	109
6.3.2	Bedform types	110
6.3.3	Bedform dimensions	112
6.3.4	Equivalent roughness sizes	115
6.4	Discussion.....	117
7	Conclusions.....	119
	References	125
	Erklärung.....	133
	Curriculum Vitae	135

List of Figures

2.1	Development of bedforms after Simons & Richardson [1966]	6
2.2	Nomenclature of bedforms.....	7
2.3	Classification of bedforms after Liu [1957].....	9
2.4	Classification of bedforms after Simons & Richardson [1966]	10
2.5	Classification of bedforms after Athaullah [1968].....	11
2.6	Classification of bedforms after Bogardi [1974].....	11
2.7	Classification of bedforms after Van Rijn [1993]	13
2.8	Heights of megaripples after Van Rijn [1993]	16
2.9	Heights of dunes after Van Rijn [1993]	17
2.10	Form roughness due to ripples after Van Rijn [1993]	21
2.11	Form roughness due to dunes after Van Rijn [1993].....	22
2.12	Flow velocity layers	23
3.1	Investigation area and bathymetric map of the Central Dithmarschen Bight ..	30
3.2	Lack and availability of sediments after Mayerle et al. [2002]	31
3.3	Characteristics of sediments in tidal channels after Mayerle et al. [2002]	31
3.4	Water level measured at Tertius and Buesum in August 22, 2000	33
3.5	Coverage of field measurements of bedforms in the tidal channels.....	33
3.6	Klein 595 side scan sonar used to map the bottom of channels	34
3.7	Field measurements of current velocities in tidal channels. Cross sectional profiles at the measuring locations are shown in Figures 3.9 and 3.17.	36
3.8	Deployment of moored ADCP.....	36
3.9	Cross sections at which ADCPs with 50cm bin resolution were placed. See Figure 3.7 for the location of the cross sections.	37
3.10	Water level and depth integrated current velocities. ADCP measurements with 50cm bin resolution	38
3.11	Typical velocity profiles during a spring tide in the Suederpiep channel. ADCP measurements with 50cm bin resolution.	39
3.12	Research vessel "Suedfall"	39
3.13	Water level and depth integrated velocities in the Piep channel. ADCP measurements with 25cm bin resolution.....	40
3.14	Typical current velocity profiles in the Piep channel. ADCP measurements with 25cm bin resolution	40
3.15	Average current velocities in the Piep channel. ADCP measurements with 5cm bin resolution	41
3.16	Typical current velocity profiles in the Piep channel. ADCP measurements with 5cm bin resolution	41

3.17	Bottom profile at which echo sounder measurement was performed. See Figure 3.7 for the location of the cross section.	42
3.18	Vessel employed for measurements of bedform dimensions.....	43
3.19	Plan view of vessel paths of echo sounder measurements selected for calculation of bedform dimensions	44
3.20	ADCP measurements with 15cm bin resolution from a stationary rubber boat.....	44
3.21	Water level and depth integrated velocity in the inner Piep channel. ADCP measurements with 15cm bin resolution.....	45
3.22	Typical current velocity profiles in the inner Piep channel. ADCP measurements with 15cm bin resolution.....	45
3.23	Proposed measurement set-up for obtaining bedforms and current velocities.....	46
4.1	Distribution of bedforms in tidal channels after Mayerle et al. [2002]	50
4.2	Side scan sonar images showing the bedforms in tidal channels	50
4.3	Typical profiles of echo sounder showing the bedforms in the Piep channel after Razakafoniaina [2001]	51
4.4	Typical bed profiles taken with echo sounder in the Norderpiep and Suederpiep channels.....	52
4.5	Echo sounder profiles in the North transect of the inner Piep channel	53
4.6	Echo sounder profiles in the South transect of the inner Piep channel.....	54
4.7	Bed profile 20 plotted using same horizontal and vertical scales	55
4.8	Three dimensional view of bedforms in the North transect.....	55
4.9	Three dimensional view of bedforms in the South transect	56
4.10	Determination of bedform orientation from the bed profiles.....	56
4.11	Approach considered in the estimation of bedform lengths for non perpendicular vessel tracks	57
4.12	Bedform dimensions over a tidal cycle at the inner Piep channel	59
4.13	Migration of bedforms during a tidal cycle in inner Piep channel	60
4.14	Bedform types on the basis of several classification schemes	62
4.15	Comparison of the measurement data in the inner Piep channel with a proposed equation for heights of megaripples.....	65
4.16	Comparison of the measurement data in the inner Piep channel with a proposed equation for heights of dunes.....	65
5.1	Relation between correlation coefficient and equivalent roughness sizes. ADCP measurements with 50cm bin resolution	71
5.2	Variation of correlation coefficients with velocity magnitudes. ADCP measurements with 50cm bin resolution.....	72
5.3	Relation between correlation coefficient and depth integrated velocity. ADCP measurements with 50cm bin resolution	73
5.4	Measured velocity magnitude and direction on August, 16, 2000. ADCP measurements with 50cm bin resolution.....	74
5.5	Relation between correlation coefficient and velocity direction. ADCP measurements with 50cm bin resolution.....	75
5.6	Variation of velocity direction with velocity magnitude. ADCP	

	measurements with 50cm bin resolution.....	76
5.7	Resulting velocity profiles by considering different averaging of ensembles. ADCP measurements with 15cm bin resolution in the inner Piep channel	78
5.8	Effect of averaging ensembles. ADCP measurements with 5cm bin resolution during flood phase. Piep channel (Point 3 in Figure 5.12)	79
5.9	Effect of averaging ensembles. ADCP measurements with 15cm bin resolution during flood phase. Inner Piep channel (Point 5 in Figure 5.12).....	79
5.10	Effect of averaging ensembles. ADCP measurements with 25cm bin resolution during flood phase. Piep channel (Point 4 in Figure 5.12)	80
5.11	Effect of averaging ensembles. ADCP measurements with 50cm bin resolution during flood phase. Norderpiep channel (Point 1 in Figure 5.12) ..	80
5.12	Locations of current velocity measurements	81
5.13	Average velocity and water level. ADCP measurements with 5cm bin resolution in Piep channel (Point 3 in Figure 5.12)	82
5.14	Velocity profiles (average of 10 ensembles covering 36 seconds). ADCP measurements with 5cm bin resolution in the Piep channel	83
5.15	Equivalent roughness sizes (average of 10 ensembles covering 36 seconds). ADCP measurements with 5cm bin resolution in the Piep channel.....	84
5.16	Equivalent roughness sizes (average of 10 ensembles covering 36 seconds). ADCP measurements with 5cm bin resolution in the Piep channel.....	84
5.17	Velocity profiles (average of 50 ensembles covering 1 minute and 16 seconds). ADCP measurements with 15cm bin resolution in the inner Piep channel	85
5.18	Equivalent roughness sizes and shear stresses. Average of 50 ensembles (1 min, 16 sec) and 250 ensembles (5 minutes). ADCP measurements with 15cm bin resolution in the inner Piep channel.....	86
5.19	Velocity profiles (average of 5 ensembles covering 20 minutes). ADCP measurements with 50cm bin resolution.....	87
5.20	Equivalent roughness sizes and velocities in the Norderpiep channel. ADCP measurements with 50cm bin size resolution (average of 5 ens covering 20 minutes).....	89
5.21	Equivalent roughness sizes and velocities in the Suederpiep channel. ADCP measurements with 50cm bin size resolution (average of 5 ens covering 20 minutes)	90
5.22	Equivalent roughness sizes and shear stresses in the Norderpiep channel. ADCP measurements with 50cm bin size resolution (average of 5 ens covering 20 minutes)	91
5.23	Equivalent roughness sizes and shear stresses in the Suederpiep channel. ADCP measurements with 50cm bin size resolution (average of 5 ens covering 20 minutes)	92
5.24	Equivalent roughness sizes in the Norderpiep channel. During spring tide considering various minimum velocities. ADCP measurements with 50cm bin size resolution (average of 5 ens covering 20 minutes).....	93
5.25	Equivalent roughness sizes in the Norderpiep channel. During neap tide considering various minimum velocities. ADCP measurements with 50cm	

	bin size resolution (average of 5 ens covering 20 minutes).....	94
5.26	Development of bed shear stress on the basis of depth integrated velocities and constant bed roughness. ADCP measurements with 15cm bin resolution	96
5.27	Comparison of shear stress obtained from depth integrated velocity and log law. ADCP measurements with resolution of 15cm	97
5.28	Shear stress in the Norderpiep channel. ADCP measurements with 50cm resolution	98
5.29	Shear stress in the Suederpiep channel. ADCP measurements with 50cm resolution	99
5.30	Comparison of shear stress obtained from depth integrated velocity and log law. ADCP measurements with 50cm bin resolution	101
5.31	Equivalent roughness sizes, shear stresses and bedform dimensions	102
5.32	Comparison of the form roughness due to ripples from existing and inner Piep channel data.....	104
5.33	Comparison of the form roughness due to dunes obtained from existing and inner Piep channel data.....	105
6.1	Maps of transport stage parameters for maximum current velocity.....	109
6.2	Predicted bedform types on the basis of classification by Van Rijn [1993].....	111
6.3	Comparison of observed and predicted bedform types.....	112
6.4	Predicted bedform heights for high transport stage parameters	113
6.5	Predicted bedform lengths for high transport stage parameters	114
6.6	Comparison of observed and predicted bedform lengths	115
6.7	Predicted equivalent roughness sizes during high transport stage parameters	116
6.8	Map of equivalent roughness sizes using local variability after Palacio [2002].....	117

List of Tables

2.1	Summary of bedform classification after Van Rijn [1993].....	12
2.2	Summary of data used in the investigations of form roughness	19
3.1	Measuring configurations of ADCP during the measurements.....	35
3.2	Depth integrated velocities. ADCP measurements with 50cm bin resolution..	37
4.1	Bedform heights and lengths at the inner Piep channel.....	58
4.2	Selected profiles for verification of bedform classifications	61
4.3	Summary of the predicted and observed bedforms in the inner Piep channel	63
5.1	Probability of uncorrelated variables after Taylor [1997].....	70
5.2	Percentage of shear stress values within a factor of 2. ADCP measurements with 15cm bin resolution.....	96
5.3	Percentage of shear stress values within a factor of 2. ADCP measurements with 50cm bin resolution.....	100
5.4	Bedform dimensions and equivalent roughness sizes. ADCP measurements with 15cm resolution in the inner Piep channel	103
6.1	Configuration of the Central Dithmarschen Bight model.....	108

Notations

c	speed of sound
C	Chezy coefficient
D_*	dimensionless particle diameter parameter
d_{35}	sediment grain diameter in which 35% of sample by mass is smaller
d_{50}	sediment grain diameter in which 50% of sample by mass is smaller
d_{80}	sediment grain diameter in which 80% of sample by mass is smaller
d_{90}	sediment grain diameter in which 90% of sample by mass is smaller
f_d	Doppler shift frequency
f_s	frequency of the sound source
Fr	Froude number
Fr_*	Froude number due to shear velocity
g	acceleration due to gravity
h	flow depth
k_s	equivalent roughness size
k'_s	grain roughness size
k''_s	form roughness size
$k''_{s,d}$	form roughness due to dunes
$k''_{s,r}$	form roughness due to ripples
m	slope of best fit line
n	number of data
r	correlation coefficient
r_f	discrepancy ratio
R	hydraulic radius
Re_*	grain shear Reynolds number
T	transport stage parameter
t	time
u_d	velocity direction
$\overline{u_d}$	average of velocity direction
u_r	relative velocity between sound source and sound receiver
u_z	velocity distribution at a distance z from the bottom

u_*	shear velocity
U	depth integrated velocity
w	stream power
z	distance to the bottom
z_b	the lowest distance to the bottom
z_m	profile gradient
z_t	the highest distance to the bottom
z_0	zero velocity level
\tilde{z}_0	corrected zero velocity level
Δ	height of bedforms
Δ_d	height of dunes
Δ_{mer}	height of megaripples
Δ_{mir}	height of miniripples
Δ_r	height of ripples
δ	displacement height
γ_d	dune presence factor
γ_r	ripple presence factor
κ	Von Karman constant
Λ	acceleration length scale
λ	length of bedforms
λ_d	length of dunes
λ_{mer}	length of megaripples
λ_{mir}	length of miniripples
λ_r	length of ripples
ν	kinematic viscosity
ρ	sea water density
ρ_s	sediment density
σ_{u_d}	standard deviation of velocity direction
τ_b	bed shear stress
τ_b'	bed shear stress due to the grains
$\tau_{b,cr}$	critical bed shear stress

Chapter 1

Introduction

1.1 Significance and statement of the problem

One of the most important contributions to the resistance to flow is the bed roughness which indicates how the seabed profile interacts with the flow velocity. The knowledge of bedforms and bed roughness is essential to the understanding of flow characteristics. The presence of bedforms affects the near bed velocity distribution, bed shear stress and the amount of transported sediment. Hence, the study of bedforms and equivalent roughness sizes is necessary for improving the understanding of the process in the vicinity of the bottom.

In this dissertation, the bedforms and equivalent roughness in tidal channels at the central Dithmarschen Bight are examined. Extensive field measurements of bedform dimensions and velocity profiles were carried out for different conditions at several locations of the tidal channels using acoustic devices. This study addresses mainly three problems:

1. How should the field measurements of bedform dimensions and current velocities be carried out to provide the required information?
2. What are the typical characteristics of bedforms in the tidal channels in question and their variation over a tidal cycle?
3. How can equivalent roughness sizes be estimated from current velocity profiles?
4. How can bedform dimensions be related to bed shear stresses?

1.2 Background

The investigations about bedforms and equivalent roughness have been conducted since several decades. Classifications of bedforms have been covered by Simons and Richardson [1966], Allen [1968] and Yalin [1972]. Formulas to predict bedform types

were proposed among others by Yalin [1964], Allen [1968] and Van Rijn [1993]. Studies on equivalent roughness sizes estimated from the dimensions of bedforms were examined by Wikramanayake [1993], Grant & Madsen [1982], Nielsen [1983], Raudkivi [1988] and Van Rijn [1993]. Most of the results in these studies were derived from flume and river experiments. Very little information is available on bedforms and equivalent roughness for field conditions especially in tidal channels. In tidal environments, the flow depth, current magnitude and direction change continuously which make such studies on bedforms challenging and necessary.

For estimation of the shear stresses and equivalent roughness sizes due to bedform measurements and velocity profiles near the bottom have been used. Results are summarized in Sternberg [1968], Carling [1981], Soulsby & Dyer [1981], Schauer [1987], Cacchione, et al. [1995] and Cheng et al. [1999]. Most of investigations employed the velocity data acquired from current meters. In this study, data from acoustic devices are used instead. This dissertation analyzes several factors and methods relevant to the estimation of bedform dimensions and the associated equivalent roughness sizes.

1.3 Objectives

The objectives which will be accomplished by this study are as follows:

1. Propose methods to measure bedforms and current velocities in tidal channels,
2. Observation of the effects of flow conditions on the dimensions of bedforms,
3. Examination of the spatial variability of bedforms in the study area,
4. Comparison of the observed bedforms with predictions made through existing bedform classification,
5. Improvement of existing equations to estimate bedform dimensions on the basis of sediment properties and flow conditions,
6. Investigation of the main factors relevant to the estimation of equivalent roughness sizes,
7. Description of the effectiveness of measured velocity profiles to estimate equivalent roughness sizes and
8. Adoption of existing equations relating bedform dimensions and equivalent roughness sizes to the conditions in the study area.

1.4 Outline

This dissertation consists of six chapters. In chapter 2, previous works on bedforms which include development, classification and estimation of bedforms are reviewed.

The equivalent roughness size is discussed in terms of grain and form roughness. Several studies to estimate equivalent roughness sizes are also described. Chapter 3 describes the study area and the field measurements. The results of the measurements of bedform dimensions using side scan sonar and echo sounder are summarized. In addition, the current velocities measured by acoustic profilers are presented and discussed. In Chapter 4, the observed bedforms are analyzed on the basis of side scan sonar images and echo sounder profiles. The development of bedforms in a tidal cycle is studied using echo sounder profiles. In addition, the observed bedforms are compared with existing bedform classifications and empirical equations. Chapter 5 covers the estimation of equivalent roughness sizes from the best fit line of current velocities in the bottom boundary layer and using depth integrated velocities. The existing equations and the data used in the estimation of equivalent roughness sizes are analyzed by using the data from tidal channels. In Chapter 6, the modified equations are applied by using numerical model simulations to produce maps of bedform types, dimensions and equivalent roughness sizes in the study area. In the last chapter, the main results of this research are summarized. Recommendations for further studies in this field are mentioned.

Chapter 2

Literature review

2.1 Introduction

In this chapter, the theoretical background of the dissertation is provided. Previous studies about bedforms and bed roughness are reviewed. The development of bedforms as a result of flow conditions is analyzed. Classifications of bedforms based on sediment characteristics and flow properties, and equations proposed for estimation of bedform dimensions are introduced. Equations developed for estimation of equivalent roughness sizes on the basis of grain and form roughness are presented. Approaches for estimation of equivalent roughness sizes using the best fit line of velocity profiles in the bottom boundary layer are described. Some studies of equivalent roughness sizes are also summarized in this chapter.

2.2 Bedforms

The bed of tidal channels is generally not flat. Small and large sediment features covering the bed are known as bedforms. Brush et al. [1996] defined bedforms as “any deviations, from a flat bed, that are readily detectable by eye or higher than the largest sediment size present in the parent bed material.” Other terms have been used by scientists sand waves [Yalin, 1972], bed irregularities [Garde & Ranga Raju, 1977] and bed configurations [Simons & Sentürk, 1992]. In this writing, the term “bedforms” is employed since it has been used quite often in the recent literature.

The bedforms in tidal channels hold a significant role in the study of sediment transport. Masselink and Pattiaratchi [2000] pointed out three important roles of bedforms. First, the bed roughness obtained from geometry of bedforms influences the near bed velocity profile and the transport of suspended sediment [Grant & Madsen, 1982 and Van Rijn, 1993]. Secondly, since the presence of bedforms increases the

shear stress, more sediments can be entrained by the flow [Nielsen, 1986]. Studies which indicated that the dimensions of bedforms influence the sediment resuspension coefficient were conducted by Drake & Cacchione [1989], Vincent et al. [1991] and Li et al. [1996]. Third, the presence of bedforms influences the sediment mixing over the flow depth [Lee and Hanes, 1996]. In addition, the migration of bedforms can be used as an indication of the bedload transport [Williams and Rose, 2001].

2.2.1 Development of bedforms

The development of bedforms has been studied extensively from the results of flume experiments. Allen [1968] has defined hierarchies of bedforms on the basis of flow conditions and sediment properties. The development of bedforms described by Simons & Richardson [1966] is mostly discussed in the literature. They classified the bedforms observed in a tilting recirculating flume with 45.7m length, 2.4m width and 0.6m depth. The slope of the flume could be varied from 0 to 0.013 and the discharge from 0.06 m³/s to 0.62m³/s. The bed sediment was quartz sand with median diameter from 0.19mm to 0.93mm. The sketches of bedforms observed during the flume experiment are shown in Figure 2.1.

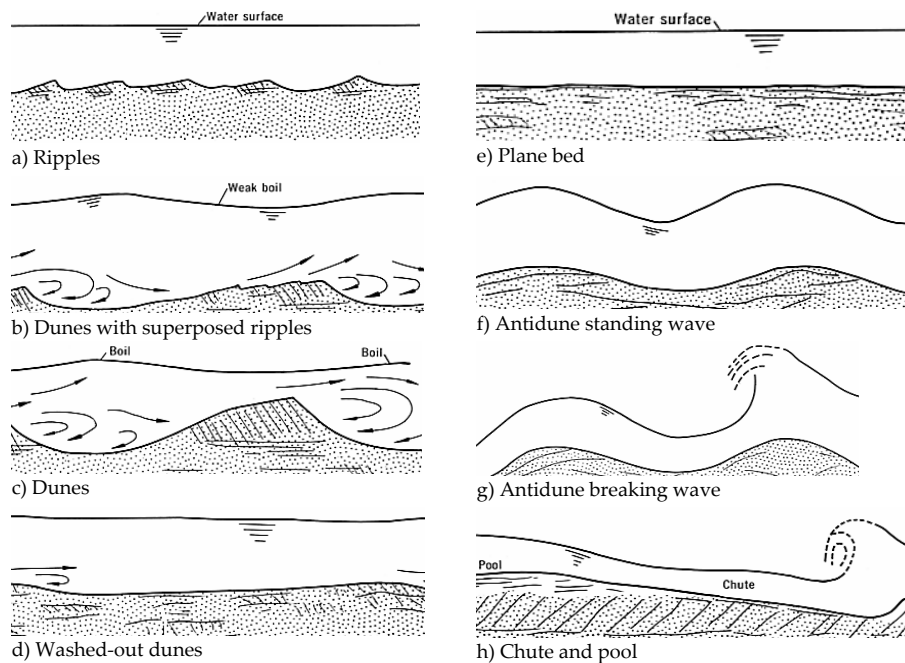


Figure 2.1: Classification of bedforms after Simons & Richardson [1966]

Figure 2.2 shows the typical profile of a bedform. The top and bottom parts of a bedform are called crest and trough. The height of a bedform is the vertical distance between crest and trough. The length is defined as the horizontal distance, at right

angle to the crest, between troughs [Reineck & Singh, 1980]. The stoss and lee sides are respectively the gentle and steep slopes of a bedform. The current usually flows in the direction from stoss to lee side.

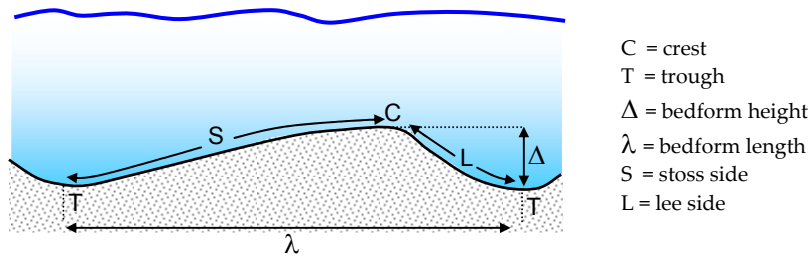


Figure 2.2: Nomenclature of bedforms

The study of bedform development is based on shape characteristics of bedforms, type of sediment transport, dissipation of energy and phase difference between bed and flow surface [Simons & Richardson, 1961]. The flows are divided into lower and upper regimes which are separated by a transition regime.

Lower flow regime

It is characterized by relatively slow flow velocities and low rates of sediment transport. Yalin [1972] described that the flow condition in this regime is subcritical with Froude numbers less than one. The dimensionless Froude number (F_r) is defined as:

$$F_r = \frac{U}{\sqrt{gh}} \quad (2.1)$$

where U is the depth integrated velocity (m/s), g is the acceleration due to gravity ($\approx 9.81 \text{ m/s}^2$) and h is the flow depth (m).

Ripples (Figure 2.1.a) which are formed as soon as the current velocity is able to move the sand grains. According to Van Rijn [1993], ripples can be divided into mini-ripples and megaripples. The length of miniripples is much smaller than the water depth, while the length of megaripples is about half of the flow depth. The maximum slope of ripples (ripple height divided by ripple length) is about 0.2 [Yalin, 1972].

If the flow velocity and thus the shear stress increase over the ripples, dunes are formed (Figure 2.1.c). At smaller shear stresses, several ripples are sometimes superposed on the upstream face of the dunes (Figure 2.1.b). The longitudinal profile of a dune resembles a triangle with gentle upstream surface and lee side which is equal to the angle of repose. The geometry of dunes is much larger than ripples and depends on the flow depth and bed shear stress. The maximum height and length of dunes is respectively about 0.4 times and between 6 and 7 times the flow depth.

Transition regime

The transition regime is characterized by the conditions between lower and upper regimes. It covers a wide range of shear stresses. As the current velocity increases, dunes decrease in amplitude and increase in length. Then, they are washed out and a plane bed with sediment transport is observed (Figures 2.1.d and 2.1.e).

Upper flow regime

This flow regime is characterized by high current velocities, low flow resistance and high sediment transport rates. According to Yalin [1972], the flow condition in the upper regime is classified as supercritical with Froude numbers of more than one. The types of bedforms in the upper flow regime are antidunes, chutes and pools. Antidunes have more symmetrical shape than ripples and dunes (Figures 2.1.f and 2.1.g). When the bed slope is very steep, chutes and pools can be formed (Figure 2.1.h).

2.2.2 Classification of bedforms

Several studies on the classification of bedforms on the basis of flow conditions and sediment properties have been conducted. Dimensional and nondimensional parameters of bedforms are plotted from primarily flume data supported with some observations in natural channels. In this section, some approaches of bedform classification are presented.

Liu [1957]

A bedform classification between the ratio of bed shear velocity (u_*) and particle fall velocity (ω) and the grain shear Reynolds number ($Re_* = u_* d_{50} / \nu$) was proposed in which d_{50} is median grain size (m) and ν is kinematic viscosity (m^2/s).

To understand the beginning of ripple formation, an experiment was conducted in a flume with 12.2m length, 0.3m width and 0.6m depth. River sands with median diameter from 0.20mm to 0.69mm were used. Flow depths and bed shear velocities up to 0.12m and 0.03m/s respectively were recorded. Figure 2.3 shows the proposed classification. According to this classification, ripples are present in the hydraulically smooth beds up to transition. On the other hand, antidunes can be found in all flow regimes. According to Simons & Sentürk [1992], the bedform classification proposed by Liu [1957] is not able to predict bedforms in field conditions.

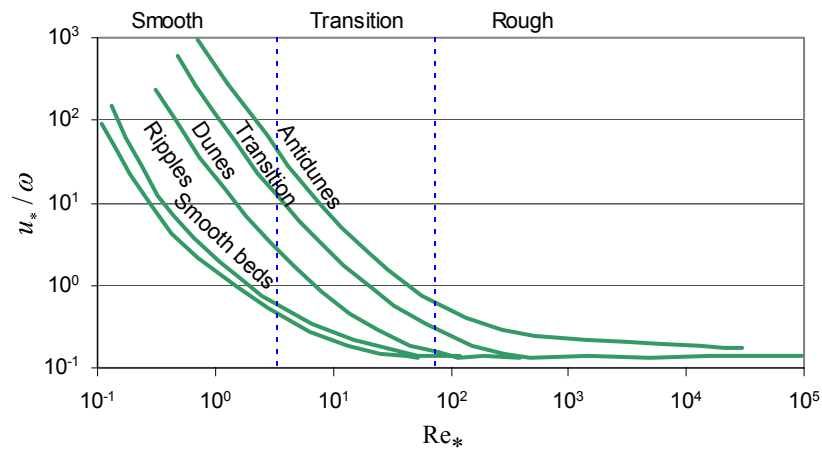


Figure 2.3: Classification of bedforms after Liu [1957]

Simons & Richardson [1966]

A classification on the basis of the medium grain size (d_{50}) and stream power ($w = \tau_b U$) was proposed in which τ_b is the bed shear stress and U is the depth integrated velocity.

The data were collected from a flume with 45.7m length, 2.4m width and 0.6m depth. Quartz sands with median diameter between 0.19mm and 0.93mm were used in the experiments. Additional data covering lower and upper flow regimes obtained from rivers in USA, India and Pakistan were also employed. The proposed classification is shown in Figure 2.4. The stream power is in Newton per second meter and the median grain size is in mm. This approach was applied successfully for shallow streams [Julien, 1995]. However, it fails to predict dunes in the Mississippi River with flow depths about 15m.

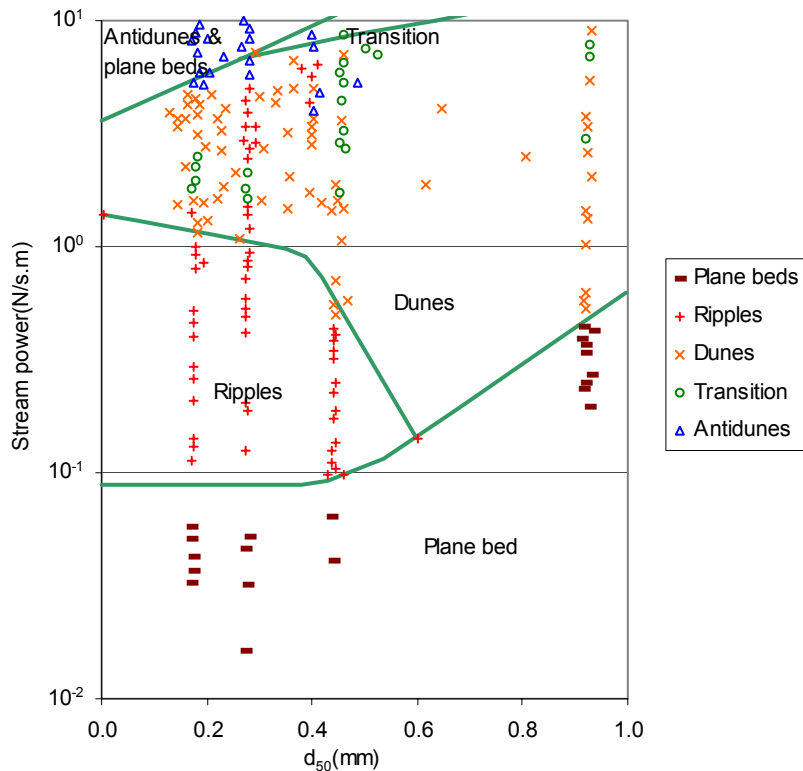


Figure 2.4: Classification of bedforms after Simons & Richardson [1966]

Athallah [1968]

Athallah [1968] studied several dimensionless parameters which are associated with bedform types such as hydraulic radius, slope of energy grade line, diameter of bed material, Froude number, shear velocity, fall velocity, Reynolds number and kinematic viscosity. Some plots of these parameters showed considerable scatter. The best fit was obtained by relating the Froude number (Fr) which accounts for the inertial effects with the relative roughness (R/d_{50}) in which R is the hydraulic radius and d_{50} is the median bed sediment size. The relative roughness is related to the stream turbulence due to bedforms. The data were collected from flume experiments and canals in USA and India.

The plot of data is shown in Figure 2.5. It can be seen that the Froude number decreases with relative roughness. Dunes can be observed for a wide range of relative roughness values, while ripples are limited to the lower regime and relative roughness values between 500 and 1050. According to Simons & Sentürk [1992], this approach cannot distinguish bedforms in natural systems.

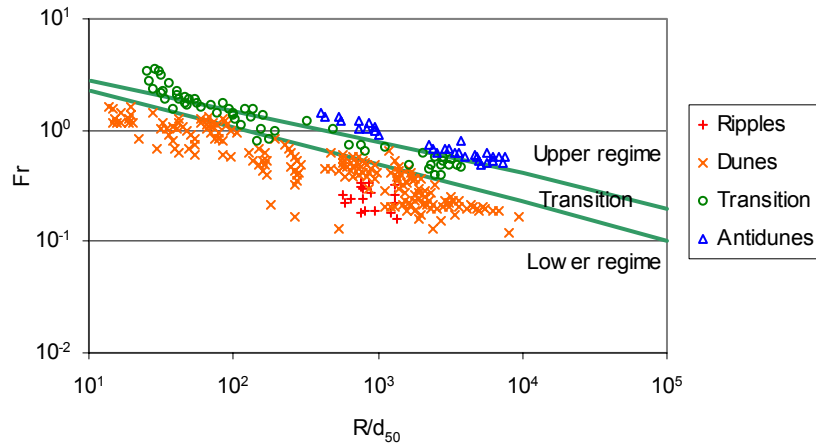


Figure 2.5: Classification of bedforms after Athallah [1968]

Bogardi [1974]

Bogardi [1974] extended the approach by Liu [1957] by separating the different boundary conditions in order to describe the initial motion of bedform types. Figure 2.6 shows the graph of bedforms with the median grain size along the horizontal axis. The vertical axis is the particle stability factor which is inversely proportional to the Froude number due to shear velocity ($Fr_* = gd_{50}/u_*^2$). Where u_* is the shear velocity (m/s), g is the acceleration due to gravity (m/s^2) and d_{50} is the median grain size (m).

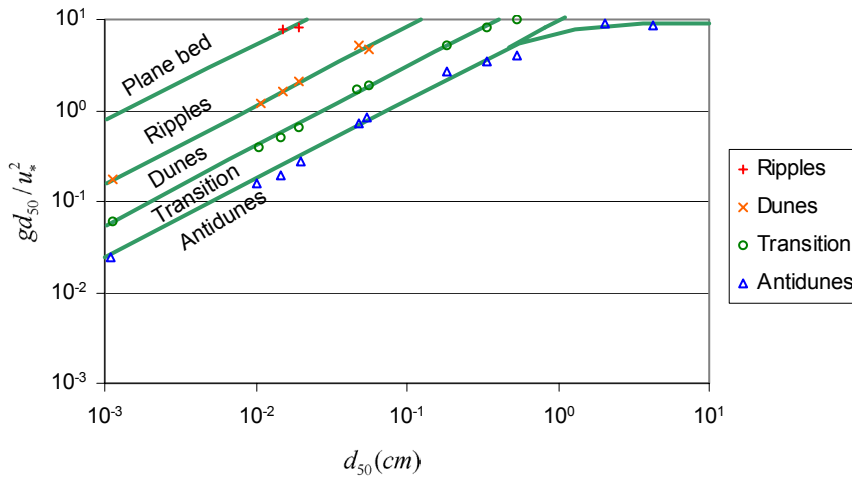


Figure 2.6: Classification of bedforms after Bogardi [1974]

It can be seen that ripples and dunes are mostly formed in the experiments with smaller particle diameter. Simons & Sentürk [1992] stated that the bedform classification by Bogardi [1974] is not appropriate for field conditions.

Van Rijn [1993]

Van Rijn [1993] classified bedforms on the basis of particle size and transport regime. The particle size is represented by the dimensional particle parameter (D_*) defined as:

$$D_* = d_{50} \left(\frac{((\rho_s/\rho) - 1)g}{\nu^2} \right)^{1/3} \quad (2.2)$$

where d_{50} is the median grain size (m), ρ_s is the sediment density (kg/m³), ρ is the water density (kg/m³), g is the acceleration due to gravity and ν is the kinematic viscosity (m²/s).

The transport regime is measured by a transport stage which is the dimensionless parameter of the shear stress (T) defined as follows:

$$T = \frac{\tau_b' - \tau_{b,cr}}{\tau_{b,cr}} \quad (2.3)$$

where τ_b' is the bed shear stress (N/m²) due to the grains and $\tau_{b,cr}$ is critical bed shear stress (N/m²).

Figure 2.7 is developed from large number of flume and field data. Several zones of bedforms are identified. Unlike other classifications, Van Rijn [1993] distinguished ripples into miniripples and megaripples. The bedform classification is summarized in Table 2.1. The lower regime is defined with transport stage parameter less than 15, while the upper regime is with transport stage parameter exceeding 25. In the lower regime, ripples are found for particle parameters less than 10. Dunes are mostly predicted with particle diameter greater than 10.

Table 2.1: Summary of bedform classification after Van Rijn [1993]

Transport regime	Particle size		
	$1 \leq D_* \leq 10$	$D_* > 10$	
Lower	$0 \leq T \leq 3$	Miniripples	Dunes
	$3 < T \leq 10$	Megaripples and dunes	Dunes
	$10 < T \leq 15$	Dunes	Dunes
Transition	$15 < T < 25$	Washed-out dunes, sandwaves	
Upper	$T \geq 25, Fr < 0.8$	(symmetrical) sandwaves	
	$T \geq 25, Fr \geq 0.8$	Plane bed and/or antidunes	

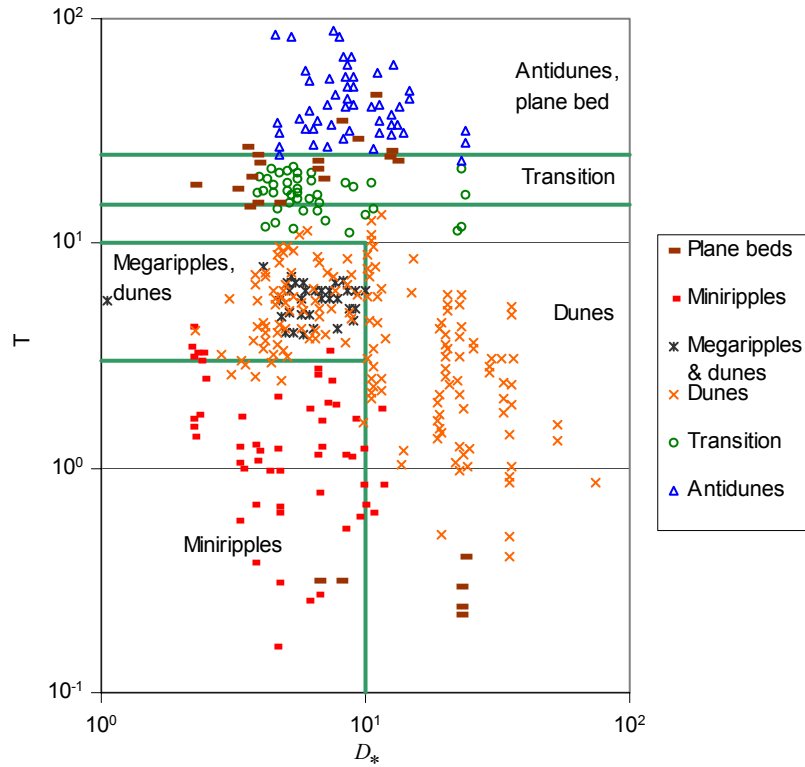


Figure 2.7: Classification of bedforms after Van Rijn [1993]

2.2.3 Estimation of bedform dimensions

Several studies have been conducted to relate the dimensions of bedforms to the flow conditions and/or sediment properties. The studies by Yalin [1964, 1972], Allen [1968] and Van Rijn [1993] are reviewed in this section.

Yalin [1964, 1972]

Flume data and field observations were analyzed using dimensional analysis and physical processes. The tilting flume had the width of 0.65m and length of 18m. The grain sizes of the bed sediment were from 0.14mm to 2.45mm. By using dimensional analysis, Yalin [1972] suggested a relation between bedform length and other parameters as follows:

$$\frac{\lambda}{d_{50}} = f\left(\frac{u_* d_{50}}{\nu}, \frac{h}{d_{50}}\right) \quad (2.4)$$

where d_{50} is median grain size (m), u_* is the shear velocity (m/s), ν is the kinematic viscosity (m²/s). For small values of u_*d_{50}/ν in which ripples are present, he found that the ripple length (λ_r) is related to the median grain size (d_{50}):

$$\lambda_r = 1000d_{50} \quad (2.5)$$

For high values of u_*d_{50}/ν , dunes are formed with the length of dunes (λ_d) related to the flow depth (h):

$$\lambda_d = 6.3h \quad (2.6)$$

Yalin's equation is based on two assumptions. Firstly, the dune length is much longer than the dune height and median grain size. Secondly, the shear stress at the trough of bedforms is roughly equal to the critical shear stress. The following equation was proposed for estimating the height of dunes (Δ_d):

$$\frac{\Delta_d}{h} = \frac{1}{6} \left(1 - \frac{\tau_{b,cr}}{\tau_b} \right) \quad (2.7)$$

where $\tau_{b,cr}$ and τ_b are respectively the critical shear stress and the bed shear stress in N/m².

Allen [1968]

Field measurements of bedforms were carried out in St. Andrew Bay, Gulf of Mexico. The samples of bed sediment consisted of fine-grained sand with median diameter of 0.14mm. During the measurements, the average flow depth and the maximum current velocity were respectively equal to 12.2m and 0.50m/s. Allen [1968] related that the height (Δ_r) and length (λ_r) of ripples with the flow depth (h) as follows:

$$\frac{\Delta_r}{h} = 0.086h^{0.19} \quad (2.8)$$

and

$$\lambda_r = h^{1.6} \quad (2.9)$$

Van Rijn [1993]

Based on flume and field data, Van Rijn [1993] proposed expressions for the bedform dimensions as a function of sediment and flow properties. Expressions for describing dimensions of bedforms from lower to upper regime have been developed. In this

section, the bedforms in the lower regime such as miniripples, megaripples and dunes are discussed because they have been observed in the current study area.

Miniripples

Miniripples are usually found for transport stage parameters smaller than 3. They present ripple spacing much smaller than the water depth. The approach by Yalin [1985] can be applied to estimate the dimensions of miniripples (Δ_{mir} and λ_{mir}) which are related to median grain size (d_{50}) as follows:

$$\Delta_{mir} = 50 \text{ to } 200d_{50} \quad (2.10)$$

and

$$\lambda_{mir} = 500 \text{ to } 1000d_{50} \quad (2.11)$$

Megaripples

The heights of megaripples were derived from field data of irrigation channels in Pakistan. The flow conditions are characterized by flow depths from 1.5m to 4m and average velocities between 0.5m/s and 1m/s. The median grain size is from 0.10mm to 0.35mm. The length (λ_{mer}) and height (Δ_{mer}) of megaripples [Van Rijn, 1993] are defined as:

$$\lambda_{mer} = 0.5h \quad (2.12)$$

$$\frac{\Delta_{mer}}{h} = 0.02(1 - e^{-0.1T})(10 - T) \quad (2.13)$$

Figure 2.8 shows the variation in height of megaripples for transport stage values (bed shear stress parameter) smaller than 10. The decrease of relative bedform height for low transport stage values indicates the presence of megaripples with low height of bedforms. The maximum height of megaripples is found for transport stage values of about 4. Equation 2.13 is limited to transport stage values of 10 for which dunes are expected to develop.

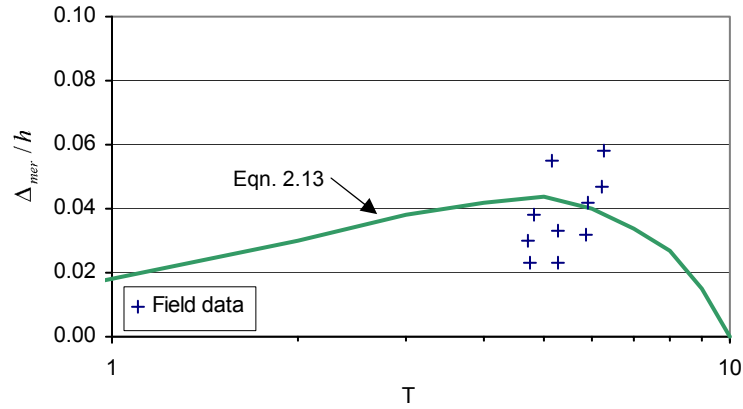


Figure 2.8: Heights of megaripples after Van Rijn [1993]

Dunes

To establish an equation for estimation of dune dimensions, data from 84 flume experiments were employed. The medium grain size was from 0.19mm to 1.35mm. The flow conditions were characterized by flow depths of 0.10-0.49m and flow velocities between 0.34m/s and 1.17m/s. In addition, 22 data sets from measurements in rivers with flow depth from 0.25m to 12.7m and flow velocity between 0.53m/s and 1.55m/s were used. The median grain size in the field ranged from 0.35mm to 3.60mm.

By assuming that geometry and migration of bedforms can be derived from the bed load sediment transport, Van Rijn [1984] found that the height and length of dunes are functions of median grain size, flow depth, particle parameter and transport stage parameter. The length (λ_d) and height (Δ_d) of dunes were proposed as:

$$\lambda_d = 7.3h \quad (2.14)$$

$$\frac{\Delta_d}{h} = 0.11 \left(\frac{d_{50}}{h} \right)^{0.3} (1 - e^{-0.5T})(25 - T) \quad (2.15)$$

Figure 2.9 shows the variation of dune height with the transport stage parameter. It can be seen that the role of grain size is not significant in affecting the height of dunes for a given flow depth. The maximum height of dunes is found between 0.1 and 0.2 of flow depth for transport stage parameter values of about 5. Dunes are expected to be washed out for transport stage parameter values exceeding 25.

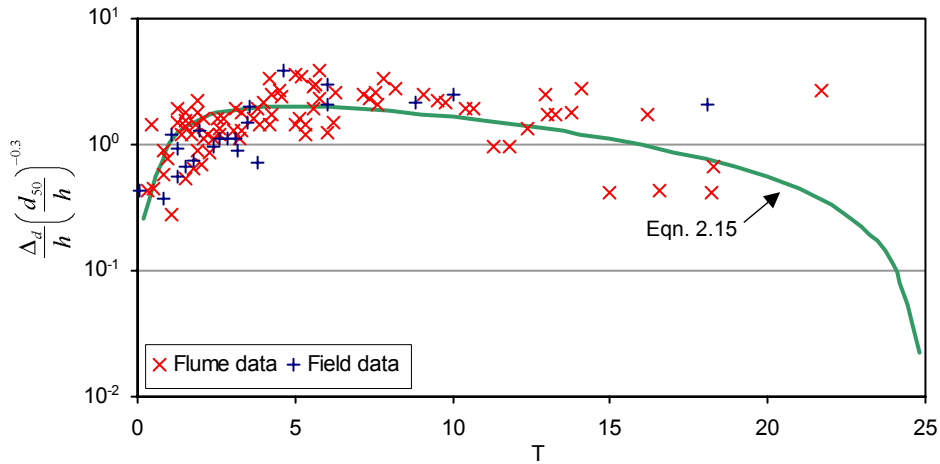


Figure 2.9: Heights of dunes after Van Rijn [1993]

2.3 Equivalent roughness sizes

The equivalent roughness size indicates the unevenness of the bottom. As previously mentioned, it influences the velocity distribution and it is one of the important factors controlling sediment transport. In this section, the relation between equivalent roughness sizes, grain sizes and bedform dimensions is presented. In addition, the estimation of equivalent roughness sizes from the best fit line of the velocity profile is also discussed.

Other factors can also contribute to the roughness. According to Harris [2003], the bed roughness in coastal environments is also influenced by biogenic factors. This type of roughness is predominant in muddy environments. The biogenic roughness can be due to mounds and burrows created by benthic organisms [Harris and Wiberg, 1997]. The bed roughness can also be due to the saltation of bottom sediments. The relation between bed roughness from saltating sediment, grain size and bed shear stress over plane beds with transport of sand was studied by Wiberg and Rubin [1989]. The saltation roughness of about 0.1cm is found in sandy coastal environments during high sediment transport.

2.3.1 Grain roughness

Although grain roughness (k'_s) usually contributes only slightly to the total roughness, it can be used as the minimum equivalent roughness size value for a plane bed. The concept of grain roughness was introduced by Nikuradse [1933]. He studied the flow in smooth and rough pipes. On the basis of flume and field measurements,

some researchers have suggested various coefficients and particle diameters to account for the grain roughness. The results of a few studies are summarized below.

Ackers & White [1973]

About 1000 sets of flume data with flow depth below 0.4m were used to determine the grain roughness. The bed sediments were sands (1.35mm) and gravels (from 6.2mm to 28.1mm). The grain roughness (k'_s) was found to be related to the sediment size for which 35% by weight is finer (d_{35}):

$$k'_s = 1.25d_{35} \quad (2.16)$$

Kamphuis [1974]

Experiments were conducted in a 15m tilting flume with 0.38m width. The sizes of bed sediments in terms of d_{90} were from 0.54mm to 46mm. The range of k'_s/d_{90} was found between 1.5 and 2.5. The following relation was proposed:

$$k'_s = 2d_{90} \quad (2.17)$$

Gladki [1975]

Field measurements carried out in the Vistula river in Poland were considered. Using data of eleven cross sections, the roughnesses were evaluated in relation to different channel filling bed, slope and velocities and thus discharges. Gladki [1975] found that the equivalent roughness size due to grain size (k'_s) is better represented with the d_{80} :

$$k'_s = 2.3d_{80} \quad (2.18)$$

Van Rijn [1982]

About 120 sets of flume and field data were considered to determine the bed roughness due to grains. The range of flow depths was from 0.02m to 1.7m. The average velocities were between 0.2m/s and 2.6m/s. The bed sediment sizes were from 0.14mm to 5mm. Van Rijn [1982] suggested the following relation:

$$k'_s = 3d_{90} \quad (2.19)$$

2.3.2 Form roughness

The equivalent roughness size due to the bedforms is related to the geometry of bedforms. In the simplest expression, the form roughness (k_s'') is equivalent to the height of bedforms (Δ):

$$k_s'' \approx \Delta \quad (2.20)$$

However, many studies show that other factors such as the length (λ) and slope of bedforms (Δ/λ) can have an effect on the form roughness. Hence, the equivalent bedform roughness is found to be a function of:

$$k_s'' = f\left(\Delta, \lambda, \frac{\Delta}{\lambda}\right) \quad (2.21)$$

A number of relations between equivalent roughness sizes and dimensions of bedforms have been proposed. The relations proposed by Wikramanayake [1993], Grant & Madsen [1982], Nielsen [1983], Raudkivi [1988] and Van Rijn [1993] are described hereafter. The ranges of flume and field conditions are summarized in Table 2.2. The ranges of conditions in some of the studies are similar since parts of the used data are from the data collected by Carstens et al. [1969].

Table 2.2: Summary of data used in the investigations of form roughness

	Wikramanayake [1993]	Grant & Madsen [1982]	Nielsen [1983]	Raudkivi [1988]	Van Rijn [1993]
Source of data⁽¹⁾	C, L, M, R	B, C	C, L	C	A, BL, H, ME, NV, VB
Lab/field condition	Wave flume & wave tunnel	Wave tunnel	Wave tunnel	Wave tunnel	Flume and river
Sediment size(mm)	0.12-0.59	0.19-0.59	0.19-0.59	0.19-0.59	0.10-1.44
Velocity (m/s)	0.14-0.84	0.14-0.84	0.14-0.84	0.14-0.84	0.24-1.50
Depth (m)	NA ⁽²⁾	NA ⁽²⁾	NA ⁽²⁾	NA ⁽²⁾	0.08-4.50
Bedform height(cm)	0.48-6.93	0.48-6.93	0.48-6.93	0.48-6.93	12-30
Bedform length(cm)	0.24-46	0.24-46	0.24-46	0.24-46	60-914

Note:

1. Abbreviations for reference of source data: A (Ackers [1964]), B (Bagnold [1946]), BL (Barton & Lin [1985]), C (Carstens et al. [1969]), H (Havinga [1992]), L (Lofquist [1986]), M (Mathisen [1989]), ME (Mahmood et al. [1984]), NV (Nap & Van Kampen [1988]), R (Rosengaus [1987]) and VB (Vanoni & Brooks [1957]).
2. NA means not available.

Wikramanayake [1993]

Four data sets from a wave flume and tunnel were used to obtain the flow over a rippled sand bed with regular waves. The mean diameters of bed sediments were between 0.12mm and 0.59mm. The significant wave period was between 2.5s and 12s. The heights of ripples ranged between 0.48cm and 6.93cm, while their lengths are from 0.24cm to 46cm. Wikramanayake [1993] drew the best fit line between effective roughness (roughness divided by height of bedforms) and slope of bedforms. The results indicated that the form roughness ($k_{s,r}''$) simply depends on the height of ripples (Δ_r) as follows:

$$k_{s,r}'' = 4\Delta_r \quad (2.22)$$

Grant & Madsen [1982]

The roughness due to wave-formed ripples was studied by using dimensional analysis of the turbulent wall layer over a rough boundary. A semiempirical equation was derived considering the law of the wall expression. The form roughness related to ripples ($k_{s,r}''$) was expressed as:

$$k_{s,r}'' = 27.7\Delta_r \frac{\Delta_r}{\lambda_r} \quad (2.23)$$

This equation was also tested with two data sets from Bagnold [1946] and Carstens et al. [1969]. It was found that the equation is capable of describing the equivalent roughness sizes due to bedforms quite well.

Nielsen [1983]

A semiempirical expression of bedforms was derived from the study of the water and sediment transport over a rippled bed in oscillatory flow. Two data sets from experiments in wave tunnels by Carstens et al. [1969] and Lofquist [1986] were considered. The bed sediment sizes were from 0.19mm to 0.59mm, while the flow velocities ranged between 0.14m/s and 0.84m/s. The equation for describing the equivalent form roughness ($k_{s,r}''$) and ripple dimensions (Δ_r, λ_r) is approximated as:

$$k_{s,r}'' = 8\Delta_r \frac{\Delta_r}{\lambda_r} \quad (2.24)$$

Raudkivi [1988]

Based on the law of the wall, Raudkivi [1988] derived empirically the expression of form roughness from the dimensions of ripples. The data by Carstens et al. [1969] were considered. The bed sediment consisted of sand with the median size between 0.19mm and 0.59mm. The maximum height and length of ripples were 6.93cm and 46cm. The relation between form roughness ($k_{s,r}''$) and ripple sizes (Δ_r, λ_r) is expressed as:

$$k_{s,r}'' = 16\Delta_r \frac{\Delta_r}{\lambda_r} \quad (2.25)$$

Van Rijn [1993]

Six data sets from flume experiments and measurements in rivers were collected to study the variation of form roughness. The bed sediment size was from 0.10mm to 0.35mm, while the average velocity ranged between 0.35m/s and 1.00m/s. The ripples had maximum height of 0.30m and maximum length of 9.14m. Figure 2.10 shows the fit line between effective form roughness and ripple steepness. It can be seen that smaller ripple heights and longer ripple lengths are observed in rivers.

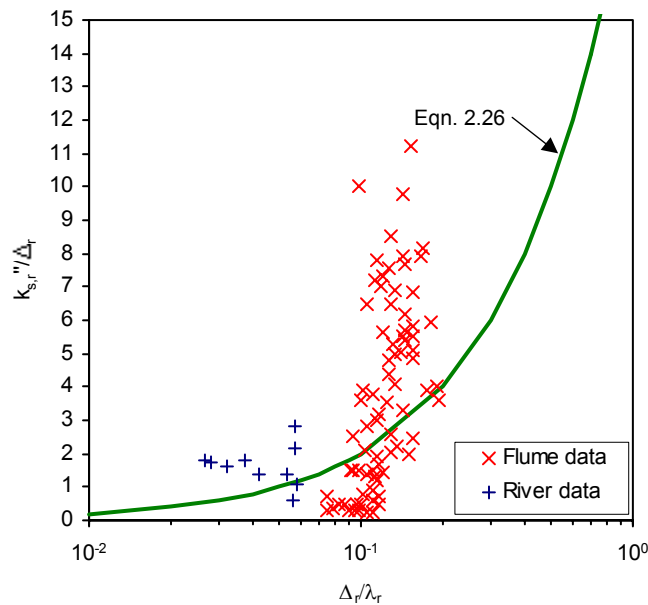


Figure 2.10: Form roughness due to ripples after Van Rijn [1993]

The relation between form roughness ($k_{s,r}''$) and ripple dimensions (Δ_r, λ_r) is formulated as:

$$k_{s,r}'' = 20\gamma_r \Delta_r \frac{\Delta_r}{\lambda_r} \quad (2.26)$$

where γ_r is the ripple presence factor which is 1 for ripple bed and 0.7 for ripples superimposed on dunes or sandwaves.

For the equivalent roughness due to dunes, Van Rijn [1982] analyzed 40 data sets from flume experiments and field measurements. The median size of bed sediments was from 0.10mm to 1.44mm. The flow depths covering flume and rivers were between 0.08m and 4.5m with the average velocity of 0.24-1.5m/s. The experimental data with ratios of flow width to depth larger than 5 and ratios of flow depth to equivalent roughness sizes larger than 10 were considered. The second condition was considered because large equivalent roughness sizes may disturb the uniformity of the flow. Figure 2.11 shows the fit line of equivalent form roughness due to dunes. The observed dunes have heights of 0.12-0.30m and lengths of 0.60-9.14m. For dune steepnesses between 0.01 and 0.20, the form roughness related to dunes ($k_{s,d}''$) is represented by:

$$k_{s,d}'' = 1.1\gamma_d \Delta_d \left(1 - e^{-25\Delta_d/\lambda_d}\right) \quad (2.27)$$

where γ_d is the dune presence factor which is 0.7 for field conditions.

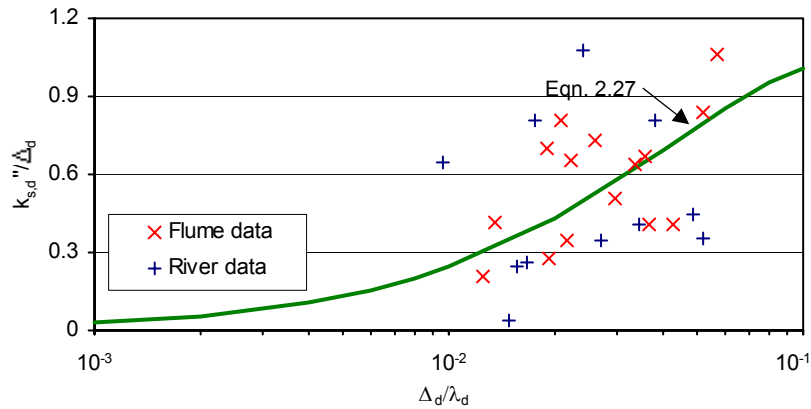


Figure 2.11: Form roughness due to dunes after Van Rijn [1993]

2.3.3 Estimation of equivalent roughness sizes

Equivalent roughness sizes can be estimated from the best fit line of velocity profile. Figure 2.12 shows a typical velocity profile over the vertical. In general, the velocity profile is divided into free-stream and boundary layer flows [Soulsby, 1983]. The ve-

velocity magnitudes in the free-stream flow are uniform up to the surface. The boundary layer is the flow region which is affected by the frictional resistance of the bed [Aagaard and Masselink, 1999]. It can be divided into bed, logarithmic and outer layers. The outer layer is largely influenced by the free-stream flow. The velocity magnitudes in the logarithmic layer increase logarithmically with respect to the height above the bed and are used to estimate the equivalent bed roughness sizes.

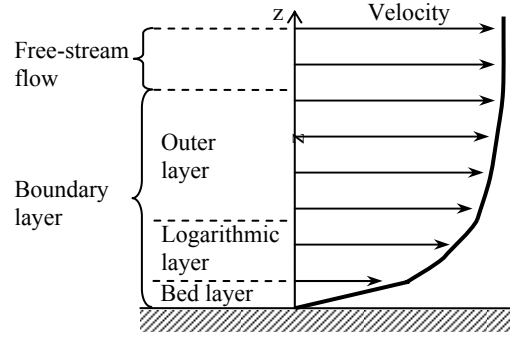


Figure 2.12: Flow velocity layers

The velocity profile in the bottom boundary layer can be expressed in terms of the law of the wall [Schlichting, 1951] as follows:

$$\frac{u_z}{u_*} = \frac{1}{\kappa} \ln \left(\frac{z}{z_0} \right) \quad (2.28)$$

where u_z is velocity distribution at a distance z from the bottom (m/s), u_* is the shear velocity (m/s), κ is the Von Karman constant (0.40) and z is the distance from the bottom (m). The zero velocity level (z_0) is only a mathematical parameter which defines the height z above the bottom at the velocity (u_z) equal to zero. To obtain z_0 , the best fit line of velocity profile within the logarithmic part of boundary layer is drawn with logarithm of z on the vertical axis. The best fit line is obtained by the least square method which determines a line having minimum deviation to the data.

From studies of flow in pipes, Nikuradse [1933] found a relationship between relative roughness (z_0/k_s) and roughness Reynolds number (u_*k_s/ν). Three flow regimes were identified, i.e. smooth, transition and rough regimes. The smooth regime is characterized by Reynolds number values of less than 5, while rough regime occurs for Reynolds number value exceeding 70. Since flows in tidal channels are usually in the rough regime, the equivalent roughness sizes (k_s) related to zero velocity level (z_0) defined by Nikuradse [1933] is used:

$$k_s = 30z_0 \quad (2.29)$$

Several studies have been performed regarding the estimation of equivalent roughness sizes from the velocities in the bottom boundary layer. These studies were carried out under different flow conditions and bed sediment properties. The studies by Sternberg [1968], Carling [1981], Soulsby & Dyer [1981], Schauer [1987], Cacchione, et al. [1995] and Cheng et al. [1999] are summarized hereafter.

Sternberg [1968]

Field measurements were carried out in six tidal channels in Puget Sound and the Strait of Juan de Fuca, USA. The flow depths were between 8m and 42m. The size of bed sediment ranged from 0.062mm to 1.087mm. Six current meters within 1.5m from the bottom were mounted on a bottom tripod. The maximum velocities were recorded between 0.30m/s and 0.45m/s. In addition, underwater television and stereo cameras were used to observe bottom sediment transport and bed geometry.

The measured velocities over 10 minute intervals were plotted on semi logarithmic paper. Logarithmic velocity profiles having at least four out of six point velocity measurements within 10% discrepancy to the fit line were selected. The limit of 10% was defined on the basis of the accuracy of the current meter. Average equivalent roughness sizes of about 2cm resulted from the measurements.

Carling [1981]

The flow velocity profiles were recorded in intertidals of South Wales, UK. The mean flow depth during the measurements was 8m. Well-sorted fine sand with average grain size of 0.125mm was found on the bed. Carling [1981] employed five direct-reading current meters at 0.08m, 0.24m, 0.44m and 0.77m from the bottom. The time interval between measured velocity profiles was 40 seconds. Velocity measurements were gathered at two stations over spring and neap tidal cycles. The maximum flow velocities ranged between 0.30m/s and 0.50m/s.

The velocity profiles having correlation coefficient of the best fit line of 0.90 were selected. To observe the effects of tidal phases, the average of the bed roughness was calculated separately for the ebb and flood phases. Equivalent roughness sizes of about 6.6cm and 5.1cm resulted respectively during ebb and flood phases.

Soulsby & Dyer [1981]

Field measurements were carried out in the Southwest coast of UK. Propeller current meters were attached to a frame at 0.17m, 0.42m, 0.82m and 1.78m above the seabed. The range of flow depth was from 14m to 27m. The bed sediment was characterized as poorly sorted sandy gravel with mean size of 0.22mm.

Soulsby and Dyer [1981] introduced a method to account for the effect of accelerating and decelerating tidal flows on the bed roughness sizes. The tidal acceleration and deceleration are characterized by a length scale (Λ) as follows:

$$\Lambda = \frac{u_* |u_*|}{du_*/dt} \quad (2.30)$$

where du_*/dt is the change of bed shear velocity (u_*) in time. Positive values of acceleration length refer to accelerating flows and negative value refers to decelerating flows.

The zero velocity level was corrected by the following equation:

$$\tilde{z}_0 = z_0 \exp\left[\frac{\ln(z_m/z_0) - 1}{1 - 0.04\Lambda/z_m}\right] \quad (2.31)$$

where \tilde{z}_0 is the corrected zero velocity level (m), z_0 is zero velocity level (m), and z_m is the profile gradient which is related to the top (z_t) and bottom (z_b) distances:

$$z_m = \sqrt{\frac{z_t}{z_b}} \quad (2.32)$$

Soulsby and Dyer [1981] found that z_0 determined by taking into account the acceleration length scale is underestimated by 60% at one hour after slack water and overestimated by 83% at one hour before slack water. The average roughness size resulted equal to about 15cm.

Schauer [1987]

Field measurements were carried out in Vejnaes channel (Baltic sea coast) and Jade inlet (German North sea coast). The flow conditions were characterized by flow depths of about 20m and maximum current velocities from 0.43m/s to 0.50m/s. In the Vejnaes channel, the bed sediment is characterized by fine sands of 0.063mm. In the Jade inlet, ripple heights of 0.1m and lengths of 6m were found. Six current meters were mounted from 0.29m to 3.43m and from 0.18m to 3.32m respectively in the Vejsnaes channel and Jade inlet. Minimum correlation coefficient values of 0.90 was employed to select valid velocity profiles. Averaged equivalent roughness sizes of about 36cm and 45cm resulted respectively in the Vejnaes channel and Jade inlet.

Schauer [1987] found that the effect of the acceleration and deceleration as pointed out by Soulsby & Dyer [1981] can be neglected. Insignificant effects of tidal acceleration on the estimation of equivalent roughness sizes were due to the contradicting effects of nonstationary flows.

Cacchione, et al. [1995]

Cacchione et al. [1995] conducted current velocity measurements in the Amazon delta with flow depth of 65m. Velocities up to 0.50m/s were recorded. The bed sediment is very fine with 0.001mm in size. Three electronic current meters were installed at elevations of 0.1m, 0.5m and 0.8m from the bottom. Minimum correlation coefficient of 0.90 was defined to obtain valid profiles. Averaged equivalent roughness sizes approximately equal to 8cm resulted.

Cheng et al. [1999]

Acoustic Doppler Current Profiler (ADCP) measurements were carried out by Cheng et al. [1999] in the San Francisco Bay, USA. The bed sediments were silt with some clays and mud. The median grain size was 0.06mm. The flow conditions in the Bay were characterized by depths of about 16m and maximum velocities of 0.75m/s. Two broad band ADCPs with a frequency of 1200kHz were mounted on a bottom platform. One device with 50cm bin sizes was directed upward to measure velocities above 3.5m from the bottom. The second ADCP with a bin size of 5cm was directed downwards and set for high resolution recording. Thirty velocity bins at heights from 0.1m to 1.5m above seabed were recorded. Only profiles resulting in minimum correlation coefficients of 0.90 were taken in the analysis. Cheng et al. [1999] obtained equivalent roughness sizes of 2.4cm and 3.1cm respectively during ebb and flood phases. It was found that the differences of equivalent roughness sizes could not be attributed to the different flow conditions during flood and ebb phases.

2.4 Discussion

In this chapter, previous studies on the bedforms and equivalent roughness sizes have been reviewed. Most of the investigations are based on data from flume experiments and some from measurements in rivers. The development of bedforms was firstly investigated in flumes. Bedforms were observed in different flow regimes. In the lower regime, ripples with about 6cm heights and lengths less than 60cm were found. Dune heights resulted of about 0.4 times of flow depth and dune lengths between 6 and 7 times of flow depth. Several bedform classifications and estimation of bedform dimensions were proposed from flume experiments and measurements in rivers.

The equivalent roughness sizes were found to be dependent on the size of bed sediment and bedforms. The grain roughness size was found to be dependent mainly on the larger particle sizes. The form roughness is explained in terms of bedform

heights and lengths. Most of existing expressions have been derived from flume experiments and measurements in rivers. In flumes, bedform heights up to 0.07m and bedform lengths up to 0.46m were observed. Larger bedform sizes, i.e. with heights from 0.12m to 0.30m and lengths from 0.60m to 9.14m resulted from measurements in rivers. Currents in flumes and rivers are characterized by a unidirectional flow. In tidal channels, the velocity magnitude, flow direction and flow depth constantly change during a tidal cycle. As a result, it is expected that, in tidal channels, the bedforms are not able to adapt to the changes in hydrodynamic conditions. Therefore, the equations derived from flume experiments and river measurements under unidirectional flows may fail to give an adequate estimation [Soulsby, 1997].

The estimation of equivalent roughness sizes on the basis of current velocity measurements has been carried out also in tidal channels (Sternberg [1968], Carling [1981], Soulsby & Dyer [1981], Schauer [1987], Cacchione, et al. [1995] and Cheng et al. [1999]). Equivalent roughness sizes ranging from 2cm to 45cm resulted. Most studies employed current meters. The use of acoustic profilers for measuring current velocities to estimate equivalent roughness sizes is rarely found in the literature. In the current study, velocity data acquired by acoustic profilers with different configurations are analyzed to identify the best setup of device for measuring current velocities in the bottom boundary layer.

Chapter 3

Study area and field measurements

3.1 Introduction

The objectives of this chapter are to describe the characteristics of the study area and to explain the devices and procedures of field measurements. The characteristics of the study area in the Central Dithmarschen Bight in terms of meteorology, geology, morphodynamics and hydrodynamics are introduced. The field measurement data are primarily acquired by acoustic devices including a side scan sonar, echo sounder and acoustic profiler. The principles and specifications of these devices are described. Initially, measurements of bedforms and velocity profiles were conducted separately during various tidal conditions. Then, to study the relation among flow, bedforms and equivalent roughness sizes, simultaneous measurements of bedform dimensions and velocity profiles were conducted.

3.2 Description of study area

The investigation area is the Central Dithmarschen Bight (Figure 3.1). It is located in the North Sea coast of Germany. The area of study is about 600km² and it is located between the Eider estuary in the North and the Elbe estuary in the South. The eastern part is bordered by the mainland of the State of Schleswig-Holstein.

3.2.1 Meteorology

The study area which is located in the middle latitude is characterized by a sub-oceanic climate. According to the Helgoland Meteorological Station [Müller, 1996], the average monthly temperature is 9.1°C with the absolute minimum of -15.6°C and absolute maximum of 31.6°C. The mean precipitation is approximately 708mm/year.

The predominant wind direction is South westerly winds between September and March.

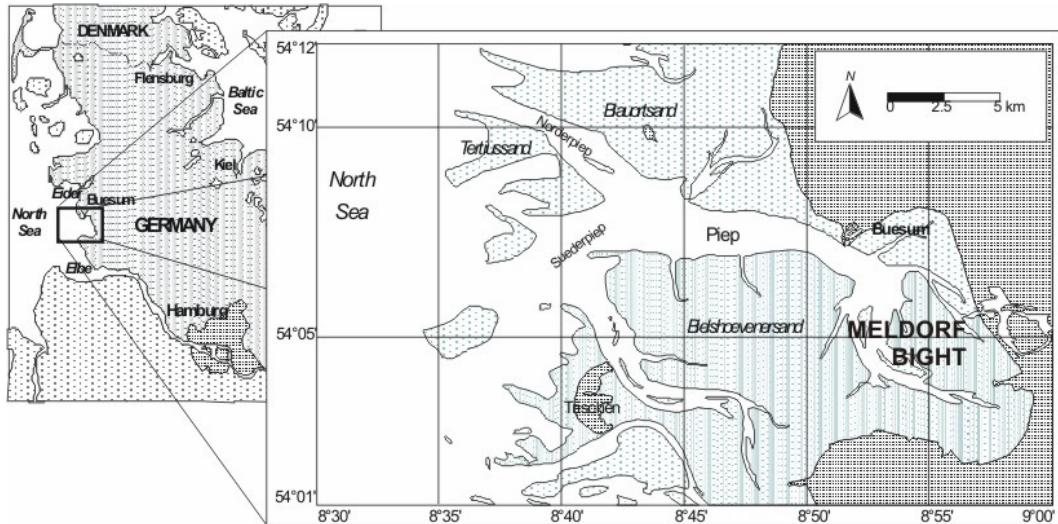


Figure 3.1: Investigation area and bathymetric map of the Central Dithmarschen Bight

3.2.2 Geology

Silica clastic sediments of Holocene age characterize the main geological setting of the study area [Ricklefs, 2002]. In the post Pleistocene, the deposition started with a peat layer above Pleistocene glacio-fluviatile sands. The rising sea level at the early post Pleistocene has eroded the peat and deposited the silty clay. The sedimentation occurred under permanent submarine conditions which is indicated by the presence of shells in the "Dithmarcher Klei" [Dittmer, 1938].

The silty clay of Holocene age consists of discordant and concordant layers which are superimposed by sand sediments with some deposits of cohesive mud. The change of facies from clay sediments to sandy deposits indicates the change from deep to shallow water conditions. The deposits match to the current sediments in the tidal flat. These intertidal deposits have a thickness up to 20m.

Composition, structure and distribution of outcropping sediments are affected by the geological structure. The deepest beds of channels are composed of deposits from early Holocene which are cohesive sediments and hard to be eroded (Figures 3.2 and 3.3). Younger sandy deposits are much easily eroded and influence the change in morphology.

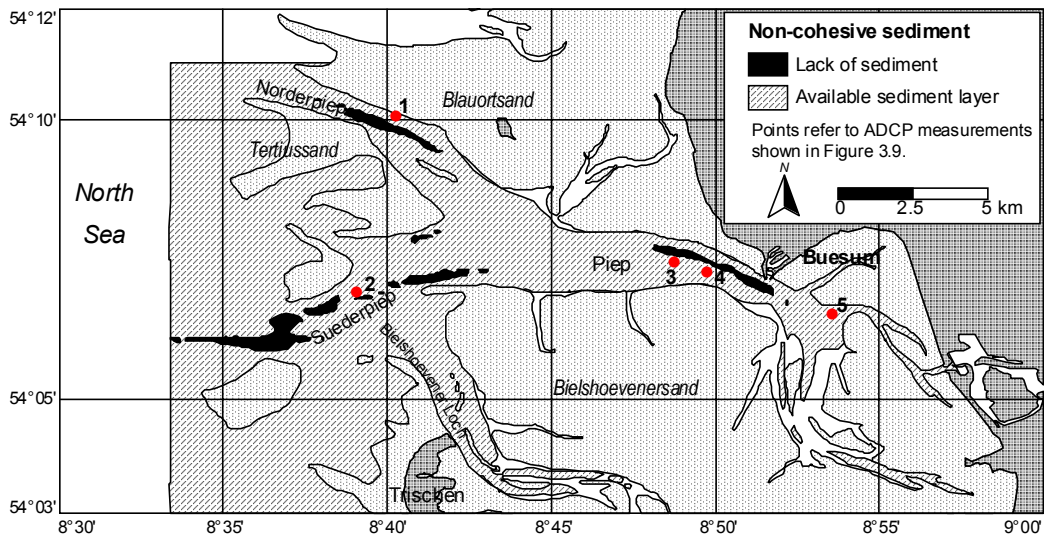


Figure 3.2: Lack and availability of mobile sediments after Mayerle et al. [2002]

Results of measurements show coarser sediment (0.15-0.23mm) in the tidal flats off the coast such as Tertiusand [Reimers, 2003]. Smaller grain sizes (0.06-0.09mm) were found in tidal flats near the coast. A sediment map in the tidal channels was obtained by combining side scan sonar records with sediment characteristics from grab samples [Vela-Diez, 2001]. The sediment types are generally very fine to fine sands (Figure 3.3). The median grain sizes of bed sediments are between 0.09mm and 0.23mm. The mud content is generally higher than 5%. About 50% of the sediment samples have mud content exceeding 10% [Vela-Diez, 2001].

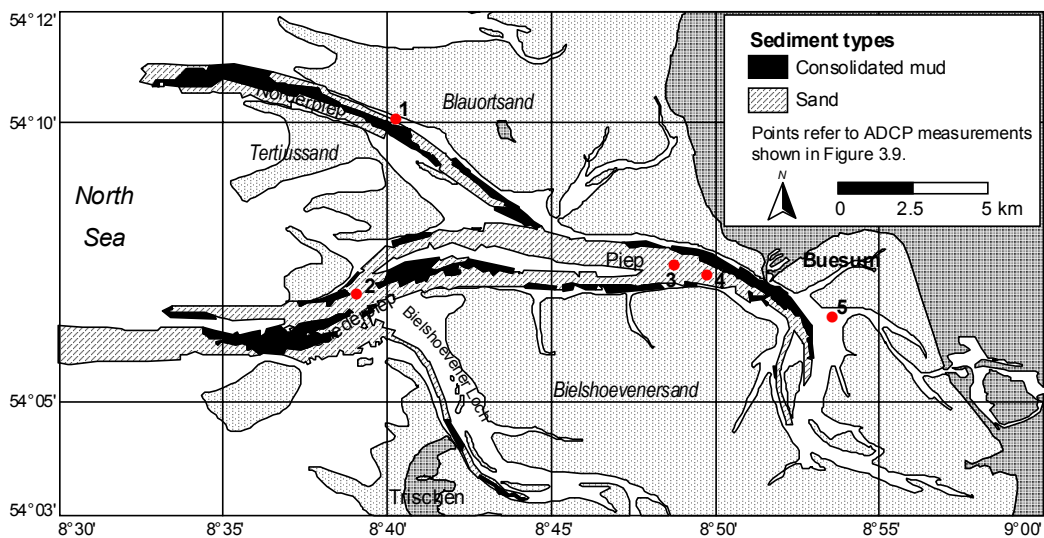


Figure 3.3: Characteristics of sediments in tidal channels after Mayerle et al. [2002]

3.2.3 Morphology

The morphology of the study area is shown in Figure 3.1. The tidal flats are characterized by the presence of several sand islands such as Blauort, Tertius and Trischen. During low tide, about 50% of the study area falls dry [Mayerle and Palacio, 2002] and the tidal flats at high water are entirely submerged. The tidal flats are relatively unstable. Trischen island has migrated eastward but its shape remained the same [Ehlers, 1988]. According to Wieland [1972], the migration rate of Trischen is about 29cm per year. An eastward displacement of 37cm per year was also observed in the Blauort island. In the winter storm, Blauort and Tertius islands can move about 80m. In the investigation area, three main tidal channels are Piep, Norderpiep and Suederpiep with maximum depths of respectively 23m, 14m and 17m. The width of tidal channel varies from a few meters to 4km. Current flows to the bight mainly through Norderpiep and Suederpiep. In the southeast of Buesum, the channel divides into three smaller channels.

3.2.4 Hydrodynamic conditions

The study area is characterized by a semidiurnal tide. Based on the German water level datum (Normal Null - NN), the mean high and low water at the gauge Buesum are 1.6m and -1.6m NN respectively. Figure 3.4 shows the water level at the gauges Tertius and Buesum during a neap tide. The location of the gauges can be seen in Figure 3.1. There is no significant tidal asymmetry in the study area. The time lag between the two locations is up to about 15 minutes. The water body is vertically well mixed. According to water level measurements at Blauort and Tertius gauges in the year 2000, the difference of tidal range between neap and spring tides is about 2.1m. The tidal range is about 1.6m and 3.7m respectively during neap and spring tidal cycles. The water level upset can be up to 5m NN during severe storm conditions.

Through Norderpiep and Suederpiep channels, the flood and ebb tides flow respectively easterly and westerly. The mean flow velocities in the tidal channel are up to about 1.2-1.5m/s [Ricklefs, 2002]. On the tidal flats, the tidal current can be as high as 0.5m/s. During storm conditions, the flows in the tidal flats can reach 1m/s [Ricklefs, 2002]. Significant heights of wind waves of up to 3-4m have been recorded in the inlets near to the open sea. Most of the wave energy is dissipated along the edge of tidal planes. The significant wave heights in the tidal flats rarely exceed 0.5m [Ricklefs, 2002].

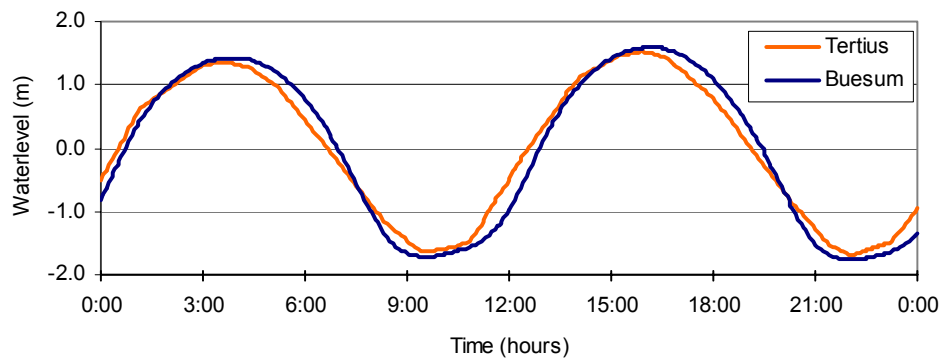


Figure 3.4: Water level measured at Tertius and Buesum in August 22, 2000

3.3 Measurements of bedforms

Field measurements of bedforms were carried out using a side scan sonar and echo sounder. Figure 3.5 shows the location of measurements in the main tidal channels. Side scan sonar measurements were conducted in 1999 and 2000. The heights of bedforms were recorded with an echo sounder in parts of Norderpiep and Piep channels in 2000. Details of the measurements of bedforms are summarized in Razakafoniaina [2001] and Vela-Diez [2001]. In 2004, additional echo sounder measurements were carried out to scan the bedforms at locations in which measurements of current velocities were previously done with moored acoustic profilers (ADCPs).

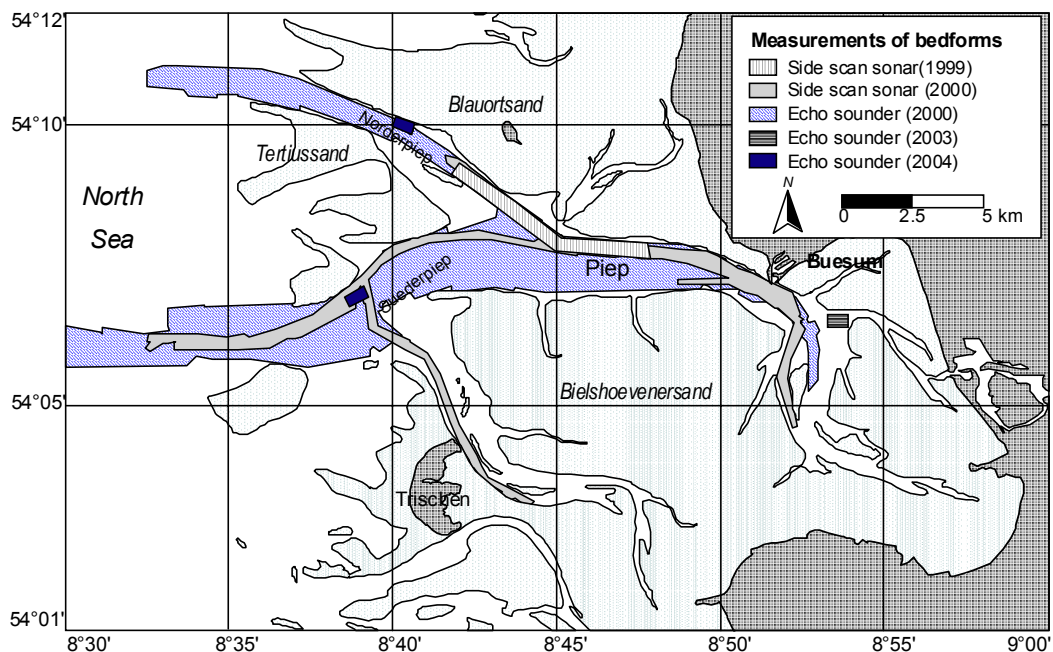


Figure 3.5: Coverage of field measurements of bedforms in the tidal channels

3.3.1 Side scan sonar

Measurements were performed in May and June 1999 as well as in September and November 2000. A Klein 595 side scan sonar with sound frequency of 500kHz was employed (Figure 3.6). It has two beams which map the left and right sides of the ship track. The total lateral coverage of the image for the conditions in question was about 150m. The returned sound is received by the device and saved as image files.



Figure 3.6: Klein 595 side scan sonar used to map the bottom of channels

3.3.2 Echo sounder

Echo sounder measurements were carried out at the intersection between the Piep and Norderpiep tidal channels (Figure 3.5). Simultaneous measurements using the echo sounder and side scan sonar were done in November 2000. Dual frequencies Fathentholz sonar (15kHz and 200kHz) was used. In 2004, the echo sounder was also used to obtain the bedforms in the Norderpiep and Suederpiep channels. The location was at the place in which stationary ADCP measurements with 50cm bin size were carried out (Points 1 and 2 in Figure 3.7). The profiles were recorded digitally and later processed to view the bedforms.

3.4 Measurements of current velocities

Current velocity profiles were measured using an Acoustic Doppler Current Profiler (ADCP). Various types of ADCP are available, i.e. self-contained, vessel mounted and direct reading and to cover a wide range of frequencies from 75kHz to 1200kHz [Gordon, 1996]. The measurement of flow speed by an ADCP is based on the Doppler effect which is defined as the change of sound frequency due to its relative motion between source and observer. The Doppler effect can be experienced when we walk on a street. As a car passes and recedes from us, the sound of its horn seems to

drop in frequency. By knowing the change of frequency, the velocity of the car can be calculated [Simpson, 2001]. The basic equation for the Doppler effect is:

$$f_d = f_s \left(\frac{u_r}{c} \right) \quad (3.1)$$

where f_d is the Doppler shift frequency (Hz), f_s is the frequency of the sound source (Hz), u_r is the relative velocity between sound source and sound receiver (m/s) and c is the speed of sound (m/s). ADCPs employ the Doppler effect by sending sound at a specific frequency and receiving echos returned by sound scatterers in the water. These sound scatterers are sediment particles or planktons which float or move in the water. Further details of the working principle of ADCP are documented in, for example, Gordon [1996] and Simpson [2001].

Equivalent roughness sizes were obtained from velocity profiles measured by ADCPs in several locations of the study area. Figure 3.7 shows the five locations at which measurements of current velocities were carried out. Measurements were carried out at the two main tidal inlets, i.e. Norderpiep (Point 1) and Suederpiep (Point 2) and at three locations along the Piep tidal channel (Points 3, 4 and 5). In this section, measurements at Point 1 to 4 which were not carried out simultaneously with bedform measurement are described and discussed. The ADCP measurements with bin size of 15cm in the inner Piep channel will be explained in Section 3.5.2.

A Workhorse Sentinel ADCP manufactured by RD Instruments was employed. Measurements with bin sizes of 50cm, 25cm and 5cm were carried out with devices either mounted on the vessel or moored to a bottom platform (Table 3.1).

Table 3.1: Measuring configurations of ADCP during the measurements

Description	50cm	25cm	15cm	5cm
Bottom track (pings/ensemble)	0	4	2	3
Maximum tracking depth (m)	0	22	7.5	10
Salinity (parts per thousand)	0	27	20	0
Time per ensemble (s)	300	4.79	1.52	3.60
Time between pings (s)	15	0.2	0.04	0.09
Blank after transmit (m)	0.44	0.25	0.50	0.10
Water profiling mode	1	1	12	5
Number of depth cells	24	52	60	30
Number of pings per ensemble	20	4	15	3
Depth cell size (cm)	50	25	15	5
Ambiguity velocity (m/s)	1.70	1.70	1.70	3.50

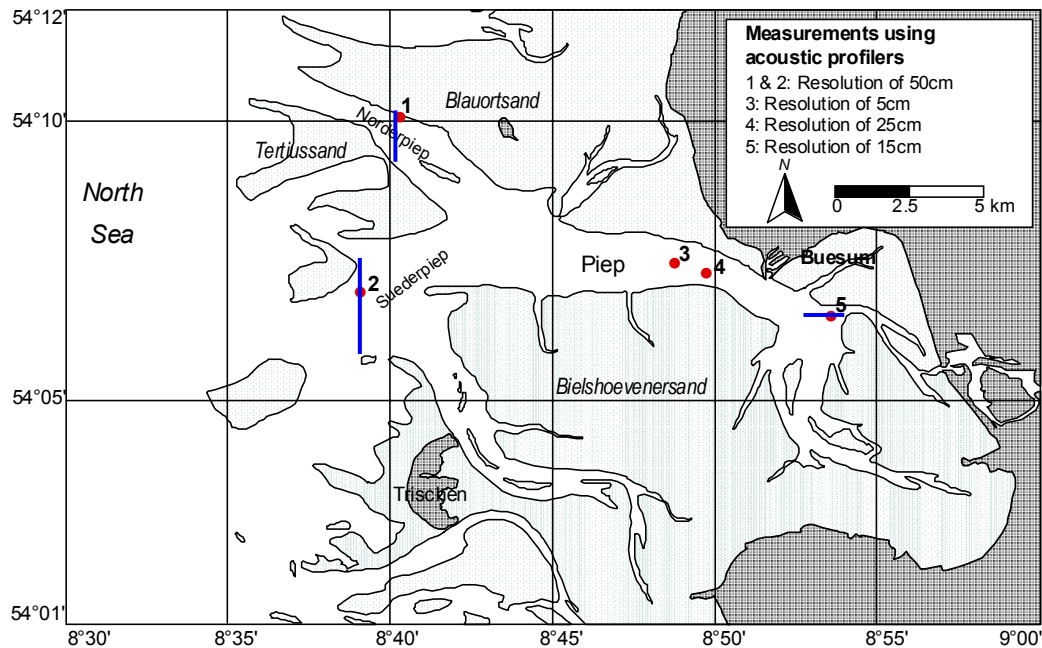


Figure 3.7: Field measurements of current velocities in tidal channels.

Cross sectional profiles at the measuring locations are shown in Figures 3.9 and 3.17.

3.4.1 Acoustic profiling with 50cm bin resolution

The ADCPs were mounted on a bottom frame and placed on the bed of the tidal channel for continuous measurements (Figure 3.8). The locations of measurements in the Norderpiep (Point 1 at $8^{\circ} 40.22'E$, $54^{\circ} 10.05'N$) and Suederpiep (Point 2 at $8^{\circ} 39.00'E$, $54^{\circ} 6.90'N$) tidal inlets are indicated in Figure 3.7. These locations are characterized by lack of sediment layers and consisting of consolidated mud (see Figures 3.2 and 3.3). The cross sections at which the measurements were carried out are shown in Figure 3.9. It can be seen that the Norderpiep channel is much narrower than the Suederpiep channel. Mean water depths at the measuring locations in the Norderpiep and Suederpiep tidal channels are respectively equal to 8m and 13m.



Figure 3.8: Deployment of moored ADCP

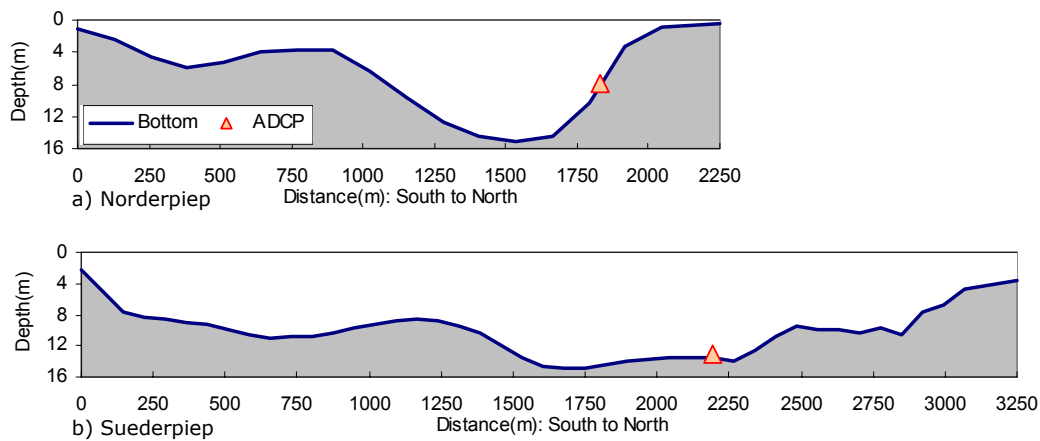


Figure 3.9: Cross sections at which ADCPs with 50cm bin resolution were placed.

See Figure 3.7 for the location of the cross sections.

The devices were configured to measure current velocities in ensembles of 20 pings per ensemble. The lowest bin is recorded at about 1m from the bottom of the channel. The velocity magnitude in each ensemble is the average of 20 pings with 15 second intervals. The time interval between adjacent velocity profiles was set to 5 minutes. To study the development of bed roughness over the same period in the Norderpiep and Suederpiep channels, the data collected from August 11 to September 11, 2000 were selected. It covers two spring tides (August 17 and 31, 2000) and two neap tides (August 25 and September 6, 2000). Figure 3.10 shows the recorded velocities during neap and spring tides in the Norderpiep and Suederpiep channels.

Table 3.2 shows the ranges of depth integrated current velocities during the measurement. Maximum depth integrated velocities up to 1.27m/s and 1.46m/s are found respectively during flood phase in the Norderpiep channel and ebb phase in the Suederpiep channel. The spring tide is characterized by higher flow velocities. The highest velocity of 1.46m/s is observed in the Suederpiep channel during spring tide. Figure 3.11 shows typical velocity profiles during a spring tide in the Suederpiep channel. Well defined velocity profiles resulted.

Table 3.2: Depth integrated velocities. ADCP measurements with 50cm bin resolution

Tidal conditions		Ranges of depth integrated current velocity(m/s)	
		Norderpiep	Suederpiep
Phases	Ebb	0.02-0.93	0.02-1.46
	Flood	0.02-1.27	0.02-1.34
Cycles	Neap	0.03-0.89	0.03-1.11
	Spring	0.03-1.27	0.03-1.46

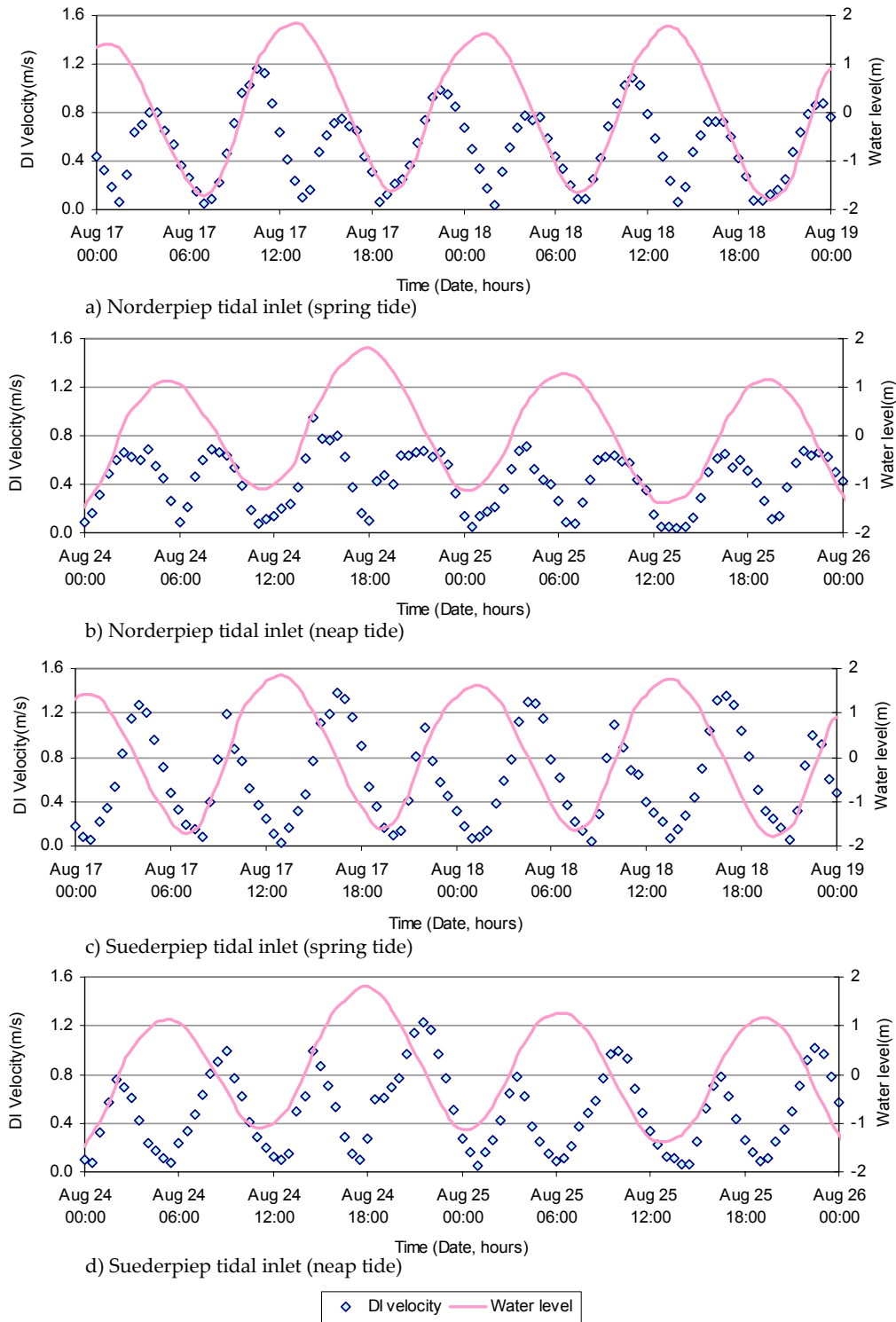


Figure 3.10: Water level and depth integrated current velocities.
ADCP measurements with 50cm bin resolution

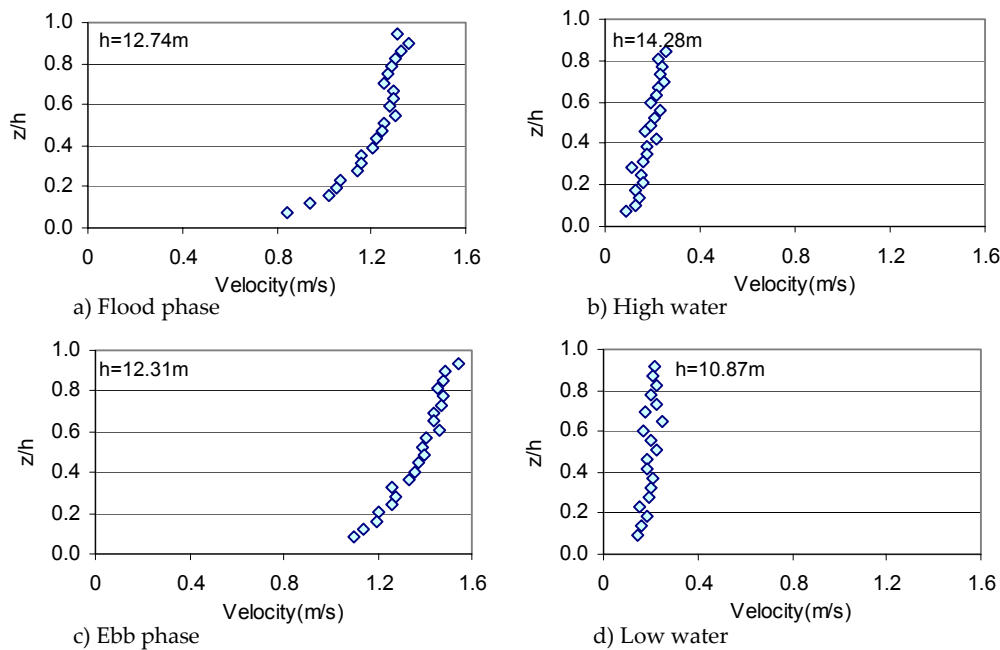


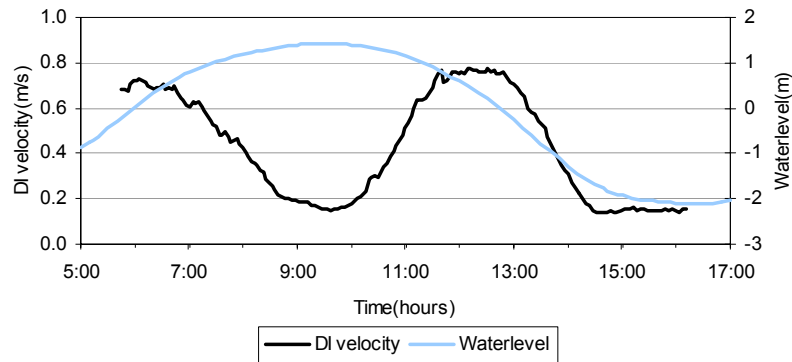
Figure 3.11: Typical velocity profiles during a spring tide in the Suederpiep channel. ADCP measurements with 50cm bin resolution.

3.4.2 Acoustic profiling with 25cm bin resolution

Stationary measurements were performed in the Piep channel on November 23, 2000 (Point 4 in Figure 3.7). Referring to Figures 3.2 and 3.3, the channel bed is characterized by the availability of mobile sediments consisting of fine to medium sands. The measurements covered a neap tidal cycle. The ADCP was mounted on the research vessel “Suedfall” (Figure 3.12). The water profiling mode 1 was employed with the bin size of 25cm (see Table 3.1). The time interval between ensembles was 4.8 seconds. The coverage of measurement was from the flood phase until low water as indicated in Figure 3.13. The depth integrated velocities were up to 0.73m/s and 0.78m/s respectively during flood and ebb phases.

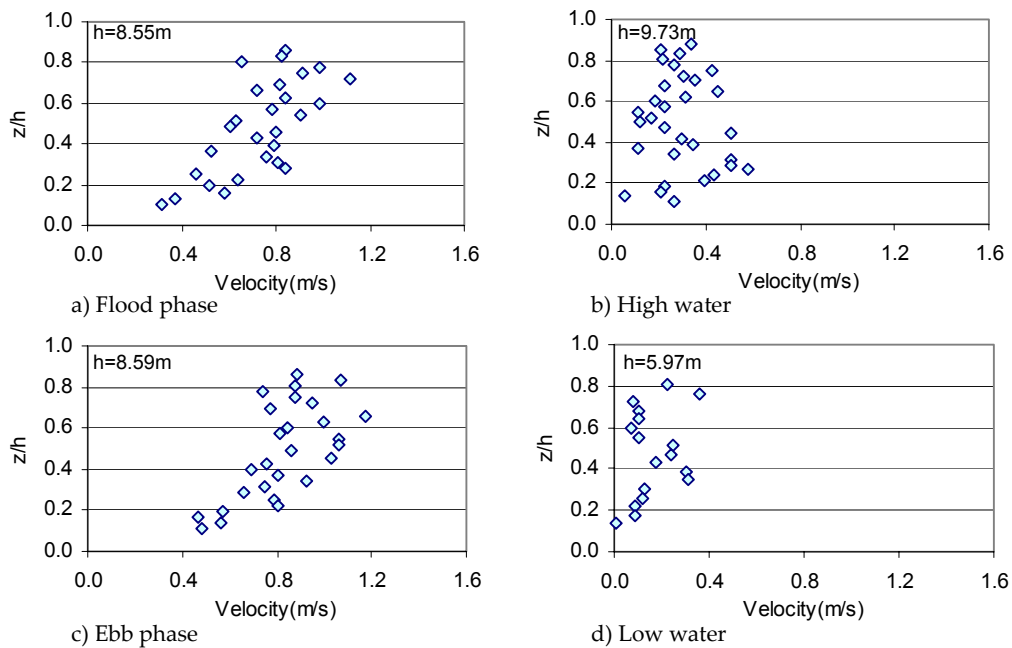


Figure 3.12: Research vessel “Suedfall”



**Figure 3.13: Water level and depth integrated velocities in the Piep channel.
ADCP measurements with 25cm bin resolution**

Figure 3.14 shows typical recorded current velocity profiles over the vertical for different tidal conditions. It can be seen that the velocity profiles are not well defined. Similar profiles are observed throughout the entire period.



**Figure 3.14: Typical current velocity profiles in the Piep channel.
ADCP measurements with 25cm bin resolution**

3.4.3 Acoustic profiling with 5cm bin resolution

Measurements were carried out using ADCP with 5cm bin size. The location of measurements is the Piep tidal channel (Point 3 in Figure 3.7). The bed at the measuring location is characterized by the presence of sandy sediments (Figures 3.2 and 3.3).

The measurements covered a neap tidal cycle on June 28, 2001. The device was attached to the NEBOSS (Near Bed Observation and Sampling System) bottom platform designed at the Research and Technology Center West Coast [Abegg et al., 2001]. The measurements focused on velocities near bed layer up to 1.4m from the bottom of channel. Nine data sets covering periods of 1 to 7 minutes were collected every hour (Figure 3.15). Some typical velocity profiles obtained for smaller velocities are plotted in Figure 3.16. Well defined profiles of velocities can be observed.

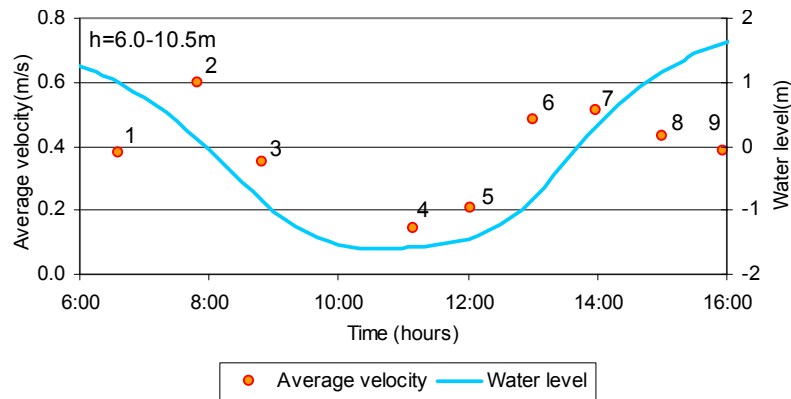


Figure 3.15: Average current velocities in the Piep channel.

ADCP measurements with 5cm bin resolution

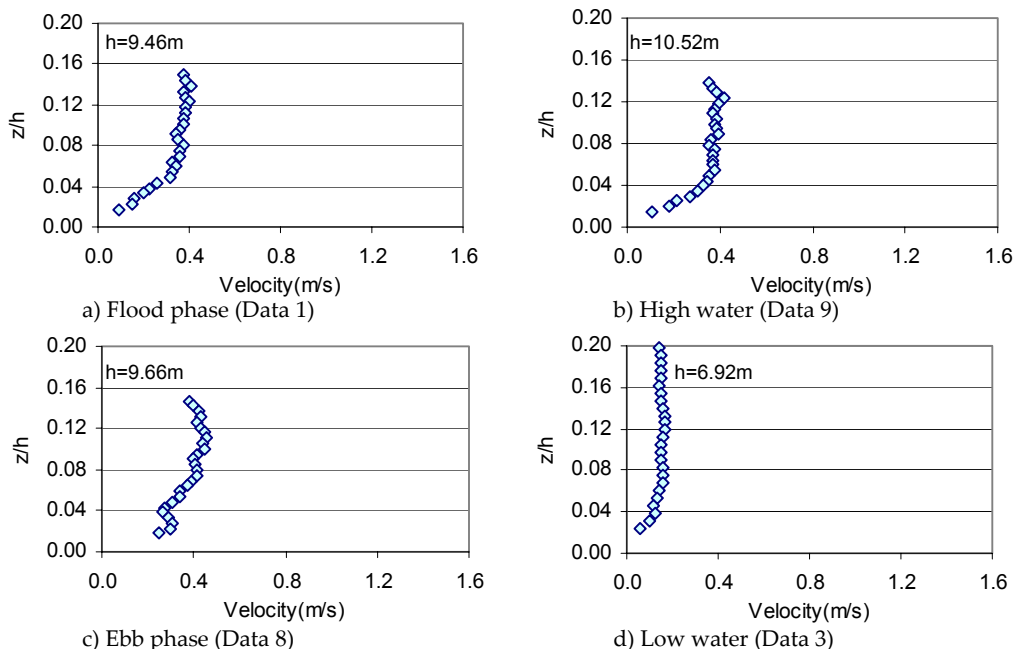


Figure 3.16: Typical current velocity profiles in the Piep channel.

ADCP measurements with 5cm bin resolution

3.5 Simultaneous measurements of bedforms and current velocities

To relate bedform dimensions to equivalent roughness sizes, simultaneous measurements were carried out. An echo sounder and an ADCP were employed simultaneously at the same location to record respectively bedforms and current velocity profiles. The location of measurements is the inner Piep tidal channel (Point 5 in Figure 3.7).

3.5.1 Echo sounder

Bedform dimensions were measured in the inner part of Piep channel in the Central Dithmarschen Bight (Point 5 in Figure 3.7). The measurements were from 09:00 to 18:30 hours on April 17, 2003. Due to tide the water depths ranged between 2.8m and 6.5m. Figure 3.17 shows the bottom profile at the location of the measurements. The bottom slope of the transect is about 0.003 from West to East.

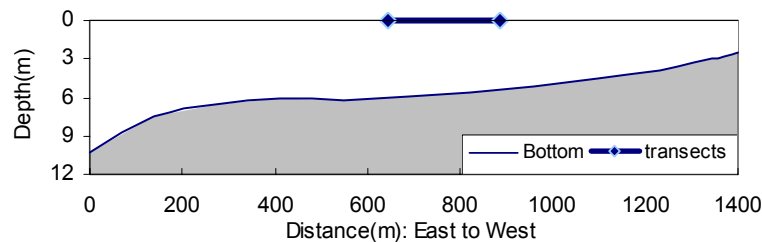


Figure 3.17: Bottom profile at which echo sounder measurement was performed.

See Figure 3.7 for the location of the cross section.

The measurements we carried out from the research vessel “Seston” (Figure 3.18.a). A 200kHz echo sounder (Lowrance Electronics) was used to acquire the profiles of bedforms. This frequency is suitable for shallow water because of low noise susceptibility. The geographic coordinates of the measuring location were recorded. The position during the transects is used to determine the length of bedforms.



Figure 3.18: Vessel employed for measurements of bedform dimensions

Forty transects were recorded along the North and South of the location at which ADCP measurement were carried out. The length of each transect is about 200m. Each data set may consist of 216 to 1441 soundings. The horizontal accuracy of the echo sounder profile depends on the speed of vessel. Measurements taken from fast moving vessel in conjunction with low resolution of data may lead to inaccuracies in the bedform lengths. Only profiles with resolution below 0.30m per sound were considered (Figure 3.19). The bedforms obtained from the echo sounder measurements can be seen in Figures 4.5 and 4.6 respectively for the North and South transects. Despite the fact that the transects do not follow exactly the same path, they have been considered in estimating bedform dimensions for the location in question (see Section 4.3.3).

3.5.2 Acoustic profiling with 15cm bin resolution

Stationary ADCP measurements were conducted from a rubber boat as shown in Figure 3.20.a. The device was attached to the back of the rubber boat (Figure 3.20.b).

The deployment configuration was based on the recommendations provided by RD Instruments [2002] and adapted for field conditions (Table 3.1). The maximum number of depth cells (bins) was set to 60 to obtain valid results in high sub-ping rate. The bin size was set to 15cm to cover flow depths up to 6.5m. Fifteen sub-pings with time intervals of 0.04 seconds were gathered per velocity profile

The profiling mode 12 was the main ADCP configuration adopted in the measuring campaign. It provides an improvement in comparison to modes 1. Previously, the ADCP sends, receives and processes a ping to measure flow velocity. With mode 12, the ADCP does not process the pulses until it collects several sub-pings into measured velocity. The major improvement of mode 12 is its ability to transmit and receive sub-pings in high frequency rate up to 20 Hz. According to RD Instruments [2003b], the advantages of water mode 12 among others are:

1. high resolution measurement can be performed from bin sizes of 1cm,
2. ability to record high flow velocities which could not be handled by previous high resolution modes,

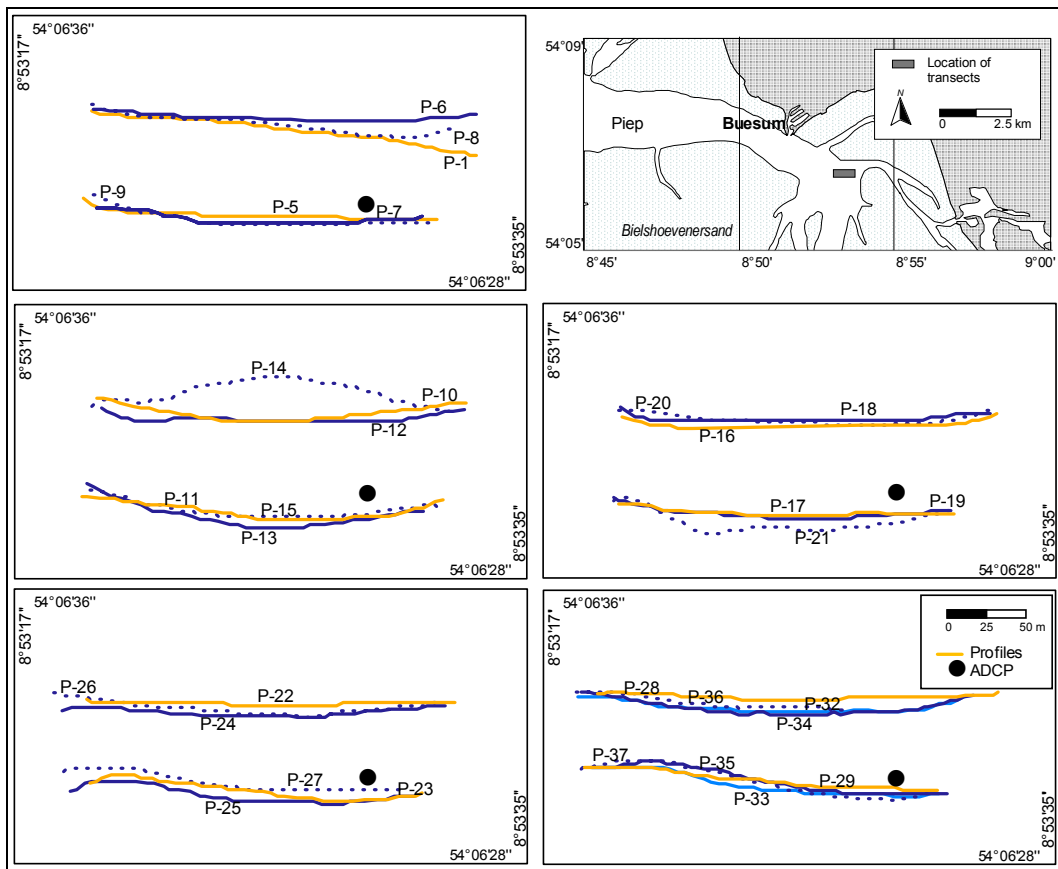


Figure 3.19: Plan view of vessel paths of echo sounder measurements selected for calculation of bedform dimensions



a) Rubber boat



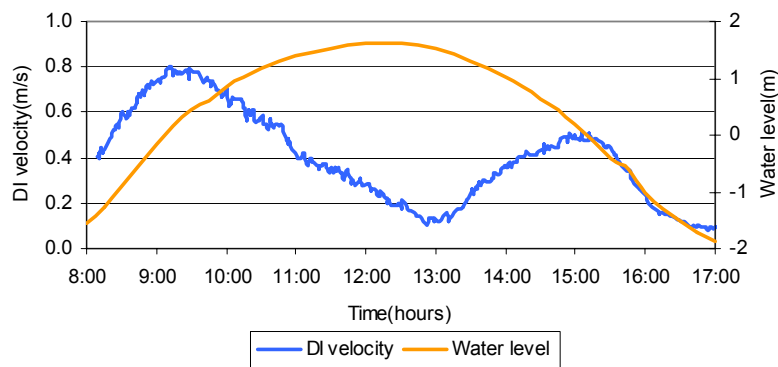
b) ADCP attached to the rubber boat

Figure 3.20: ADCP measurements with 15cm bin resolution from a stationary rubber boat

3. improvement of temporal resolution due to high rate of ping frequency. This advantage is of particular importance for turbulence studies,
4. low energy consumption due to the fact that the orientation data are processed less frequently. As a result, the measuring period can be extended significantly.

On the other hand, this mode is not suitable for flow conditions with inconsistent flow direction or when the device orientation changes over a short time. The reason is that the orientation is only recorded once at the beginning of sub-ping transmission. Therefore, changes in the orientation during transmission of sub-pings cannot be detected.

Current velocity profiles covering a tidal cycle were collected during this measuring campaign (Figure 3.21). The peak velocities in the flood and ebb phases are respectively equal to 0.81m/s and 0.52m/s. Figure 3.22 shows typical velocity profiles for different tidal conditions. In general, the resulted velocity profiles were not well defined.



**Figure 3.21: Water level and depth integrated velocity in the inner Piep channel.
ADCP measurements with 15cm bin resolution**

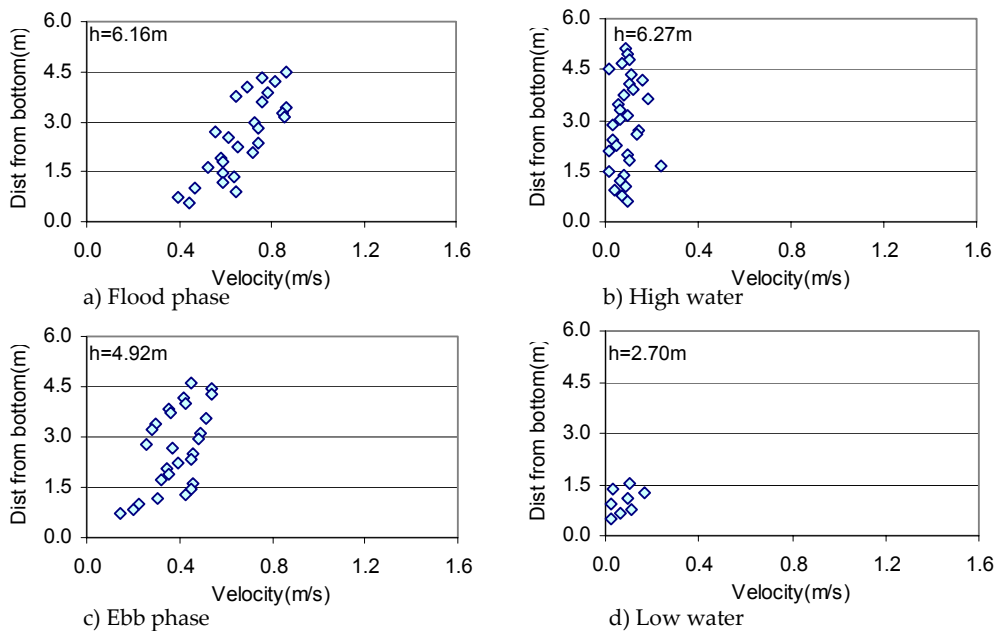


**Figure 3.22: Typical current velocity profiles in the inner Piep channel.
ADCP measurements with 15cm bin resolution**

3.6 Discussion

In this chapter, the field conditions and measurements of bedforms and current velocity profiles in the study site were discussed. The study area was described in terms of meteorology, geology, morphology and hydrodynamic conditions. Measurements of bedforms and current velocities were carried out using acoustic devices.

Current velocity profiles were measured with an acoustic profiler (ADCP) considering various configurations. Relatively well-defined profiles were recorded by ADCP. The moored ADCP with 50cm bin size averages high number of pings in an ensemble. The measurement with 25 and 5cm were carried out in low number ensemble or single ping mode. Averaging more pings should lead to better results. Less consistent current profiles were obtained by ADCP with a bin size of 15cm and 25cm. The resulting standard deviations obtained in the measurements with 5cm and 50cm bin size are respectively 0.35cm/s and 1.56cm/s, while those for 15cm and 25cm are respectively 6.45cm/s and 6.43cm/s. Lower standard deviations resulted from measurements taken from moored devices. The less well-defined records of velocities could be due to two reasons. Devices mounted on vessels are in general subjected to the tilting of ships (pitch, roll and heading) due to ship movement, waves and currents. This is in contrast to the moored ones which are fixed at a bottom platform. In addition, the less accurate current profile measurements can be also due to the bottom tracking configuration which is needed in case of vessel mounted devices.

Some methods for proper measurements of bedforms and current velocities are suggested. Figure 3.23 shows a sketch of the proposed procedure for field measurements of bedform dimensions in conjunction with current velocities and bed shear stresses.

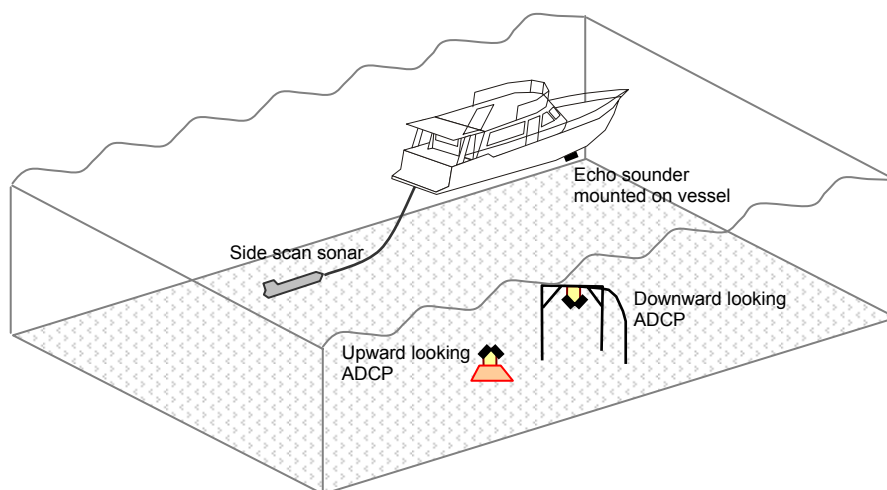


Figure 3.23: Proposed measurement set-up for obtaining bedforms and current velocities

Bedforms are scanned by echo sounder and side scan sonar from the vessel, while current velocities are recorded by two acoustic profilers moored to a bottom platform. The proposed procedure for field measurements in the investigation area can be summarized as follows:

1. Measurements of bedforms and current velocities should be carried out simultaneously. This enables to relate current velocities and bed shear stresses with the formation and development of bedforms for different tidal conditions. Besides, the flow conditions can be employed to study the classification of bedforms and to develop equations estimating bedform dimensions and equivalent roughness sizes.
2. Measurements of bedforms should provide reliable information on height, length and orientation of bedforms. Bedform heights and lengths can be obtained respectively using echo sounder profilers and side scan sonar images. The orientation of bedforms with respect to the vessel track is necessary for the accurate determination of bedform lengths. The bedform orientation can be deduced from images of side scan sonar. For more comprehensive measurement of bedforms, vessel mounted echo sounder and vessel towed side scan sonar should be employed (Figure 3.23). The scanning of the bottom by the vessel should be carried at regular time intervals defined in accordance to the changes in the bedform dimensions.
3. Regarding the measurement of current velocities, three recommendations are made:
 - a. Two acoustic profilers should be moored to fixed bottom platforms. From previous experiences, well-defined velocity profiles were recorded from devices attached to a fixed platform. The devices should be configured to record current profiles over a short period of time (less than 5 seconds). To cover an entire tidal cycle, the measurements should be repeated at regular time intervals, e.g. 5 to 10 minutes. During the data processing, about 20 to 50 ensembles covering about 1 to 4 minutes of current velocity measurements can be averaged to obtain the best fit line of velocities in the bottom boundary layer.
 - b. The downward looking acoustic profiler is set to measure the velocity in the bottom boundary layer. A high vertical resolution, e.g. 5cm, should be configured to record many velocity bins in the logarithmic layer. This enables a properly fitted profile of the near bottom velocities to be obtained.
 - c. The upward looking ADCP is installed on the bottom platform. A vertical resolution between 10cm and 20cm depending on the flow depths should be considered. The aim is to record current velocities up to the surface, so that depth integrated velocities and information outside the boundary layer can be obtained.

Chapter 4

Bedform dimensions

4.1 Introduction

In this chapter, the observed bedform types and dimensions are analyzed. Images of side scan sonar and profiles of echo sounder are used to gather information on the types and dimensions of bedforms in the study area. A detailed analysis of bedforms is done using echo sounder profiles. The development of bedforms during a tidal cycle is studied to see the effects of tidal flow on the bedforms. The observed bedform types are compared to those predicted by existing bedform classifications. Empirical equations available to estimate bedform dimensions from flow conditions and sediment properties are also verified for the conditions in the study area.

4.2 Bedform lengths throughout the tidal channels

Side scan sonar images have been acquired in tidal channels of the study area (Figure 3.5). The distribution of bedforms on the basis of these measurements is shown in Figure 4.1 [Mayerle et al., 2002]. The bedforms are observed in few sections in Piep channel and several sections in the Norderpiep and Suederpiep channels. Megaripples with lengths up to 20m are mostly found in tidal channels. Average bedform lengths from 8m to 10m was observed along Norderpiep and Suederpiep channels. In the intersection between Suederpiep channel and Bielshoevener Loch, sand dunes with lengths up to 22m were recorded.

Figure 4.2 shows four images of bedforms in tidal channels. The time during the tidal cycle at which measurements were taken is indicated in Figure 4.1. The image files are viewed and extracted using the Isis software [Triton Elics International, 1999]. To obtain bedform lengths, the images are rectilinearly rendered so that the image scale is equal for along-track and across-track directions. The along-track di-

rection is based on correction of vessel speed and across-track direction is based on correction of slant range. In Figure 4.2, the ranges of bedform lengths are 3m to 6.3m in the Norderpiep, 5m to 7m in the Suederpiep and 6.7m to 9.7m in the Piep channel.

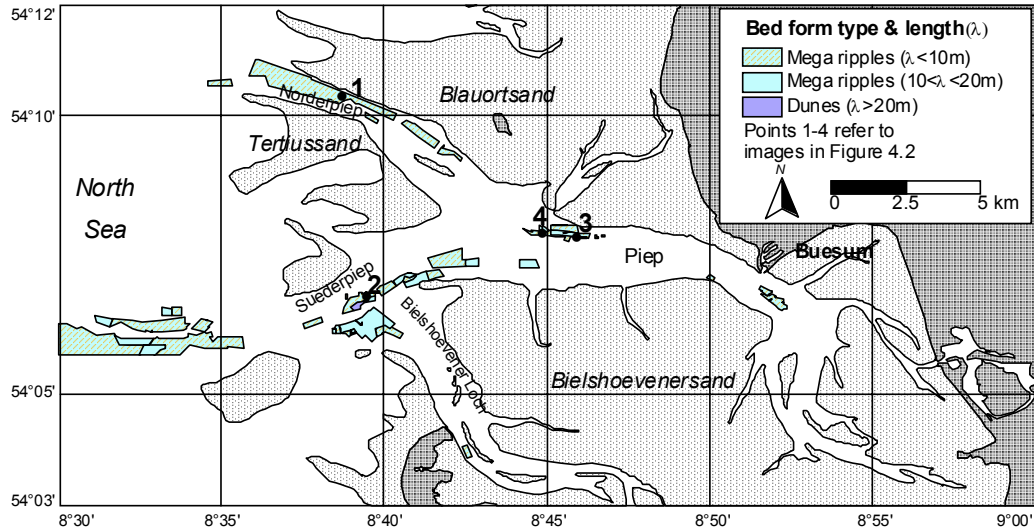


Figure 4.1: Distribution of bedforms in tidal channels after Mayerle et al. [2002]

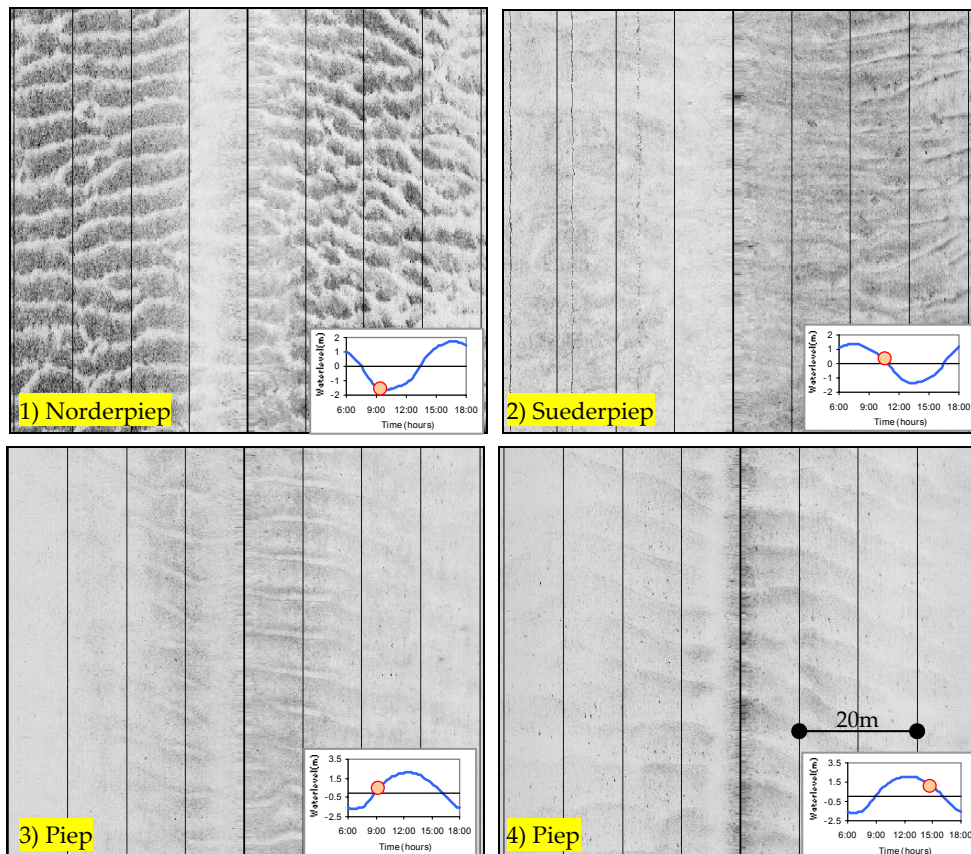
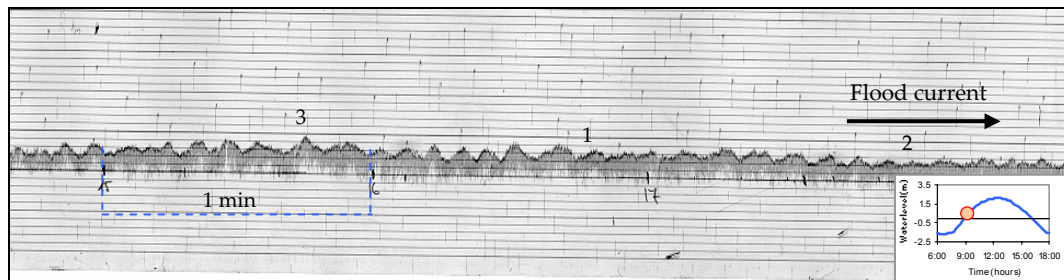


Figure 4.2: Side scan sonar images showing the bedforms in tidal channels

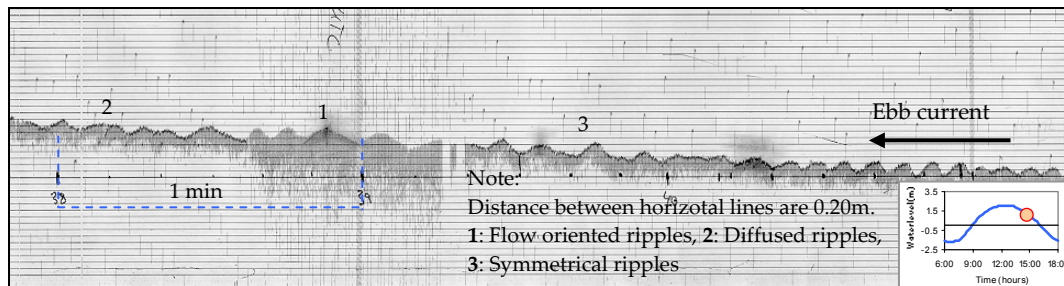
4.3 Bedform dimensions at defined locations

4.3.1 Piep channel

Profiles of echo sounder were used to obtain the height of bedforms in the Piep channel (Figure 3.5). The results were plotted on echo sounder register which consists of horizontal lines indicating 20cm interval. The echo sounder profiles obtained during flood and ebb phases are shown in Figure 4.3. Flow oriented megaripples as well as diffused and symmetrical megaripples were recorded. Bedform heights up to 0.40m were measured during flood and ebb phases. The results showed that differences in flow velocities and tidal phases do not affect significantly the height of bedforms. The length of megaripples could not be determined due to the lack of horizontal positioning.



a) Flood phase



b) Ebb phase

Figure 4.3: Typical profiles of echo sounder showing the bedforms in the Piep channel after Razakafoniaina [2001]

4.3.2 Norderpiep and Suederpiep channels

The echo sounder was used to obtain the bedforms in the Norderpiep and Suederpiep channels in 2004. The locations at which the bed profiles were taken are near the locations at which stationary ADCPs with resolution of 50cm were deployed in the year 2000 (Figure 3.5).

The measured bedforms are not typical sandy bed features such as ripples and/or dunes. According to Ricklefs [2004], the sediment characteristics in both locations are mainly fine grain sediments with some mud content. Figure 4.4 shows relatively flat beds recorded in the Norderpiep and Suederpiep channels. The undulating bedforms up to about 0.20m are outcropping bed layers which were formed by erosions of sediment layers. The bed is considered relatively flat because the spacing between the undulations is very sparse, i.e. up to 14.2m and 17.2m in the Norderpiep and Suederpiep channels respectively.

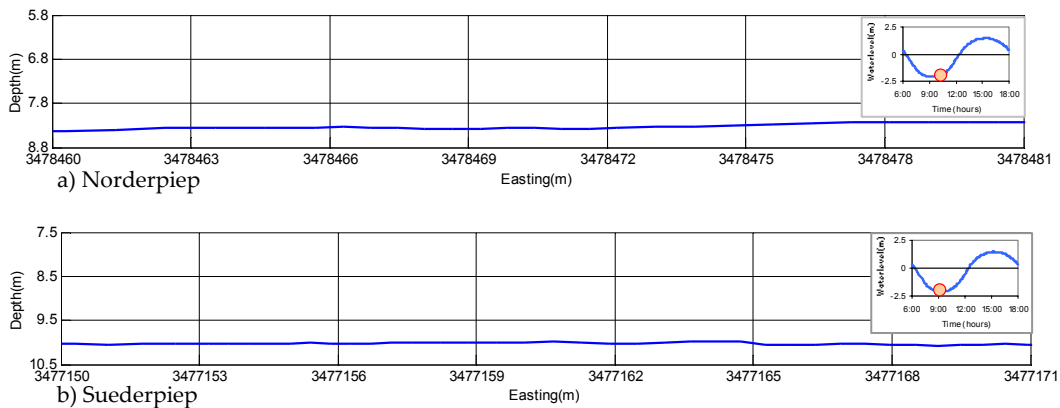


Figure 4.4: Typical bed profiles taken with echo sounder in the Norderpiep and Suederpiep channels

4.3.3 Inner Piep channel

An echo sounder was used to record the bedform dimensions in the inner Piep tidal channel (Figure 3.5). The profiles of bedforms covering a distance of about 200m are shown in Figures 4.5 and 4.6 respectively for the North and South transects. Tracks of each transect are shown in Figure 3.19. It should be pointed out that bed profiles in Figures 4.5 and 4.6 are plotted with an increased vertical scale. A plot of the bedforms without distortions is shown in Figure 4.7.

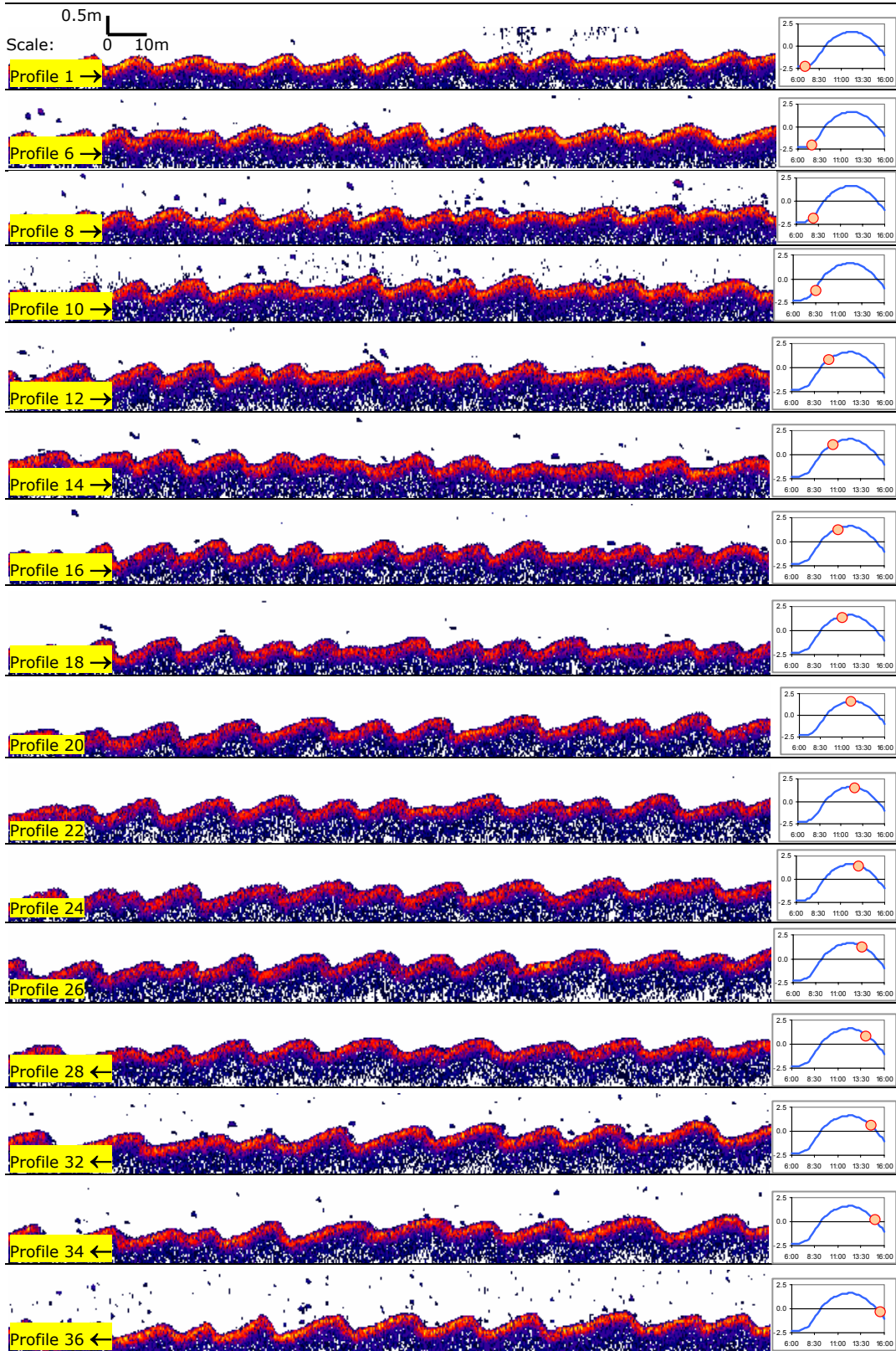


Figure 4.5: Echo sounder profiles in the North transect of the inner Piep channel

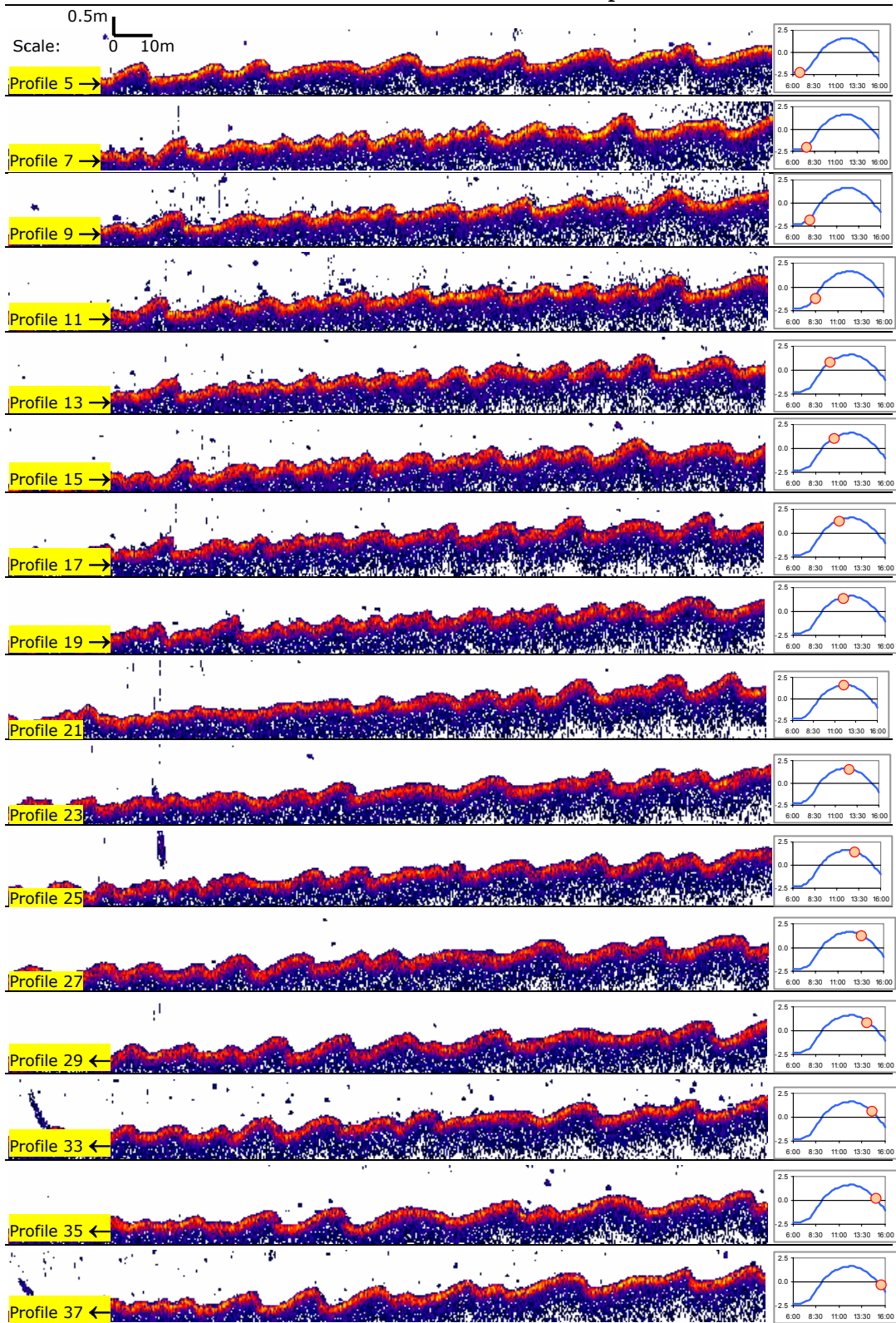


Figure 4.6: Echo sounder profiles in the South transect of the inner Piep channel

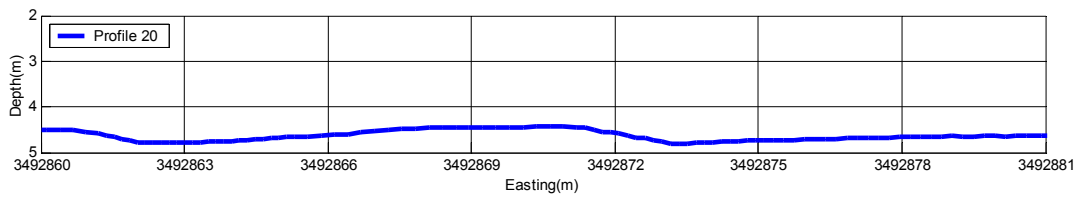


Figure 4.7: Bed profile 20 plotted using same horizontal and vertical scales

The arrows in Figures 4.5 and 4.6 indicate the flow direction and tidal phase. Right arrows stand for flood currents flowing to the East, while left arrows for ebb currents flowing to the West. The bedforms during high water are shown between profiles 20 and 27. It should be pointed out that since the vessel tracks were not always straight (see Figure 3.19), the lengths of bedforms could be slightly distorted.

Figures 4.8 and 4.9 show plots of the bedforms in three dimensions during flood and ebb phases obtained respectively at the North and South transects. The three dimensional plots have the advantage of showing the profiles and their horizontal orientations. In the figures, profiles which were not acquired at the same vessel track are shown. Some bedforms which are approximately perpendicular to the flow direction can be seen.

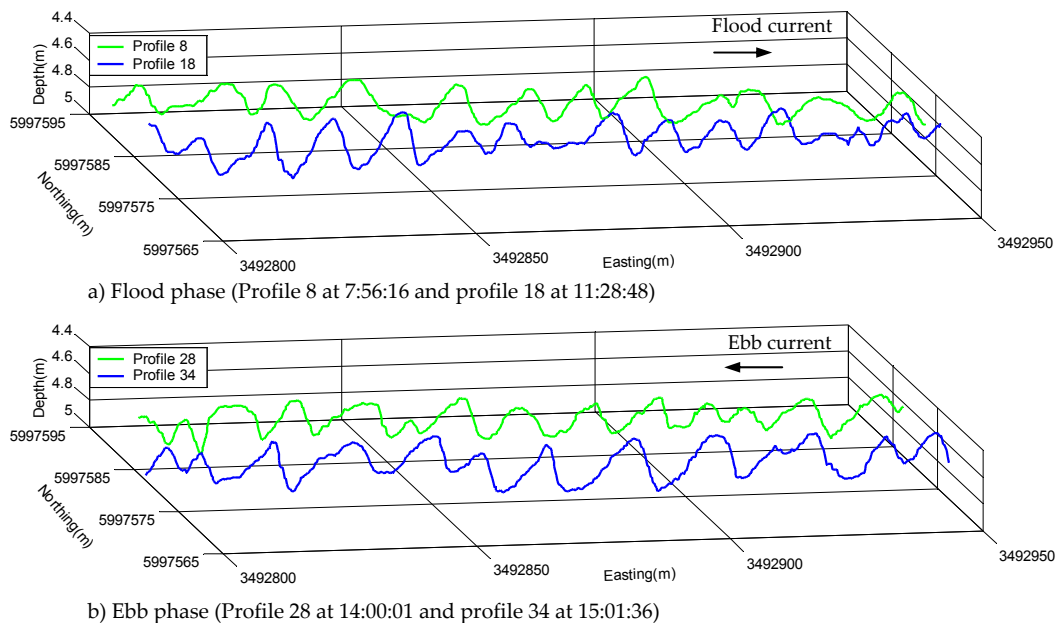


Figure 4.8: Three dimensional view of bedforms in the North transect

The dimensions of bedforms are estimated using Matlab software. The heights of bedforms are defined by the vertical difference between crests and troughs while the lengths by the horizontal distance between two troughs [Reineck & Singh, 1980]. For

the estimation of bedform lengths, the orientation of bedform crest to the vessel track was considered. The orientation of bedforms was obtained by plotting two profiles. Figure 4.10 shows two profiles about 4m apart measured during high water along the North transect. The profiles with bedforms perpendicular to the vessel track are plotted at the same horizontal coordinates (Easting). Bedforms indicated as A, B and E in Figure 4.10 are approximately perpendicular to the vessel track since their corresponding peaks are located at the same horizontal coordinates. In such circumstances, the bedform lengths are measured as the horizontal distance between two troughs.

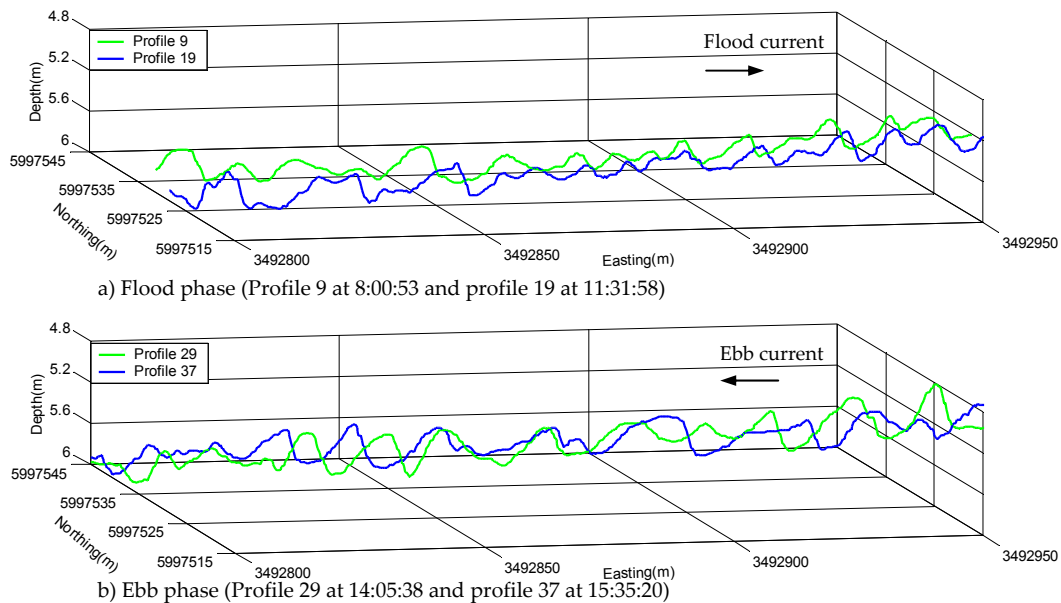


Figure 4.9: Three dimensional view of bedforms in the South transect

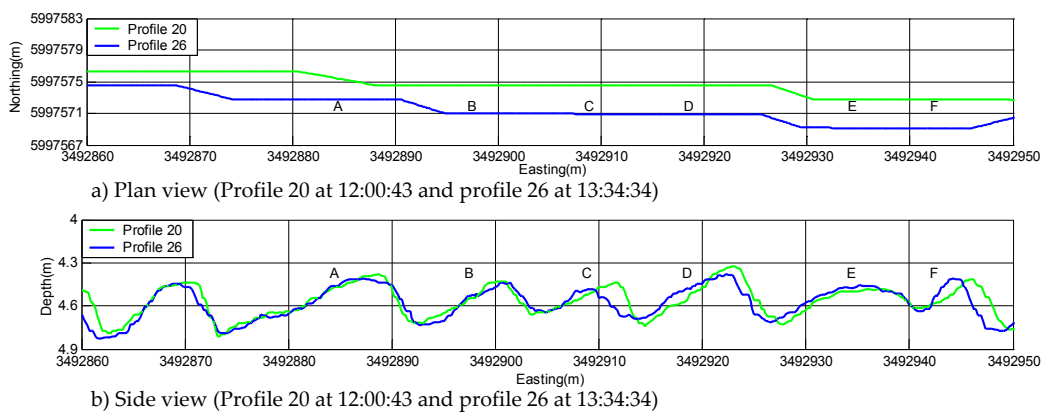


Figure 4.10: Determination of bedform orientation from the bed profiles

However, the crests of bedforms C, D and F are not aligned at the same horizontal coordinates (Easting). Figure 4.11 shows the approach adopted to estimate the length

of bedforms which are not perpendicular to the vessel track. The upper and lower figures show respectively a perspective view and a plan view of the two transects. Instead of the distance between two troughs along the vessel track (T1-T2 or T3-T4), the bedform lengths are defined as the distance between a trough and the point perpendicularly projected to another trough (T1-T1').

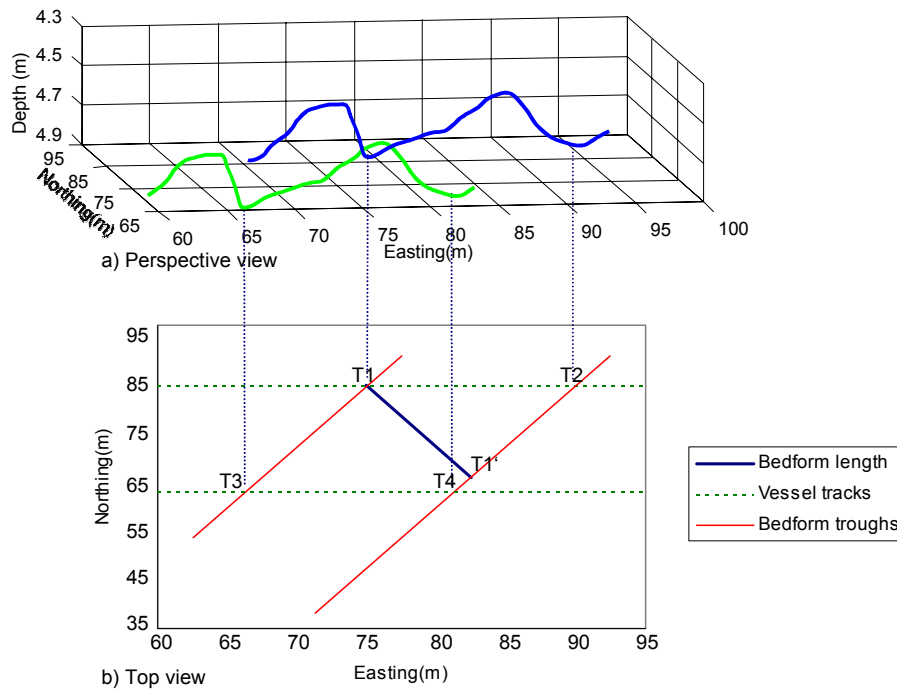


Figure 4.11: Approach considered in the estimation of bedform lengths for non perpendicular vessel tracks

4.4 Development of bedform dimensions

The development of bedforms is studied on the basis of echo sounder profiles obtained in the inner Piep channel. Table 4.1 lists the dimensions of bedforms in terms of ranges, mean values and standard deviations of bedform heights and lengths. The measured profiles are shown in Figures 4.5 and 4.6. The measuring location is indicated in Figure 3.5. The bedform heights range between 0.10m and 0.50m with the average for each profile ranging from 0.22m to 0.36m. The bedform lengths are from 3.8m to 19.2m with the average of 6.7m to 12.7m. The maximum standard deviations of bedform height and length are respectively 0.11m and 4.20m.

Table 4.1: Bedform heights and lengths at the inner Piep channel

Pro file	Tran sect	Time (UTC)	Tidal Phase	Depth (h)	DI vel (m/s)	Bedform height (m)			Bedform length (m)		
						Range	Mean	St dev	Range	Mean	St dev
1	North	06:48:21	Flood	2.48	NA	0.14-0.32	0.25	0.06	8.04-15.15	10.45	2.56
5	South	06:53:06	Flood	2.50	NA	0.24-0.41	0.32	0.05	5.99-12.46	9.18	2.78
6	North	07:34:38	Flood	2.81	NA	0.16-0.36	0.25	0.06	6.96-12.85	10.15	2.45
7	South	07:37:55	Flood	2.83	NA	0.16-0.42	0.33	0.11	6.05-11.53	8.39	2.29
8	North	07:56:16	Flood	3.18	NA	0.16-0.31	0.24	0.05	8.08-17.24	10.78	3.09
9	South	08:00:53	Flood	3.21	NA	0.16-0.38	0.27	0.09	6.13-12.74	7.99	2.76
10	North	08:29:24	Flood	3.60	0.61	0.17-0.35	0.26	0.06	8.66-12.96	10.34	1.92
11	South	08:34:06	Flood	3.73	0.56	0.14-0.39	0.30	0.10	4.73-11.74	7.44	3.05
12	North	09:58:26	Flood	5.53	0.66	0.10-0.39	0.27	0.08	6.53-13.70	10.48	2.52
13	South	10:03:14	Flood	5.56	0.66	0.10-0.37	0.25	0.09	5.01-12.69	8.15	3.41
14	North	10:27:20	Flood	5.81	0.60	0.19-0.36	0.28	0.05	8.36-13.40	11.24	1.88
15	South	10:31:31	Flood	5.89	0.57	0.15-0.40	0.27	0.10	3.78-9.72	6.76	2.51
16	North	11:02:03	Flood	6.07	0.51	0.10-0.36	0.27	0.09	7.77-14.73	10.75	2.30
17	South	11:05:37	Flood	6.09	0.49	0.19-0.40	0.29	0.08	5.62-12.33	7.43	3.27
18	North	11:28:48	Flood	6.23	0.46	0.19-0.40	0.28	0.08	4.77-12.73	9.75	3.21
19	South	11:31:58	Flood	6.26	0.41	0.13-0.37	0.26	0.09	5.15-12.09	7.87	3.05
20	North	12:00:43	HW	6.38	NA	0.21-0.41	0.32	0.06	4.93-17.91	10.36	3.51
21	South	12:04:08	HW	6.38	NA	0.16-0.44	0.31	0.11	6.80-17.00	11.28	3.70
22	North	12:29:44	HW	6.39	NA	0.20-0.45	0.31	0.08	7.76-16.46	10.85	2.64
23	South	12:33:22	HW	6.38	NA	0.13-0.33	0.24	0.07	6.50-16.27	9.91	3.73
24	North	12:59:30	HW	6.28	NA	0.24-0.41	0.34	0.07	5.96-16.12	12.65	3.26
25	South	13:03:00	HW	6.27	NA	0.16-0.38	0.27	0.07	8.66-14.54	11.06	2.33
26	North	13:34:34	HW	6.07	NA	0.17-0.38	0.30	0.07	6.21-19.14	12.08	3.78
27	South	13:38:34	HW	6.05	NA	0.14-0.36	0.26	0.08	6.69-12.74	10.60	2.44
28	North	14:00:01	Ebb	5.86	0.41	0.10-0.30	0.22	0.06	5.73-12.60	9.59	2.40
29	South	14:05:38	Ebb	5.82	0.39	0.25-0.50	0.36	0.09	6.18-15.64	10.38	3.02
32	North	14:31:28	Ebb	5.53	0.44	0.17-0.40	0.31	0.09	6.03-12.57	9.62	2.47
33	South	14:35:27	Ebb	5.49	0.45	0.14-0.41	0.30	0.09	6.53-11.85	8.59	2.12
34	North	15:01:36	Ebb	5.05	0.52	0.18-0.40	0.30	0.08	5.77-19.22	10.64	4.20
35	South	15:05:52	Ebb	5.00	0.48	0.16-0.44	0.31	0.09	6.80-14.82	10.19	3.00
36	North	15:31:28	Ebb	4.43	0.45	0.22-0.42	0.33	0.07	6.87-18.56	10.96	3.59
37	South	15:35:20	Ebb	3.37	0.43	0.11-0.41	0.30	0.08	8.17-12.11	10.05	1.63

Note:

1. NA means not available. DI velocities are not available because the ADCP was not ready at the beginning of echo sounder measurements and the depth integrated values could not be calculated during high water.
2. HW means high water.

Figure 4.12 shows the development of bedform dimensions over the measuring period. The mean and standard deviation of heights and lengths of bedforms are shown. The results show that bedforms are present throughout the entire tidal cycle. The bedform heights remain approximately constant over the entire tidal cycle. The

mean bedform heights vary from 0.22m to 0.36m. Averages of bedform lengths are from 6.76m to 11.24m in the flood phase and 8.59m to 12.65m in the ebb phase.

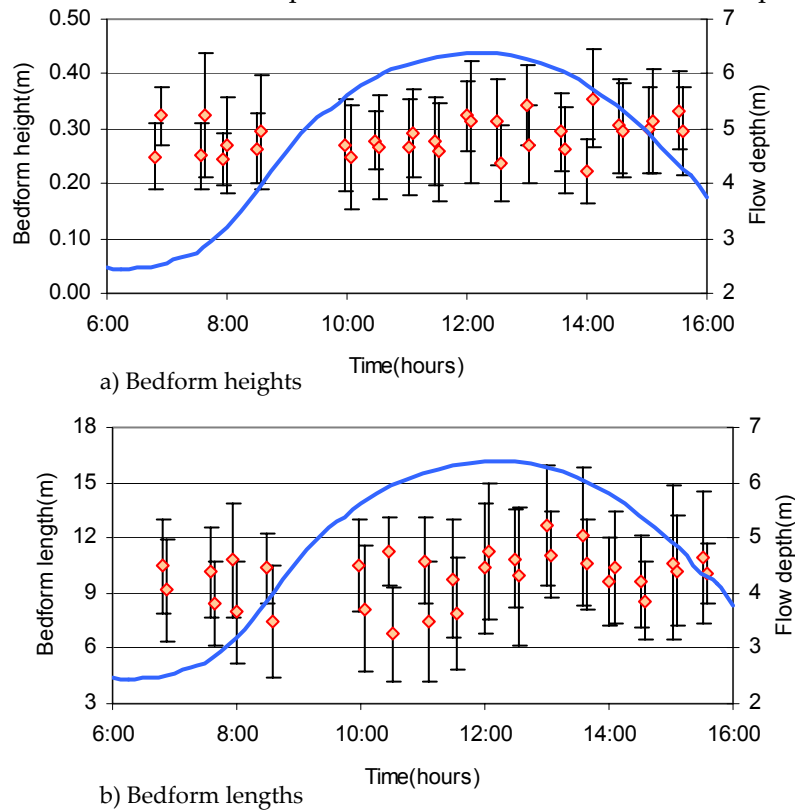


Figure 4.12: Bedform dimensions over a tidal cycle at the inner Piep channel

Bedforms acquired from echo sounder profiles are categorized as megaripples and dunes. This is based on two reasons. Firstly, megaripples and dunes are characterized by having asymmetrical bedforms with a rather steep lee side and a gentle stoss side. These shapes can mostly be seen in echo sounder profiles (Figures 4.5 and 4.6). Secondly, the ratios of bedform lengths to flow depths are in the range between megaripples and dunes. Measured bedform lengths (Table 4.1) range from 0.77 to 6.13 times the flow depth. According to Van Rijn [1993], the megaripples can be as long as the water depth, while the length of dunes are about 3 to 15 times the flow depth.

To analyze the development of bedforms during the measuring period, the echo sounder profiles obtained along the same vessel track are plotted. Figure 4.13 shows the profiles taken in the North transect during the flood phase, high water level and ebb phase. The profiles in the South transect are not used because their tracks do not overlap. It can be seen that the bedforms migrate in the direction of the current. Advances up to about 4m during flood phase can be seen at bedforms indicated as 2 and 5 in Figure 4.13. The bedform movement is identified by the sediment erosion at the

stoss side and deposition at the lee side. Moreover, the deepening of troughs can be observed at bedforms in Figure 4.13 (see bedforms 3 and 5). The scouring of troughs occurs probably due to the reverse flow which tends to erode the trough [Reineck & Singh, 1980].

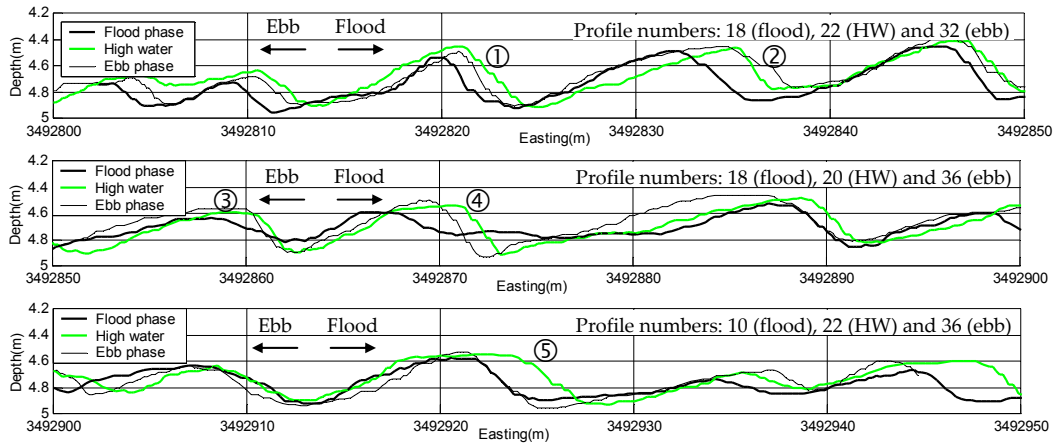


Figure 4.13: Migration of bedforms during a tidal cycle in inner Piep channel

During the measurement period covering between high water level and ebb phase, the bedforms moved in the direction of the ebb current. The sediments are eroded at the lee side and deposited at the stoss side. The crests of bedforms during ebb phase are slightly higher than those observed during the flood phase. This may be related to the maximum flow magnitudes of about 0.8m/s and 0.5m/s respectively during flood and ebb phases. Higher current velocities observed during the flood phase may flatten the peaks of bedforms so that lower bedforms are formed. Relatively low velocities during ebb phase may let the sediments to settle at the bedform crests. Slightly longer bedforms during ebb phase (see bedforms 1, 2 and 4 in Figure 4.13) are found due to sediments deposited at the lee side which cannot be eroded by low velocity magnitude of ebb current.

In general, the bedforms are present during the entire tidal cycle. Bedforms migration following the flow direction is to the East during the flood phase and to the West during the ebb phase. The gentle slope is mostly found at the West side of bedforms and the steep slope is at the East side of bedforms during both tidal phases. This may be due to stronger currents observed in the flood phase. The weaker current in the ebb phase is not able to change the shape of bedforms substantially.

4.5 Comparison with existing bedform classifications

As mentioned in section 4.4, mainly megaripples and dunes were found in the study area. The adequacy of existing bedform classifications to predict the bedform types in

tidal channels is dealt herein. The classifications proposed by Liu [1957], Simons & Richardson [1966], Athaullah [1968], Bogardi [1974] and Van Rijn [1993] were verified. These have been developed mainly on the basis of flume experiments and river measurements. In this section, field conditions during the bedform observation in the inner Piep channel are plotted in the existing classification systems. A median grain size of 0.103mm obtained from samples taken by Vela-Diez [2001] close to the measuring location was considered. The collected samples in the inner Piep channel cannot be used because they were taken from sediments above the bed. The velocity data from ADCP with bin size of 15cm are used for the calculation of the flow properties.

Data sets from eighteen profiles were selected for verifying the bedform classifications. Only the data which have transport stage parameters greater than zero were used (see Table 4.2). Figure 4.14 shows the measured data in conjunction with the five classification systems. It should be noticed that most classifications use a single term of ripples, while Van Rijn [1993] distinguishes between miniripples and megaripples.

Table 4.2: Selected profiles for verification of bedform classifications

Profile	Time	Tidal phase	Depth (m)	DI velocity (m/s)	u_* (m/s)	T	Δ (m)	λ (m)
10	8:29:24	Flood	3.60	0.61	0.03	1.94	0.26	10.34
11	8:34:06	Flood	3.73	0.56	0.04	1.50	0.30	7.44
12	9:58:26	Flood	5.53	0.66	0.05	2.21	0.27	10.48
13	10:03:14	Flood	5.56	0.66	0.06	2.23	0.25	8.15
14	10:27:20	Flood	5.81	0.60	0.06	1.62	0.28	11.24
15	10:31:31	Flood	5.89	0.57	0.06	1.39	0.27	6.76
16	11:02:03	Flood	6.07	0.51	0.05	0.93	0.27	10.75
17	11:05:37	Flood	6.09	0.49	0.05	0.73	0.29	7.43
18	11:28:48	Flood	6.23	0.46	0.03	0.56	0.28	9.75
19	11:31:58	Flood	6.26	0.41	0.04	0.25	0.26	7.87
28	14:00:01	Ebb	5.86	0.41	0.03	0.24	0.22	9.59
29	14:05:38	Ebb	5.82	0.39	0.04	0.14	0.36	10.38
32	14:31:28	Ebb	5.53	0.44	0.04	0.47	0.31	9.62
33	14:35:27	Ebb	5.49	0.45	0.05	0.51	0.30	8.59
34	15:01:36	Ebb	5.05	0.52	0.03	1.02	0.30	10.64
35	15:05:52	Ebb	5.00	0.48	0.04	0.74	0.31	10.19
36	15:31:28	Ebb	4.43	0.45	0.03	0.57	0.33	10.96
37	15:35:20	Ebb	4.37	0.43	0.04	0.44	0.30	10.05

By applying the bedform classification by Liu [1957] considering grain shear Reynolds number and the ratio of shear velocity to the particle fall velocity, ripples and

dunes are predicted in the study area (Figure 4.14.a). Only one datum with low shear stress is predicted as ripples.

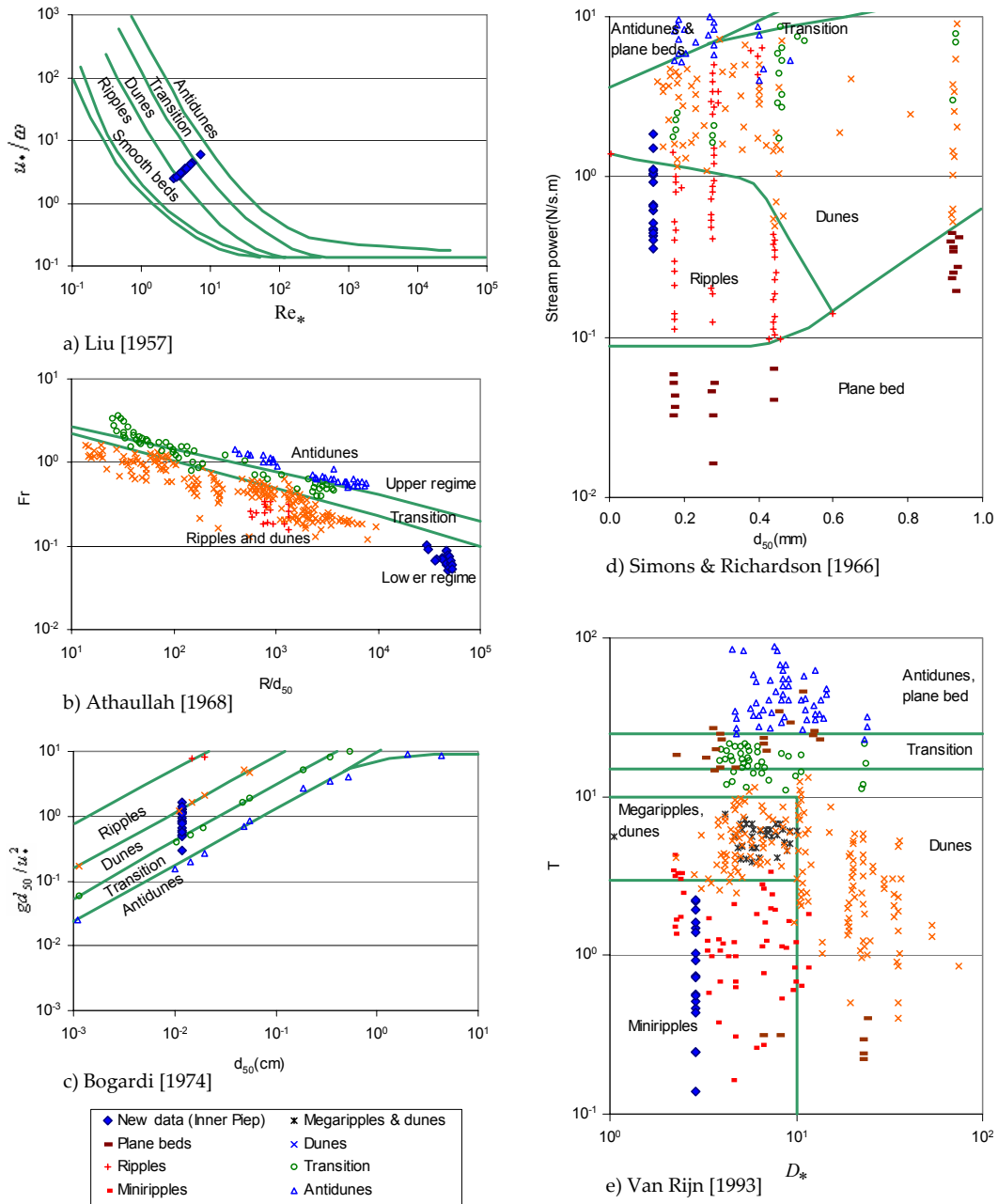


Figure 4.14: Bedform types on the basis of several classification schemes

According to the classification by Athallah [1968], the field data are plotted in the lower flow regime and at high values of R/d_{50} (Figure 4.14.b). The reason is that the data for the current study are measured in tidal channels which are characterized

by deep water depths and small grain sizes, while most of data used by Athaullah [1968] were obtained from flume experiments. According to this classification, ripples and dunes are predicted to be present in the inner Piep channel.

By using the classification by Bogardi [1974], the inner Piep data are plotted in the range of dimensionless parameter gd_{50}/u_*^2 between 0.52 and 1.67 (Figure 4.14.c). The plot suggests the presence of ripples and dunes in the study area. One datum having the lowest shear velocity is classified as ripples.

By considering median grain size and stream power, classification by Simons & Richardson [1966] predicts mainly the presence of ripples (Figure 4.14.d). Two data with the highest stream power are classified as dunes. The stream power for the inner Piep data ranges from 0.4N/s.m to 1.5N/s.m.

Van Rijn [1993] proposed that bedforms can be related to the particle parameter (D_*) and transport stage parameter (T). By using median grain size of 0.103mm, the particle parameter of 2.50 is obtained. The transport stage parameter values range from 1 to 2.23. The presence of miniripples is predicted for the conditions in the study area (Figure 4.14.e) with some data approaching megaripples and dunes. Low transport stage parameters measured in the tidal channels resulted in the prediction of miniripples.

The bedform classifications generally predict the presence of ripples and dunes in the inner Piep channel (Table 4.3). Miniripples are estimated by Van Rijn's approach [1993]. The approach by Van Rijn is recommended to be used for bedform classification since it was derived from more than 350 bedform data obtained from flumes, shallow and deep rivers. Several reviews have indicated the weakness of other classifications. According to Simons & Sentürk [1992], the classifications by Liu [1957] and Bogardi [1974] are not suitable to be used for field conditions since they are based mainly on laboratory experiments. Julien [1995] pointed out that the classification by Simons & Richardson [1966] was found appropriate only for estimation of bedforms in the shallow depths because it was derived from small scale rivers.

Table 4.3: Summary of the predicted and observed bedforms in the inner Piep channel

Classification	Predicted bedforms	Observed bedforms
Liu [1957]	Ripples and dunes	
Athaullah [1968]	Ripples and dunes	Megaripples
Bogardi [1974]	Ripples and dunes	and
Simons & Richardson [1966]	Ripples and dunes	dunes
Van Rijn [1993]	Miniripples, megaripples and dunes	

4.6 Comparison with empirical equations to estimate bedform dimensions

In this section, bedform dimensions and corresponding bed shear stresses measured in the inner Piep channel are compared with existing empirical equations for estimation of bedform heights and lengths. Since the observed bedforms are in the range between megaripples and dunes, the estimation of bedform dimensions is done hereafter for both bedforms.

4.6.1 Height of bedforms

Van Rijn [1993] proposed an expression relating bedform heights with the transport stage parameters, flow depths and median grain sizes. Equations 2.13 and 2.15 are used to estimate the height of bedforms in case of ripples and dunes respectively. The data with values of transport stage greater than zero were selected. Table 4.2 shows eighteen data sets with the transport stage parameters up to 2.23. The first ten data were recorded during flood phase, while the last eight data were obtained during ebb phase. The range of flow depths is between 3.60m and 6.26m. The depth integrated velocities are from 0.39m/s to 0.66m/s.

In Figure 4.15, the measured bedform length to water depth ratios against transport stage parameter are plotted in conjunction with the proposed approach after Van Rijn [1993]. It can be seen that the data obtained in the inner Piep fall in the region of lower transport stage parameters while those from irrigation channels [Mahmood et al., 1984] are in higher range of transport stage parameters. The relative bedform height values (Δ / h) of the Piep data are between 0.04 and 0.08. The plotted data are above the fit line by Van Rijn [1993]. The new fit line is proposed by deriving a line with minimum root mean squared error (RMSE).

The best fit line considering the data from irrigation channels and the ones measured in the present study resulted as follows:

$$\frac{\Delta_{mer}}{h} = 0.02(1.1 - e^{-0.17})(10 - T) \quad (4.1)$$

This equation is modified from Equation 2.13 by changing the coefficient in the first term in brackets to 1.1, instead of 1.0. To be noticed that the proposed equation covers also conditions with smaller transport stage parameters.

For the prediction of dune heights, Equation 2.15 by Van Rijn [2003] is considered. The measured results are composed with the proposed equation in Figure 4.16. The data are in a good agreement with the existing expression by Van Rijn [1993]. Hence, the equation by Van Rijn [1993] to estimate dune height is also applicable to the inner Piep data.

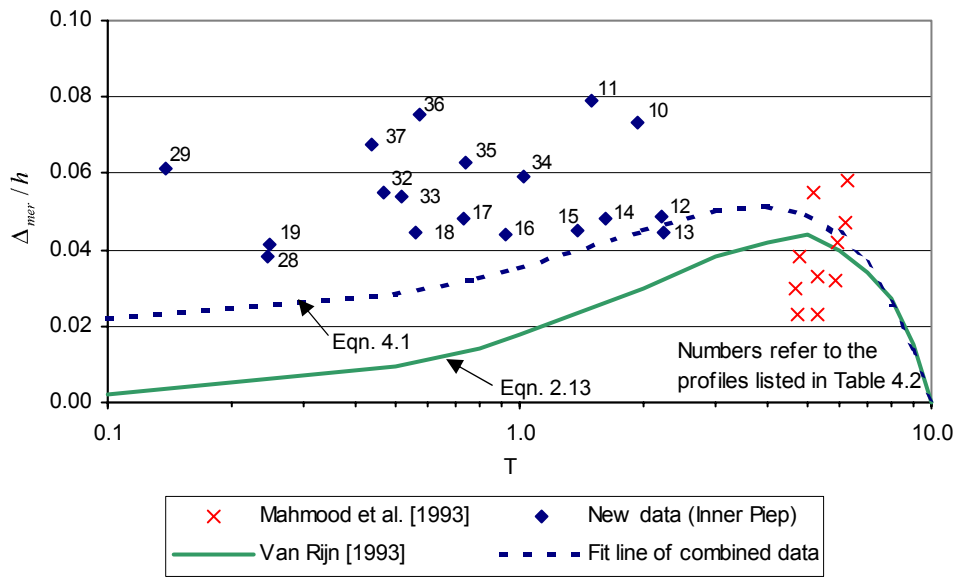


Figure 4.15: Comparison of the measurement data in the inner Piep channel with a proposed equation for heights of megaripples

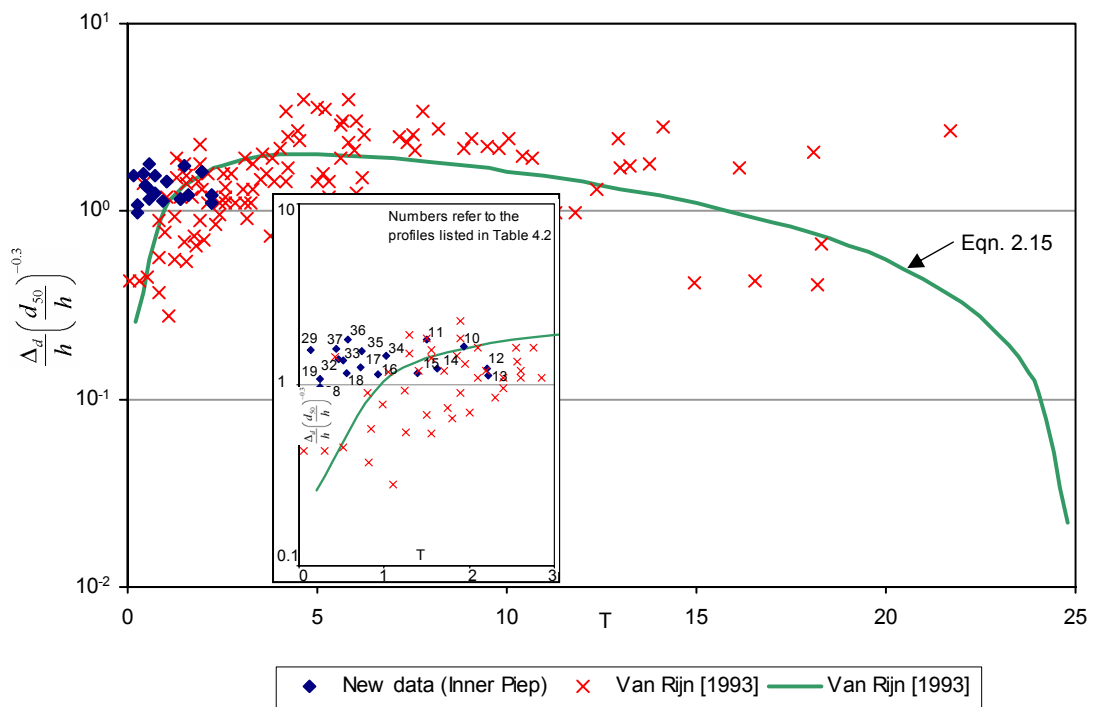


Figure 4.16: Comparison of the measurement data in the inner Piep channel with a proposed equation for heights of dunes

4.6.2 Length of bedforms

Several researchers have suggested that the length of bedforms can be related to the flow depth. Van Rijn [1993] found the lengths of megaripples to be about half of the flow depth and dunes in the order of 7.3 times the flow depth. Yalin [1972] stated that the length of dunes is about 6.3 times the flow depth. Considering the conditions in the study area with transport stage greater than zero, the length of bedforms resulted between 1.1 and 2.9 times the flow depth (Table 4.2). The average ratio of bedform lengths to flow depths (λ/h) is in the order of 1.9.

4.7 Discussion

In this chapter, the dimensions of bedforms obtained from measurements of side scan sonar and echo sounder were discussed. Side scan sonar images acquired in 1999 and 2000 show the presence of megaripples and dunes in several sections of the investigated tidal channels. In general, the lengths of these bedforms are between 10m and 22m. Profiles of echo sounder in the Piep channel show bedform heights up to 0.40m. Results of measurements carried during flood and ebb phases indicate that the bedform heights do not change significantly. Echo sounder was also used to obtain the bedforms in the Norderpiep and Suederpiep channels at which ADCPs with 50cm bin resolution were deployed. Since these channel beds were dominated by fine grain sediments with mud contents, sandy bed features such as ripples and dunes were not observed. Instead, outcropping consolidated mud layers with the height up to 0.22m were recorded.

Bedforms acquired from echo sounder profiles in the inner Piep channel are also studied. The observed bedforms are categorized as megaripples and dunes. Typical characteristics of these bedforms such as asymmetrical shapes with a steep lee side and a gentle stoss side were observed. In addition, the ratios of bedform length to flow depth lie within those for megaripples and dunes.

The bedforms were present during the entire tidal cycle for which measurements were taken. The maximum bedform height and length are respectively 0.50m and 19.22m. The bedform dimensions did not change largely during observation, although slightly higher values of bedform dimensions were found during the ebb phase. Slightly higher values of bedform height and length during ebb phase are the results of erosion and deposition of bed sediments due to tidal current. Higher depth integrated velocity of about 0.8m/s was recorded during flood phase, while depth integrated velocity of about 0.5m/s was observed during ebb phase. Relatively higher bedform dimensions during the ebb phase are probably associated with the deposition of sediments at the crest of bedforms and the scouring at the troughs. Slower ebb

currents allow sediments to settle on the bedform crest while faster flood currents tend to flatten the bedform crest. Slightly longer bedforms during ebb phase are due to the deposition of sediments on the lee side.

The migration of bedforms due to tidal currents is also identified by the deposition and erosion of bed sediments. Between flood phase and high water, the bedforms advance along the direction of flood current by erosion at the stoss side and deposition at the lee side. Between high water and ebb phase, the bedform migrations along the ebb current were observed in a few locations. It was found that only small portions of lee side are eroded. The lower velocities during the ebb phase are not strong enough to transport the sediments on the lee side back to the stoss side.

The observed bedforms in the inner Piep channel were compared to several existing approaches proposed for classification of bedforms. These classifications consider sediment properties and flow conditions to estimate bedforms. Most classifications predict the presence of ripples and dunes in the study area. The classification by Van Rijn [1993] is recommended to be used in the study area because it was derived from many data with a wide range of conditions covering both flume and field conditions. Other classifications were derived mostly from flume experiments and measurements in shallow rivers.

The empirical equations to predict the bedform dimensions by Van Rijn [1993] have been considered for the conditions in the investigated area. For the estimation of bedform heights, the equations for megaripples and dunes are considered. The Van Rijn's equation for megaripple heights is modified to best fit conditions measured in the tidal channel. The results show also a good agreement with the equation proposed for the estimation of dune heights. The measured bedform lengths resulted about 1.9 times of the flow depth.

Chapter 5

Equivalent roughness sizes

5.1 Introduction

In this chapter, the estimation of equivalent roughness sizes in tidal channels of the Central Dithmarschen Bight is studied. Initially, the equivalent roughness sizes are estimated from the best fit line of measured velocities in the bottom boundary layer. Several significant factors to obtain valid velocity profiles are identified. Then, the equivalent roughness sizes are estimated on the basis of depth integrated velocities. Finally, the results obtained in this study are compared with existing empirical formulas relating equivalent roughness sizes and bedform dimensions. Modified empirical formulas for estimation of form roughness considering the results of this study are proposed.

5.2 Criteria for selection of valid velocity profiles

The equivalent roughness sizes are estimated from the best fit line of velocities in the bottom boundary layer. Approaches by Schlichting [1951] and Nikuradse [1933] (Equations 2.28 and 2.29) summarized in Chapter 2 are employed. Six criteria for selection of valid velocity profiles for estimating of equivalent roughness sizes were identified. These include: the number of velocity bins in the log law layer, correlation coefficient of the fit line to the logarithmic velocity profile, velocity magnitude, velocity direction, displacement height and average of ensembles.

5.2.1 Number of bins

When deriving a correlation coefficient of two variables, an important question is whether both variables are indeed correlated. Table 5.1 shows the probability of un-

correlated variables of n measurements and observed correlation coefficient r [Taylor, 1997]. The probability of uncorrelated relations should be less than 0.05 to ensure that the data are really correlated. Table 5.1 helps determining the acceptable correlation coefficient for certain number of bins. For example, if there are 10 data sets, the minimum correlation of 0.70 should be considered to obtain probability of uncorrelated variables of 0.02 (less than 0.05).

Table 5.1: Probability of uncorrelated variables after Taylor [1997]

n	r										
	0	0.10	0.20	0.30	0.40	0.50	0.60	0.70	0.80	0.90	1
3	1	0.94	0.87	0.81	0.74	0.67	0.59	0.51	0.41	0.29	0
4	1	0.90	0.80	0.70	0.60	0.50	0.40	0.30	0.20	0.10	0
5	1	0.87	0.75	0.62	0.50	0.39	0.28	0.19	0.10	0.04	0
6	1	0.85	0.70	0.56	0.43	0.31	0.21	0.12	0.06	0.01	0
7	1	0.83	0.67	0.51	0.37	0.25	0.15	0.08	0.03	<0.01	0
8	1	0.81	0.63	0.47	0.33	0.21	0.12	0.05	0.02	<0.01	0
9	1	0.80	0.61	0.43	0.29	0.17	0.09	0.04	0.01	<0.01	0
10	1	0.78	0.58	0.40	0.25	0.14	0.07	0.02	<0.01	<0.01	0

According to Wright [1995], the logarithmic layer exists between 10% and 20% of the boundary layer thickness. In shallow water, the boundary layer limit may reach the free surface [Brown et al., 1991]. In this study, the logarithmic layer is defined as 20% of the flow depth to get sufficient number of velocity data.

5.2.2 Correlation coefficient

By considering the lower 20% of the flow depth from the bottom, the minimum of five bins were taken. As a result, the minimum correlation coefficient r of 0.90 should be established (Table 5.1). In addition, high correlation limit is chosen to ensure that the velocity profile is of logarithmic pattern and to avoid high estimations of equivalent roughness sizes. As discussed in Chapter 2, a correlation coefficient limit of 0.90 has been previously employed in some studies to estimate equivalent roughness sizes from measurements in the bottom boundary layer by Carling [1981], Schauer [1987], Cacchione et al. [1995] and Cheng et al. [1999].

The plots of correlation coefficient and equivalent roughness sizes during neap and spring tides in the Norderpiep and Suederpiep channels can be seen in Figure 5.1. The equivalent roughness sizes are computed by using the lowest five velocity data from the bottom. Figure 5.1 shows that low correlation coefficient values are related to very high and unrealistic estimations of equivalent roughness sizes and vice-

versa. Lower equivalent roughness sizes resulted for correlation coefficients exceeding 0.90.

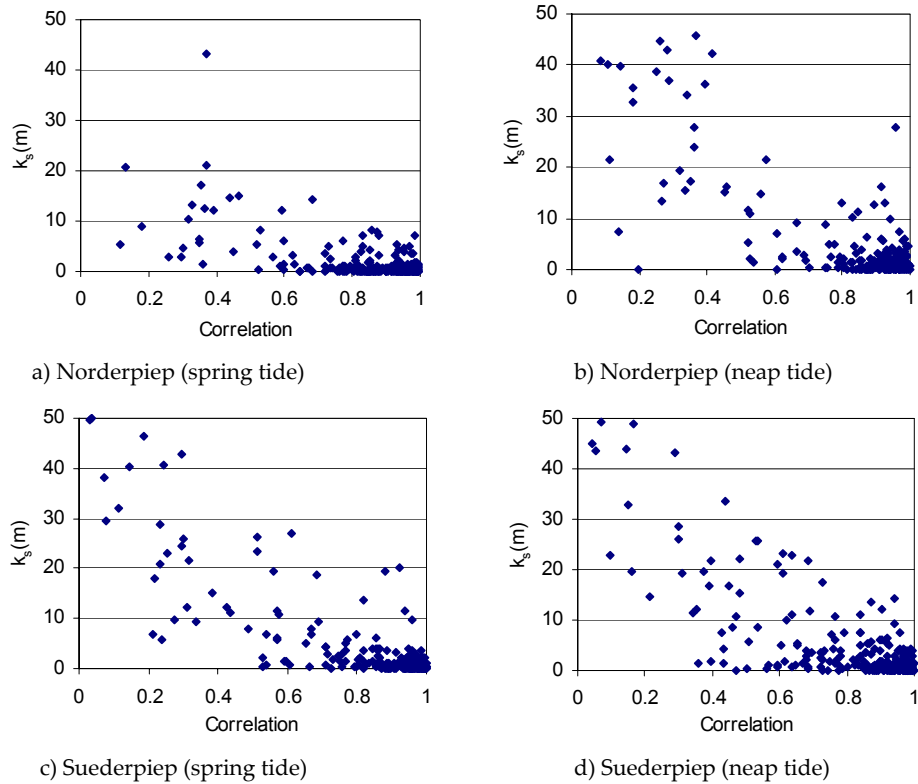


**Figure 5.1: Relation between correlation coefficient and equivalent roughness sizes.
ADCP measurements with 50cm bin resolution**

It should also be mentioned that quite low correlation coefficients resulted during high and low water when the flow velocities are small and the velocity profiles are undefined (Figure 5.2). About one hour before and after the velocity reaches its minimum value, the correlation coefficient decreases until zero. During maximum flood or ebb currents, much higher correlation coefficients (more than 0.90) are observed.

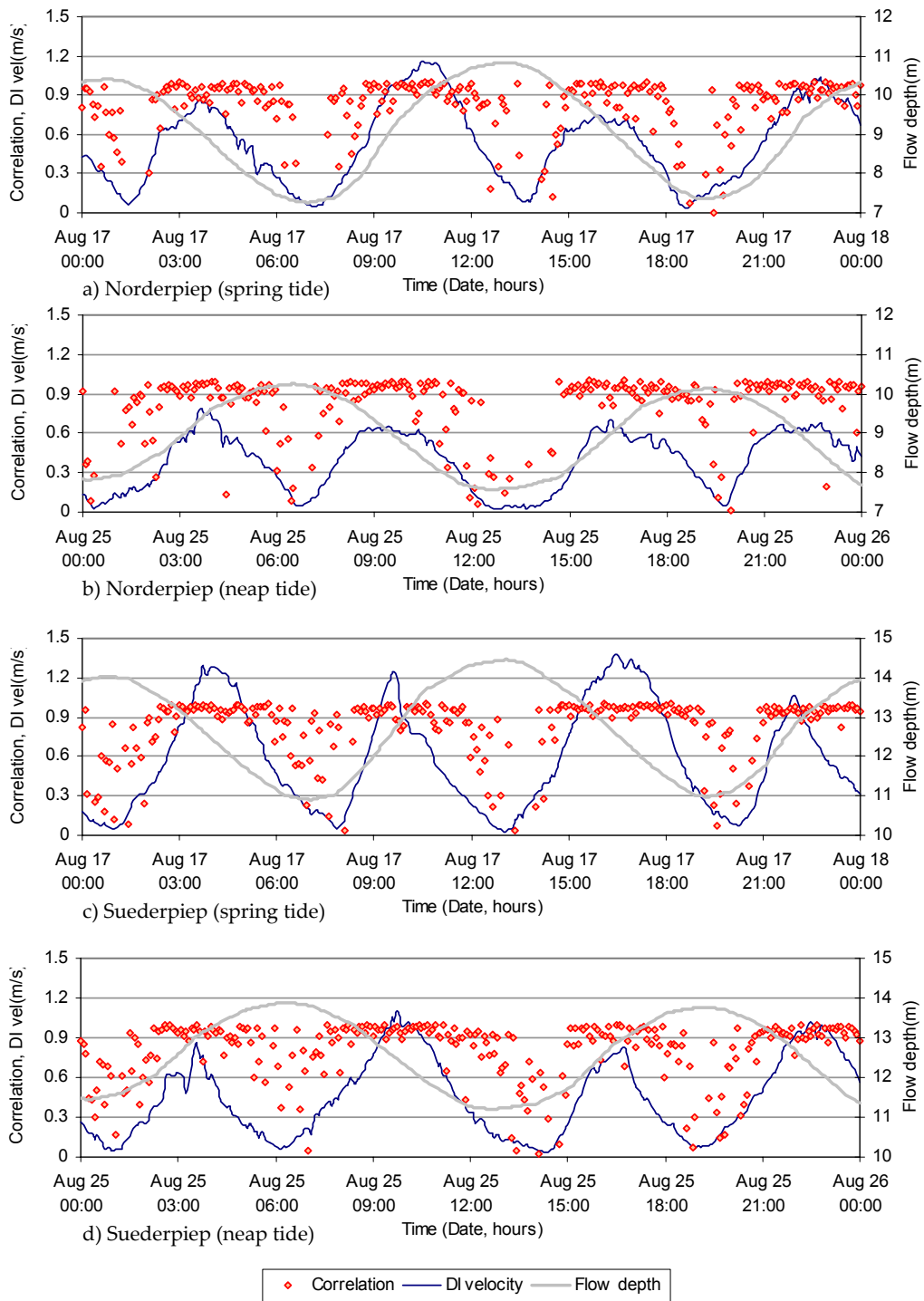


**Figure 5.2: Variation of correlation coefficients with velocity magnitudes.
ADCP measurements with 50cm bin resolution**

5.2.3 Velocity magnitude

The velocity magnitude is also identified as a parameter for selection of valid velocity profiles for estimation of equivalent roughness sizes. Figure 5.3 shows the relation between depth integrated velocity and correlation of best fit lines during neap and spring tides in the Norderpiep and Suederpiep tidal channels. The measurements were carried out with moored ADCPs with a 50cm bin resolution at the Norderpiep and Suederpiep channels (see Figure 3.7 for the location). Low correlation coefficients are related to low depth integrated velocities. However, high correlation coefficients of more than 0.90 are mostly found for velocities exceeding 0.30m/s. Hence, the depth integrated velocity of 0.30m/s is used as the minimum magnitude for selection of valid velocity profiles in this study. This ensures that the velocity profiles are well defined. In the study on the accuracy of acoustic profilers for field conditions in the Central Dithmarschen Bight [Jimenez-Gonzales et al., 2003], the data with minimum depth integrated velocity of 0.30m/s were also used.

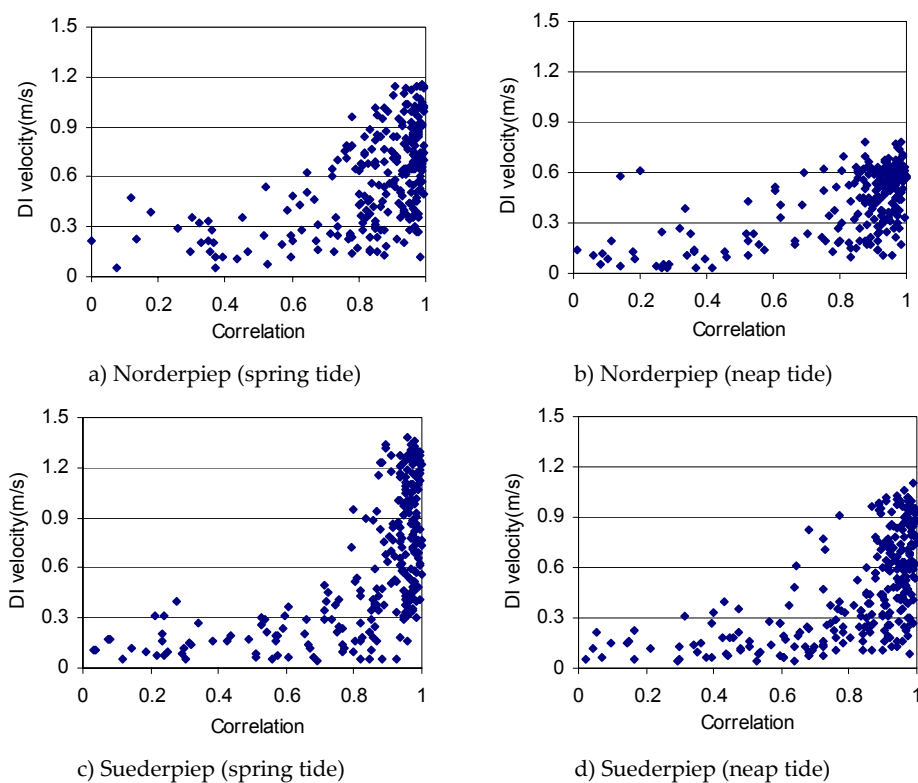


Figure 5.3: Relation between correlation coefficient and depth integrated velocity. ADCP measurements with 50cm bin resolution

5.2.4 Velocity direction

The best fit line of velocity profile assumes a uniform flow direction. In the tidal region, this assumption cannot be fulfilled especially during high and low water when the flow direction changes. One advantage of acoustic profiler is the ability to record also the flow direction. Figure 5.4 shows the velocity direction and magnitude over the vertical for two measured velocity profiles. It can be seen that both profiles show opposite flow direction between the top and bottom layers.

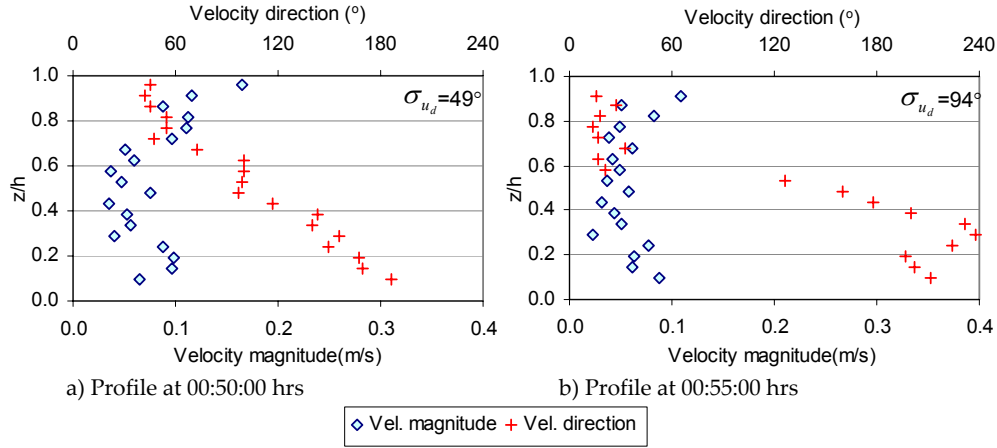


Figure 5.4: Measured velocity magnitude and direction on August 16, 2000. ADCP measurements with 50cm bin resolution

The standard deviation (σ_{u_d}) is used to measure the variability of velocity direction over the vertical in a profile. σ_{u_d} is defined as follows:

$$\sigma_{u_d} = \sqrt{\frac{\sum_{i=1}^n (u_{di} - \overline{u_d})^2}{n-1}} \quad (5.1)$$

where u_{di} is the velocity direction (degree), $\overline{u_d}$ is the average of velocity direction and n is the number of data points. Low standard deviation values mean that the flow direction is nearly uniform and high values refer to velocity profiles with non-uniform flow directions. High standard deviations of velocity direction of 49° and 94° resulted for the profiles in Figures 5.4.a and 5.4.b respectively.

The relation between standard deviation of velocity direction over the vertical and correlation coefficient of best fit line is shown in Figure 5.5. High correlation coefficients exceeding 0.90 are mostly associated with standard deviation of velocity direction lower than 10° . Hence, only those profiles with standard deviation of velocity direction over the vertical less than 10° were considered.

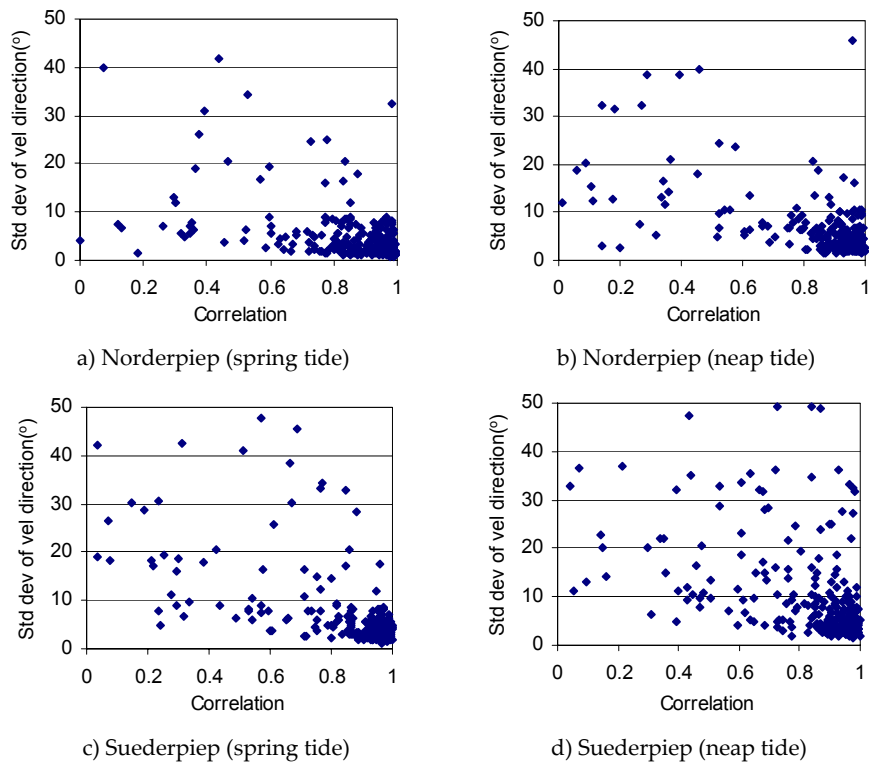
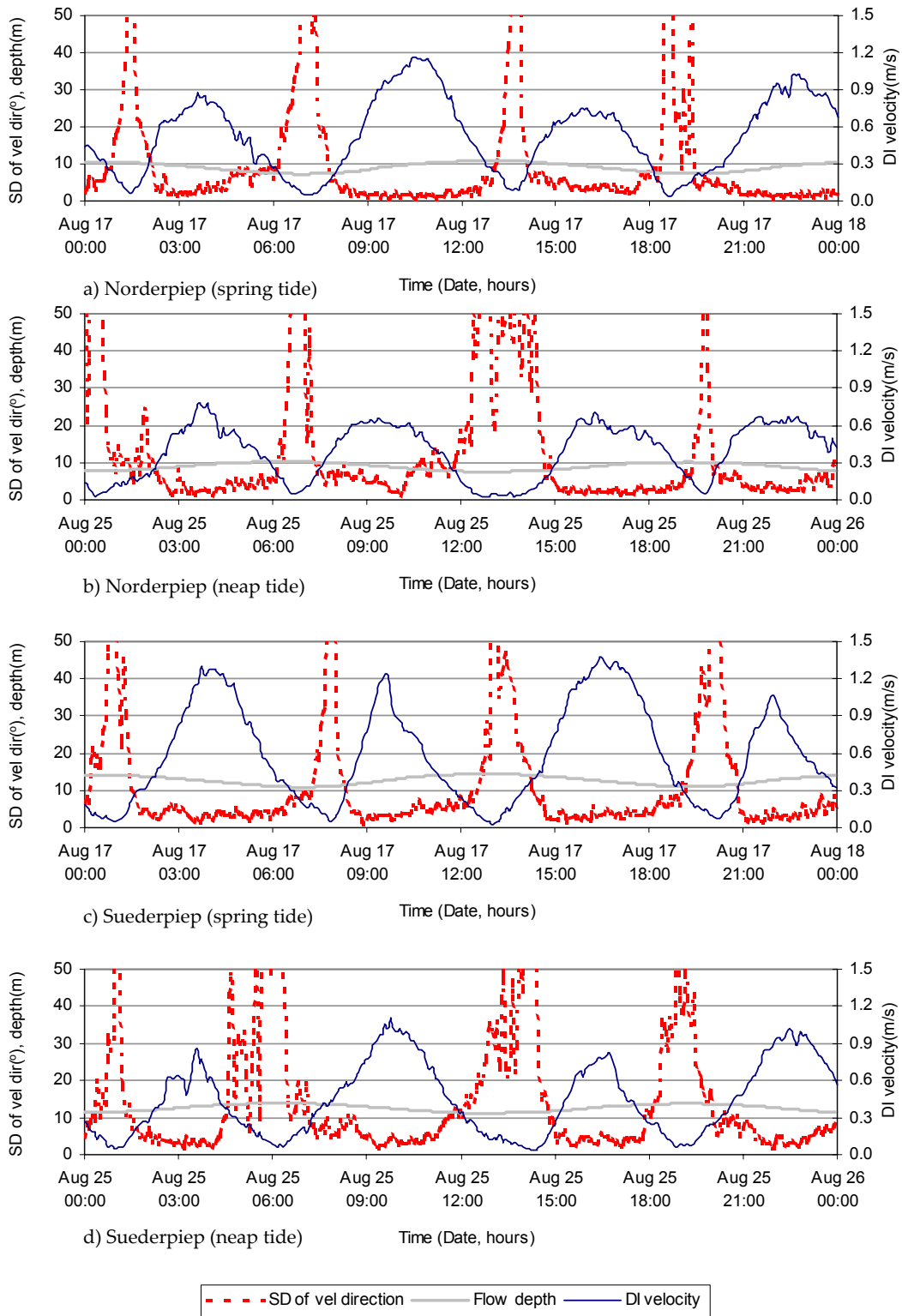


Figure 5.5: Relation between correlation coefficient and velocity direction. ADCP measurements with 50cm bin resolution

Figure 5.6 shows the development of standard deviation of velocity direction and velocity magnitude during several tidal cycles in Norderpiep and Suederpiep tidal channels. It is found that nearly uniform flow direction is related to high velocity magnitude values. However, for depth integrated velocities smaller than 0.30m/s, high standard deviations of velocity direction are observed. These occur during high and low water when the tidal phase changes.

5.2.5 Displacement height

The reference level of a velocity profile cannot be exactly defined due to the presence of bedforms. Jackson [1981] proposed a correction of the velocity profile by applying a displacement height. The proposed displacement height corresponds to the mean bed elevation when all bedforms are flattened. Displacement heights of about 70% of the roughness height, as observed by Jackson [1981] for different kinds of bed roughness, were employed.



**Figure 5.6: Variation of velocity direction with velocity magnitude.
ADCP measurements with 50cm bin resolution**

To account for the displacement height (δ), the logarithmic profile (Equation 2.28) is modified as follows:

$$\frac{u_z}{u_*} = \frac{1}{\kappa} \ln\left(\frac{z - \delta}{z_0}\right) \quad (5.2)$$

In this study, the displacement height was accounted for only to the current velocities obtained from measurements using acoustic profilers with bin size of 15cm in the inner Piep for which bedform dimensions during measurements are available.

5.2.6 Average of ensembles

The average of ensembles is carried out by taking the mean of velocity bins at the same height to create one velocity profile. This method has been employed to minimize errors due to random variations in current velocities in a tidal estuary [Wood et al., 1998]. It has also been applied with 10 minute intervals from tidal channel data collected by current meters [Heathershaw & Simpson, 1978 and Gross & Nowell, 1983] and acoustic devices [Cheng et al., 1999].

Figure 5.7 shows typical velocity profiles of single ensemble and average of ten (15 second intervals), forty (1 minute intervals) and fifty (1 minute and 15 second intervals) ensembles. The profiles were measured by the ADCP with bin resolution of 15cm. It can be seen that the profile obtained considering a single ensemble is not well defined. However, as more ensembles are averaged, the velocity distribution resembles a logarithmic one.

Figures 5.8 to 5.11 show the effect of averaging ensembles on the correlation coefficient and equivalent roughness sizes. The average of one to ten ensembles is applied to the measurements obtained on the basis of 5cm bin size data, while the average of one to fifty ensembles is applied to 15cm, 25cm and 50cm bin size data. Due to the limitation of acquired data, less ensembles can be averaged for 5cm bin size data. In all bin sizes, the correlation coefficient fluctuates as more ensembles are averaged. Relatively high correlation coefficients, close to one, resulted from the current velocity measurements using 50cm bin sizes in conjunction with the average of twenty or more ensembles.

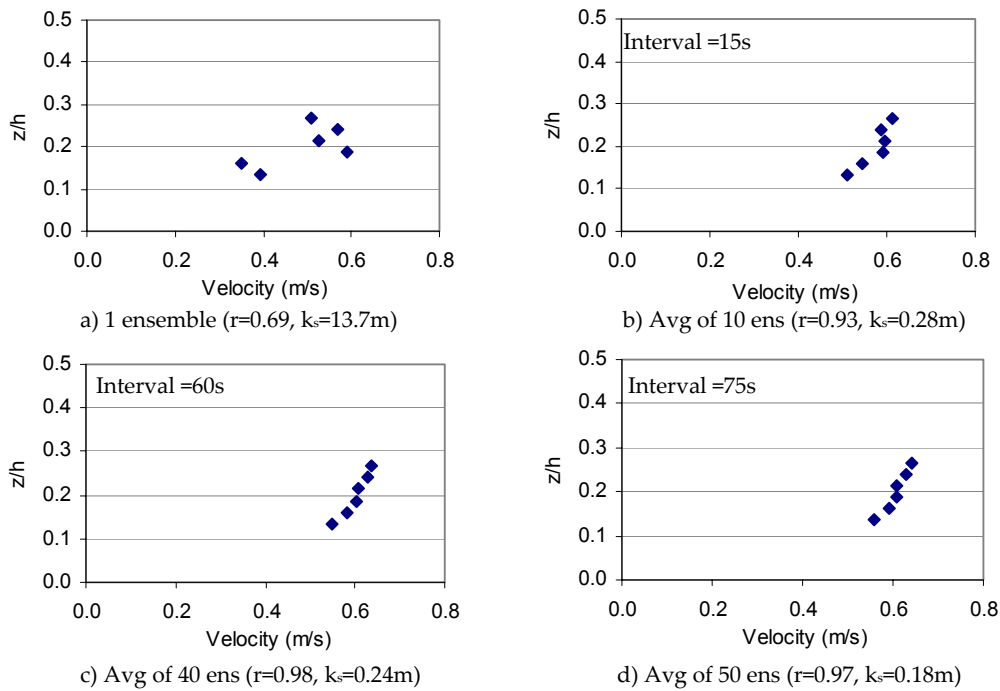


Figure 5.7: Resulting velocity profiles by considering different averaging of ensembles. ADCP measurements with 15cm bin resolution in the inner Piep channel

In general, an increase in the correlation coefficient and the bed roughness sizes tends to reach a constant value by considering more than 10 to 20 ensembles. The optimum number of ensembles to be considered is established by identifying the number of ensembles which lead to uniform estimation of equivalent roughness sizes. The number of ensembles for different bin sizes is determined as follows:

1. For the data with 5cm bin size, uniform equivalent roughness sizes are reached by considering approximately 8 to 10 ensembles. Figure 5.8 shows typical velocity profiles with 5cm bin size. Hence, the average of 10 ensembles covering a period of 36 seconds is chosen for the analysis.
2. Relatively uniform equivalent roughness sizes resulted by considering between 40 and 50 ensembles for 15cm bin size data. The typical velocity profiles are shown in Figure 5.9. As a result, 50 ensembles covering a period of 1 minute and 16 seconds are chosen for estimation of equivalent roughness sizes.
3. Some graphs of data with 25cm resolution show a decreasing trend of equivalent roughness sizes up to 50 ensembles. Figure 5.10 shows results of typical velocity profiles from measurements using 25cm resolution. Therefore, the ADCP data with 25cm bin size was excluded from the analysis. As mentioned earlier, the measurements were acquired from the acoustic profiler mounted on the vessel. The recorded profiles are less well-defined and have high standard deviation of velocities.

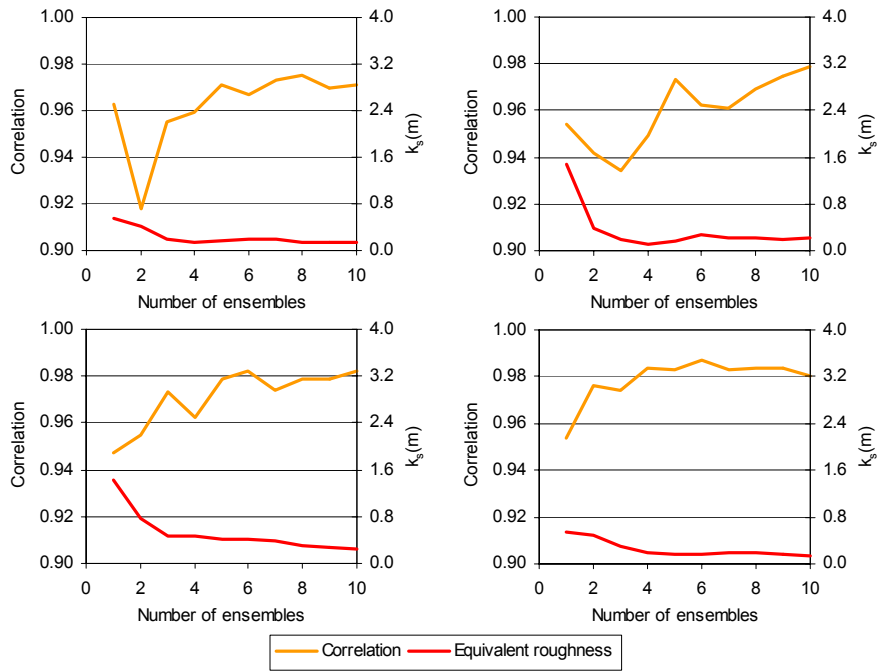


Figure 5.8: Effect of averaging ensembles.

ADCP measurements with 5cm bin resolution during flood phase.

Piep channel (Point 3 in Figure 5.12)

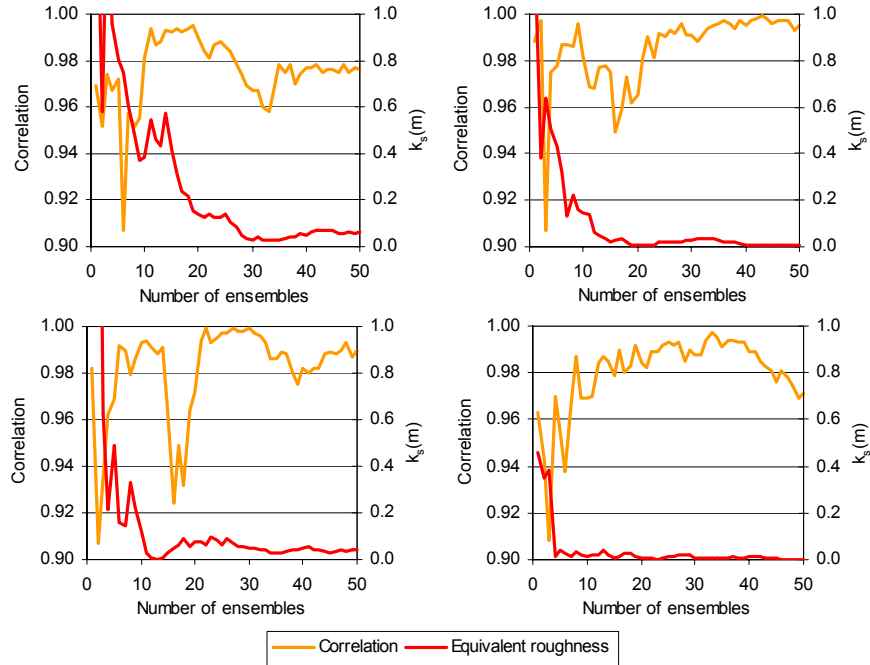


Figure 5.9: Effect of averaging ensembles.

ADCP measurements with 15cm bin resolution during flood phase.

Inner Piep channel (Point 5 in Figure 5.12)

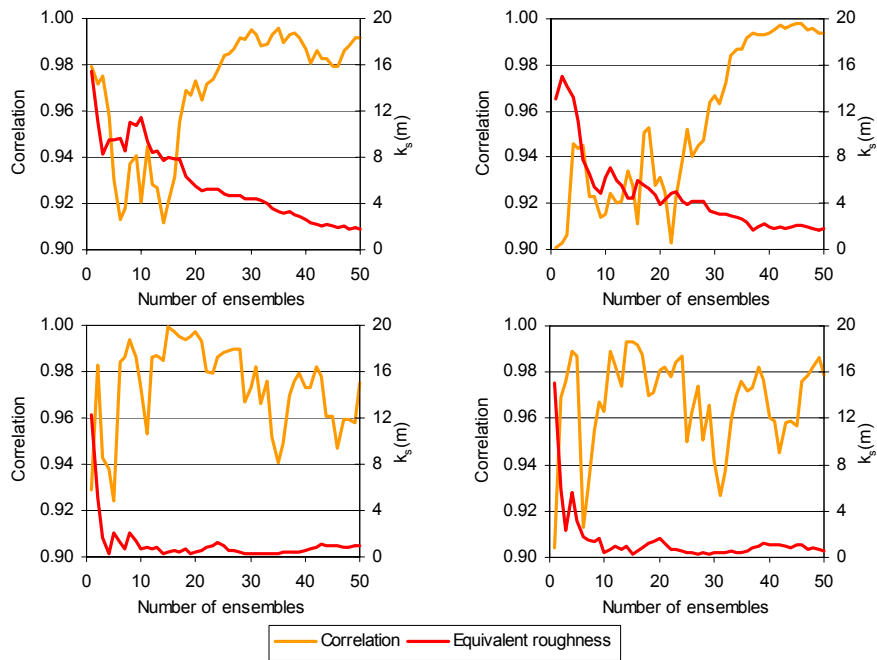


Figure 5.10: Effect of averaging ensembles.

ADCP measurements with 25cm bin resolution during flood phase.

Piep channel (Point 4 in Figure 5.12)

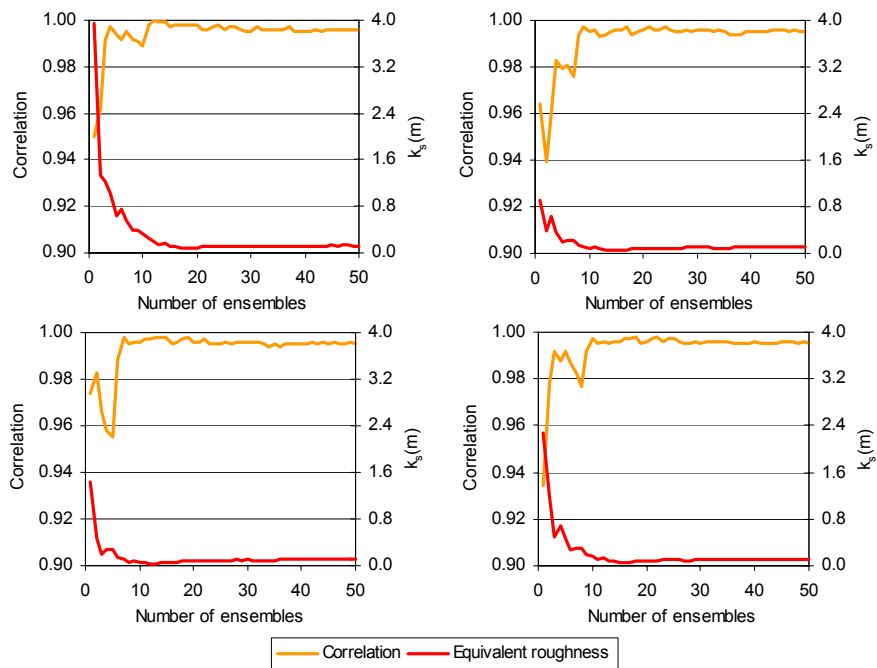


Figure 5.11: Effect of averaging ensembles.

ADCP measurements with 50cm bin resolution during flood phase.

Norderpiep channel (Point 1 in Figure 5.12)

4. For the 50cm data, the constant estimations of equivalent roughness are found between 10 and 50 ensembles. The typical velocity profiles are shown in Figure 5.11. Because the interval between ensembles is very large (5 minutes), the average of 10 ensembles covers a wide variation of velocities within 45 minutes. Hence, 5 ensembles covering a period of 20 minutes are chosen for the estimation of equivalent roughness sizes. The resulting equivalent roughness sizes should be analyzed carefully since there will probably be a tendency for overestimation.

5.3 Estimation of equivalent roughness sizes

As discussed in Chapter 3, the current velocity profiles were measured in tidal channels of the Central Dithmarschen Bight. Figure 5.12 shows the measurement locations in the Norderpiep, Suederpiep and Piep tidal channels. ADCPs with different bin size resolutions were employed. Measurements were carried out with 5cm bin size at Point 3 (Piep channel), 15cm bin size at Point 5 (inner Piep channel), 25cm bin size at Point 4 and 50cm bin size at Points 1 and 2 (Norderpiep and Suederpiep channels) as indicated in Figure 5.12.

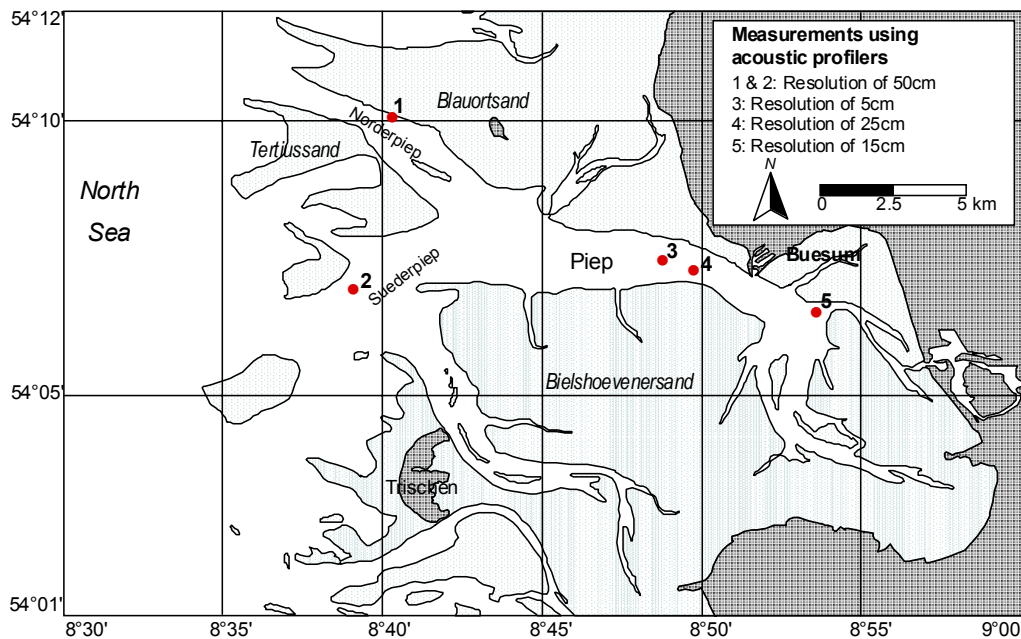


Figure 5.12: Locations of current velocity measurements

For all data sets with different bin sizes, only the measured velocities in the lower 20% of flow depth with minimum correlation coefficient of 0.90, minimum depth integrated velocity magnitudes of 0.30m/s and maximum standard deviation of velocity direction of 10° were selected. The numbers of bins employed in the log law fit are 22-23 bins for 5cm resolution and 5 bins for 15cm and 50cm resolution. Displacement heights equal to 70% of the corresponding bedform heights were considered only for

data measured with 15cm bin size resolution. As mentioned in Section 5.2.6, the average of different number of ensembles was taken. The average of 10 (36 second intervals), 50 (1 minute, 16 second intervals) and 5 (20 minute intervals) ensembles was considered respectively for measurements with bin sizes of 5cm, 15cm and 50cm.

In addition, the bed shear stress is also computed from fit line of velocities in the logarithmic layer. Assuming a von Karman constant of 0.4 (Brown et al., 1991), the shear velocity u_* is inversely related to the slope m of the best fit line:

$$u_* = \frac{1}{5.75 * m} \quad (5.3)$$

The bed shear stress τ_b estimated from the best fit line is related to the shear velocity u_* as follows:

$$\tau_b = u_*^2 \rho \quad (5.4)$$

5.3.1 Measurements with acoustic profiler with 5cm bin size

Measurements using an ADCP with 5cm bin size were carried out at nine periods of the tidal cycle as indicated in Figure 5.13. During each period, 3 minutes of continuous acoustic profile measurements were taken resulting in about 28 ensembles. Figure 5.14 shows typical current velocity profiles during ebb and flood phases. An averaging period of 36 seconds was considered. Plots of the first and last ensembles show that the current profiles do not vary significantly over the averaging period. Standard deviation values up to 0.08m/s resulted for the profile during the ebb phase. The profiles are also well defined both during ebb and flood phases. The number of bins considered in the log law fit ranged from 22 to 23 bins (up to 1.25m from the bed). As a result, high correlation coefficients of the log law fit resulted.

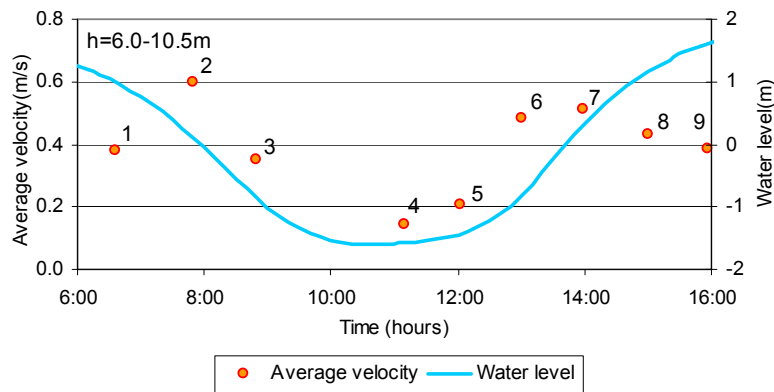
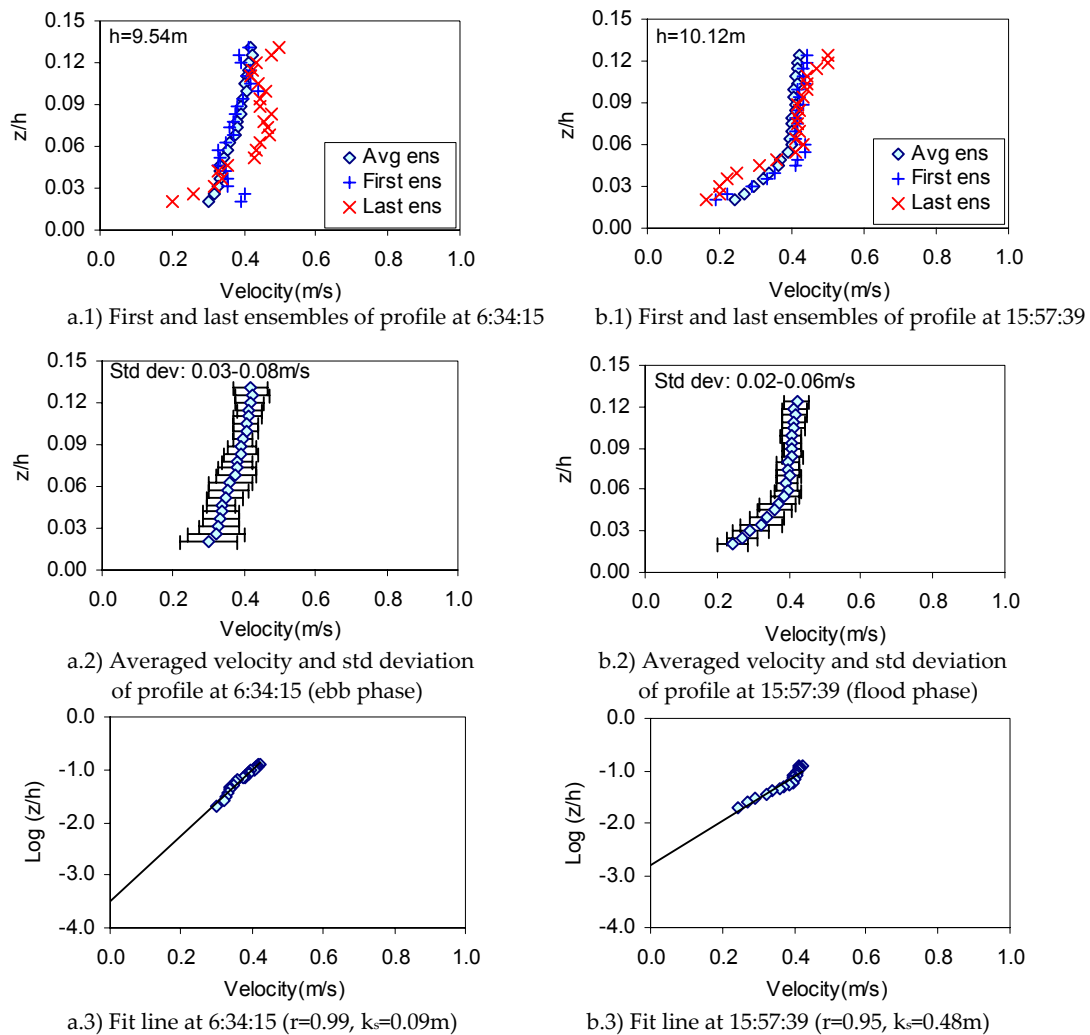


Figure 5.13: Average velocity and water level.

ADCP measurements with 5cm bin resolution in Piep channel (Point 3 in Figure 5.12)



**Figure 5.14: Velocity profiles (average of 10 ensembles covering 36 seconds).
ADCP measurements with 5cm bin resolution in the Piep channel**

Figure 5.15 shows the estimation of equivalent roughness sizes for the measuring periods 1, 5, 8 and 9 which fulfill the criteria defined for selection of valid velocity profiles (Section 5.2). Velocity data recorded during high current velocities cannot be used because the ADCP with 5cm bin size configured in water mode 5 is very sensitive to high shear and turbulence (see Section 3.4.3). No clear relation could be identified between the resulting equivalent roughness sizes during ebb and flood phases. Figure 5.16 shows that the trends of increasing and decreasing roughness are observed in all data sets. Equivalent roughness sizes ranging between 0.05m and 0.49m resulted. According to Figures 3.2 and 3.3, fine to medium sands are available at the measuring location. Therefore bedforms can develop. In summary, the results show that the velocity profiles measured with 5cm bin size seem to be appropriate for estimating equivalent roughness sizes.

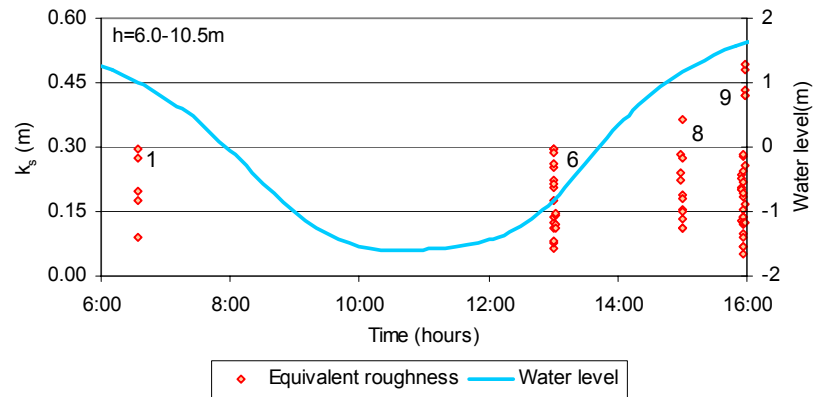


Figure 5.15: Equivalent roughness sizes (average of 10 ensembles covering 36 seconds).
ADCP measurements with 5cm bin resolution in the Piep channel

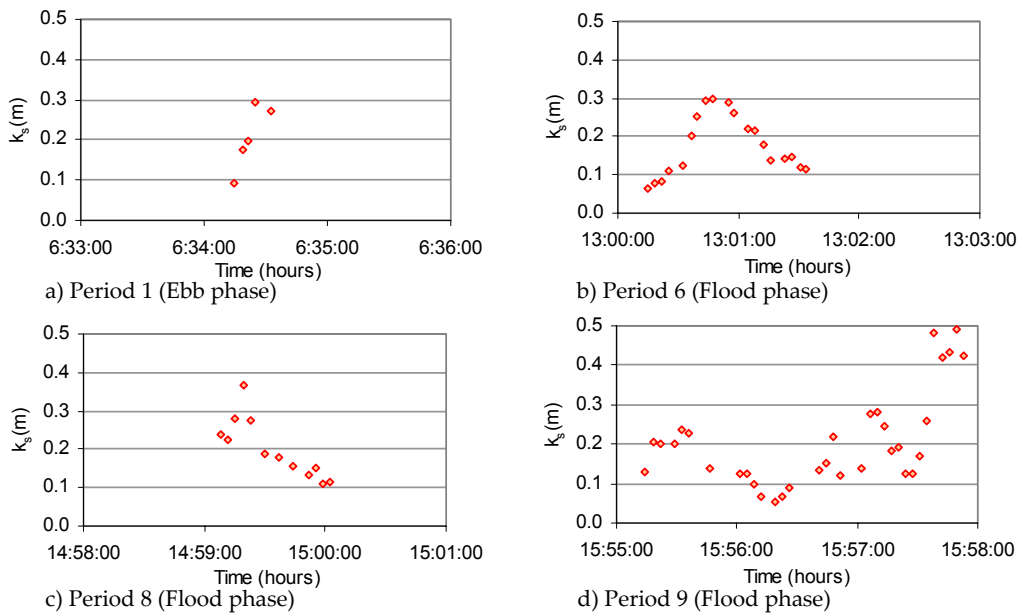


Figure 5.16: Equivalent roughness sizes (average of 10 ensembles covering 36 seconds).
ADCP measurements with 5cm bin resolution in the Piep channel

5.3.2 Measurements with acoustic profiler with 15cm bin size

Figure 5.17 shows two profiles from the average of 50 ensembles which lead to maximum equivalent roughness sizes during flood and ebb phases. Five bins of near bed velocities (up to 1.36m from the bottom) are considered in the log law fit. The standard deviations of current velocities between 0.06m/s and 0.14m/s were observed. High standard deviations are due to less defined current profiles as shown in

Figures 5.17.a.1 and 5.17.b.1. Compared to echo sounder profiles (Figures 4.5 and 4.6), the estimated roughness is in the range of bedform heights up to 0.5m.

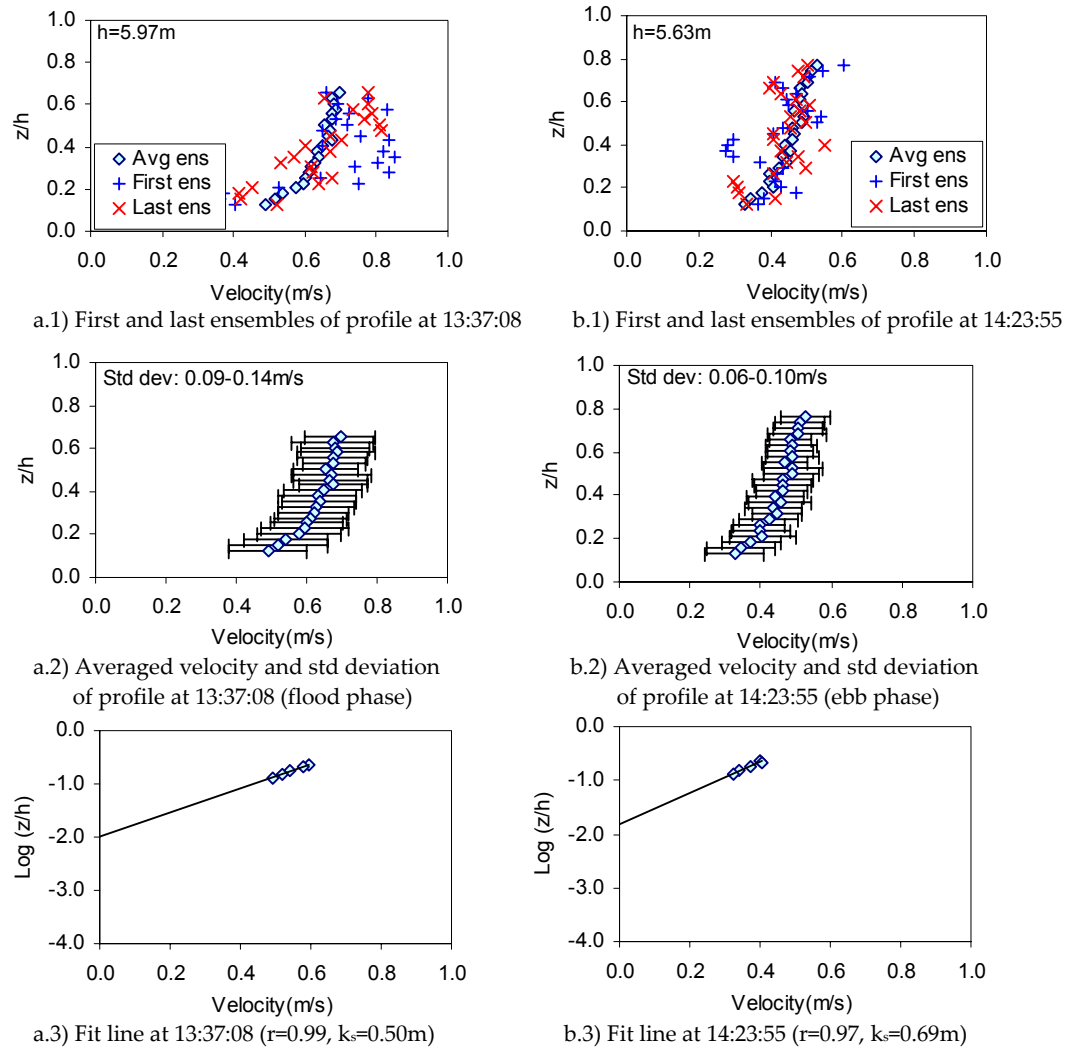


Figure 5.17: Velocity profiles (average of 50 ensembles covering 1 minute and 16 seconds). ADCP measurements with 15cm bin resolution in the inner Piep channel

Figure 5.18 shows the development of equivalent roughness sizes with respect to the current velocity expressed in terms of the depth integrated values and velocities near the bed and free surface. Bed shear stress values up to about $5N/m^2$ resulted during the flood phase (Figure 5.18.b). Higher values are obtained during periods with high current velocities during the flood phase. During the ebb phase, the estimated shear stress values resulted much lower than during the flood phase.

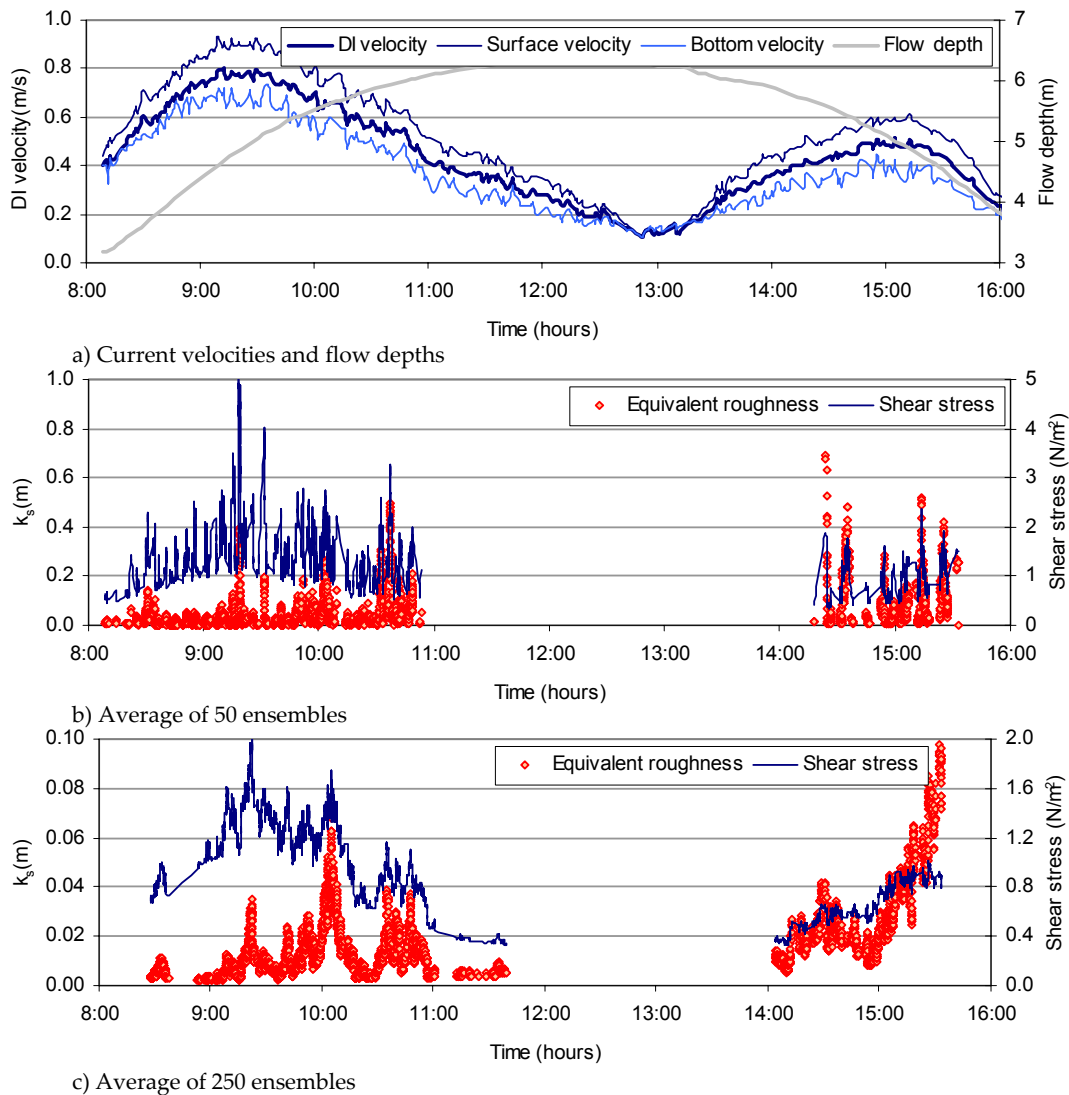


Figure 5.18: Equivalent roughness sizes and shear stresses.

**Average of 50 ensembles (1 min, 16 sec) and 250 ensembles (5 minutes).
ADCP measurements with 15cm bin resolution in the inner Piep channel**

Equivalent roughness sizes up to 0.50m and 0.69m resulted respectively during flood and ebb phases. Relatively low equivalent roughness sizes were obtained during increasing current velocities in the flood phase. The estimated equivalent roughness sizes fluctuate and depend on the velocity magnitude.

In addition, the results obtained considering the average of 250 ensembles covering 5 minute periods are also shown in Figure 5.18.c. It can be seen that much lower equivalent roughness sizes and bed shear stresses resulted. The resulting equivalent roughness sizes and bed shear stress are up to 0.10m and 2.1N/m² respectively.

5.3.3 Measurements with acoustic profiler with 50cm bin size

Figure 5.19 shows typical current velocity profiles resulting in low and high estimation of equivalent roughness sizes in the Suederpiep channel. Five bins covering velocities up to 3m from the bottom are considered for fitting the log law. The standard deviation of velocities resulted up to 0.06m/s and 0.04m/s (Figures 5.19.a.2 and 5.19.b.2). The current velocities used for averaging do not vary significantly due to well defined velocities which were obtained from the average of 20 pings over a period of 5 minutes (Table 3.1).

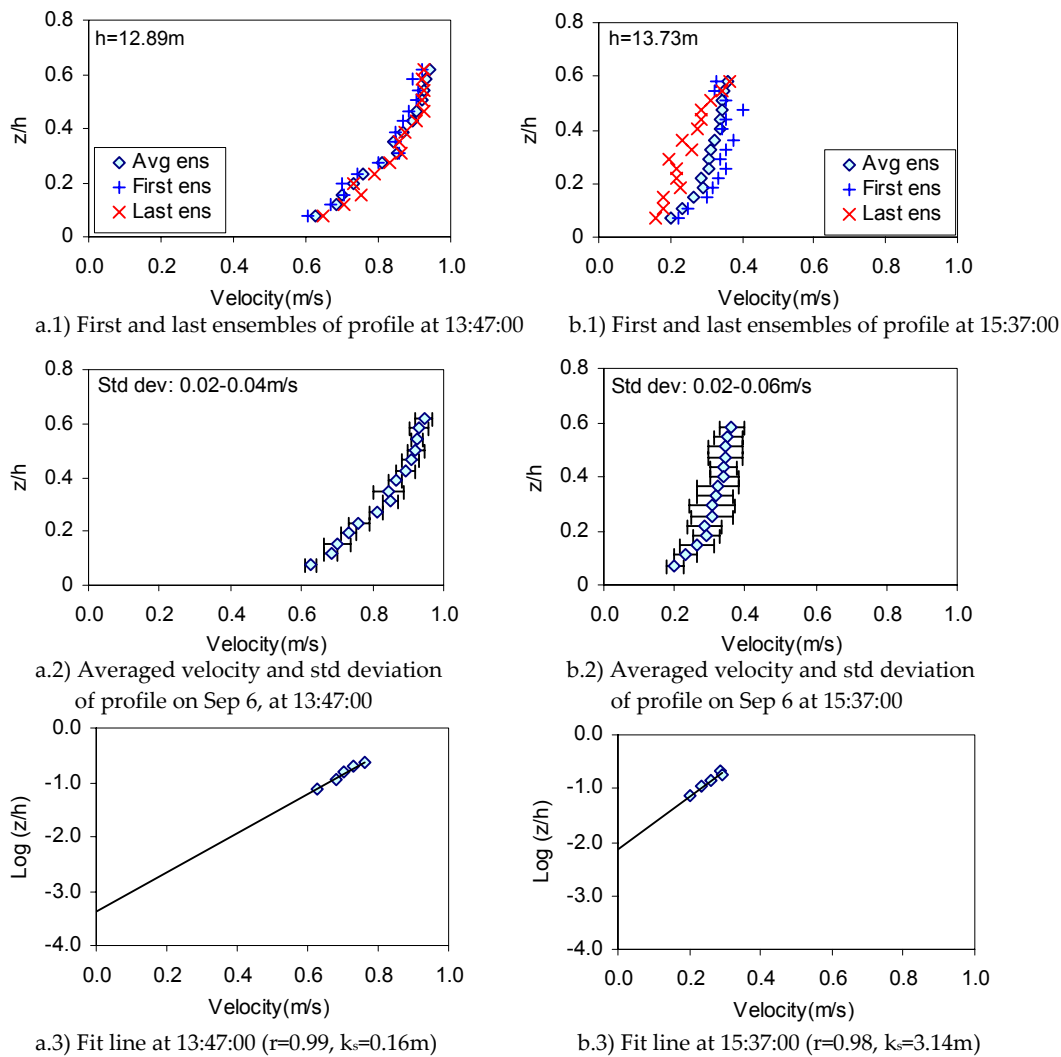


**Figure 5.19: Velocity profiles (average of 5 ensembles covering 20 minutes).
ADCP measurements with 50cm bin resolution**

The variation of equivalent roughness sizes over neap and spring tidal cycles are shown in Figures 5.20 and 5.21 respectively for Norderpiep and Suederpiep channels (Points 1 and 2 in Figure 5.12). Besides depth integrated velocities, the surface and bottom velocities are also plotted. In Figures 5.22 and 5.23, the bed shear stresses obtained from the best fit line of velocities in the logarithmic layer are shown. In both tidal channels, the bed shear stresses follow the pattern of velocity magnitudes. Higher velocities result in higher bed shear stresses. Close to low and high water, the bed shear stresses reach minimum values. In the spring tide which is characterized by higher velocities, higher shear stresses resulted. Values up to 11.4N/m^2 and 5.0N/m^2 are obtained respectively during spring and neap tides.

A wider scatter of equivalent roughness sizes estimated from single ensemble (5 minute intervals) as compared to the one obtain on the basis of the average of 5 ensembles (20 minute intervals) is observed. The estimation of equivalent roughness sizes follow the criteria for selecting velocity profiles as described in Section 5.2. Some fluctuations of equivalent roughness sizes estimated from average of 5 ensembles are also seen during spring and neap tides. High variations of estimated roughness are found during accelerating and decelerating currents.

To investigate the effects of considering different minimum velocity magnitude values for selection of valid velocity profiles for estimation of equivalent roughness sizes, limiting depth integrated velocities between 0.3m/s and 0.6m/s are employed. Figures 5.24 and 5.25 show the resulting equivalent roughness sizes during spring and neap tides obtained for the different limiting values. It can be seen that the high equivalent roughness sizes, which appear unrealistic for the conditions in question, are eliminated. It suggests that the limiting factors for selection of current velocity profiles should be further investigated.

The estimated equivalent roughness resulted much higher than the bedform dimensions observed by echo sounder profiles (Figure 4.4). The bed in the location of measurements is relatively flat with some undulations of outcropping layers of consolidated mud as high as about 0.20m . This is probably related to the large bin sizes and limited number of bins in the part of the flow that can be taken to fit the log law. Furthermore, the rate at which the measurements were taken should be increased so that the averaging of the ensembles over a relatively small period of time can be considered.

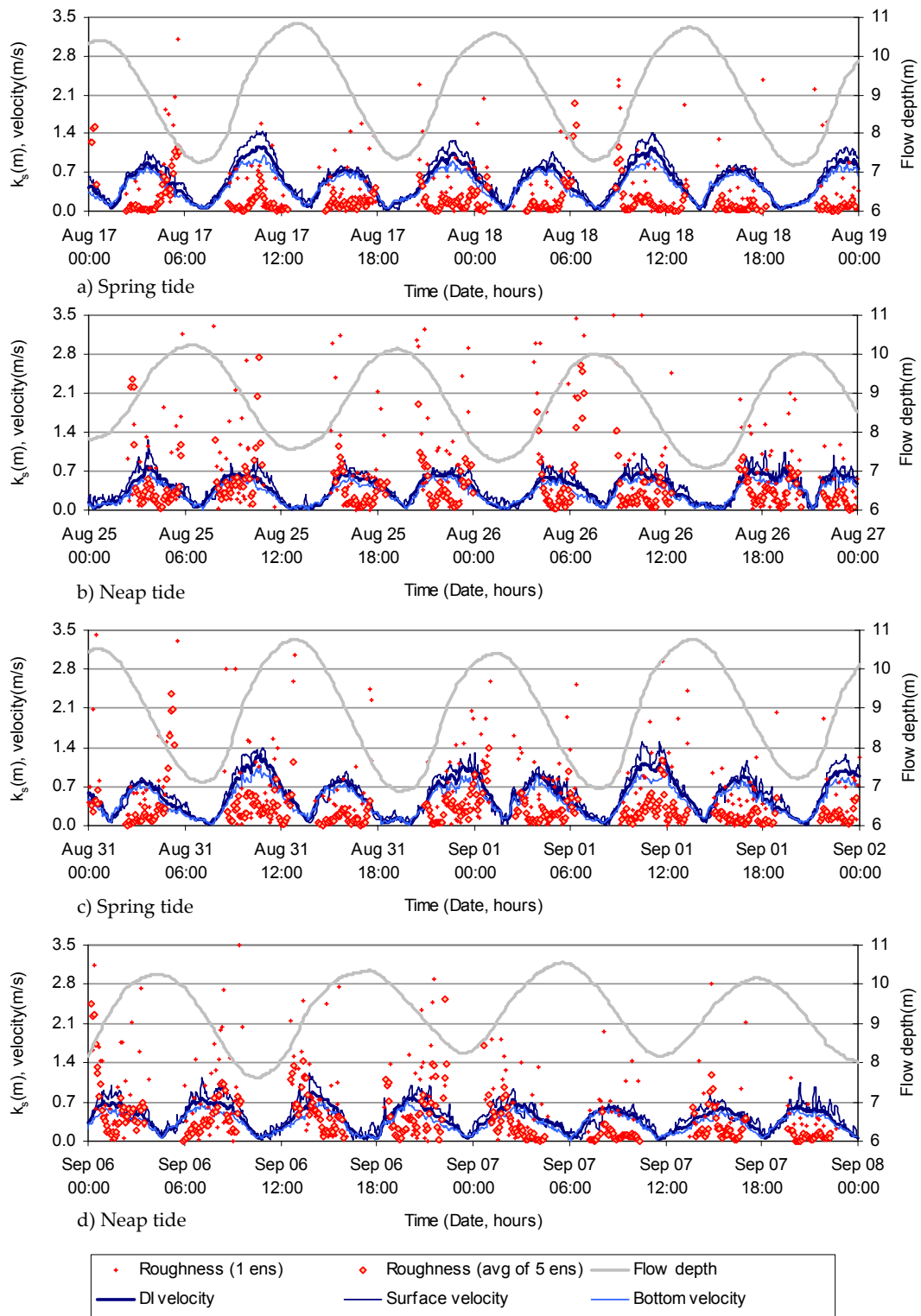


Figure 5.20: Equivalent roughness sizes and velocities in the Norderpiep channel. ADCP measurements with 50cm bin size resolution (average of 5 ens covering 20 minutes)

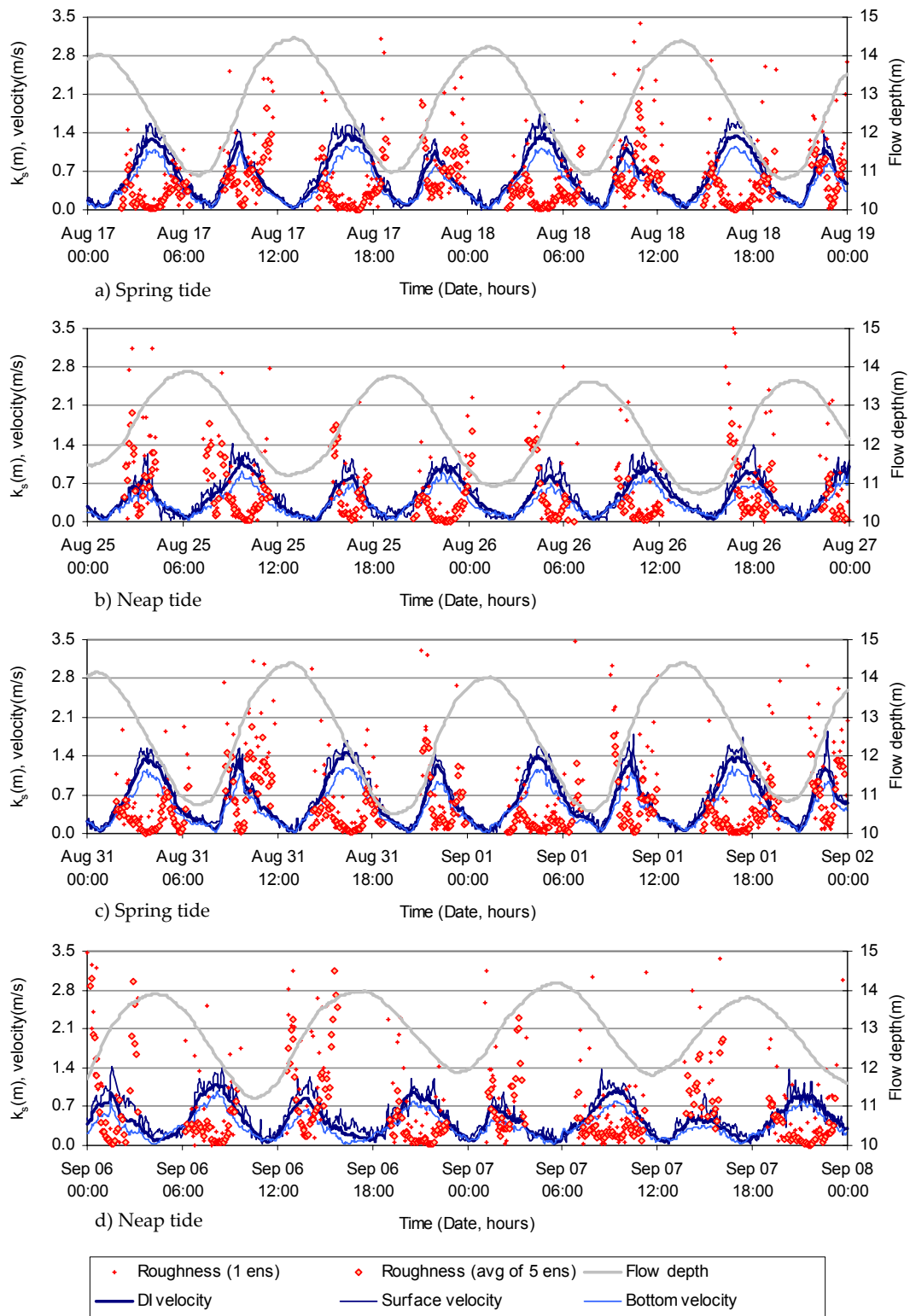


Figure 5.21: Equivalent roughness sizes and velocities in the Suederpiep channel. ADCP measurements with 50cm bin size resolution (average of 5 ens covering 20 minutes)

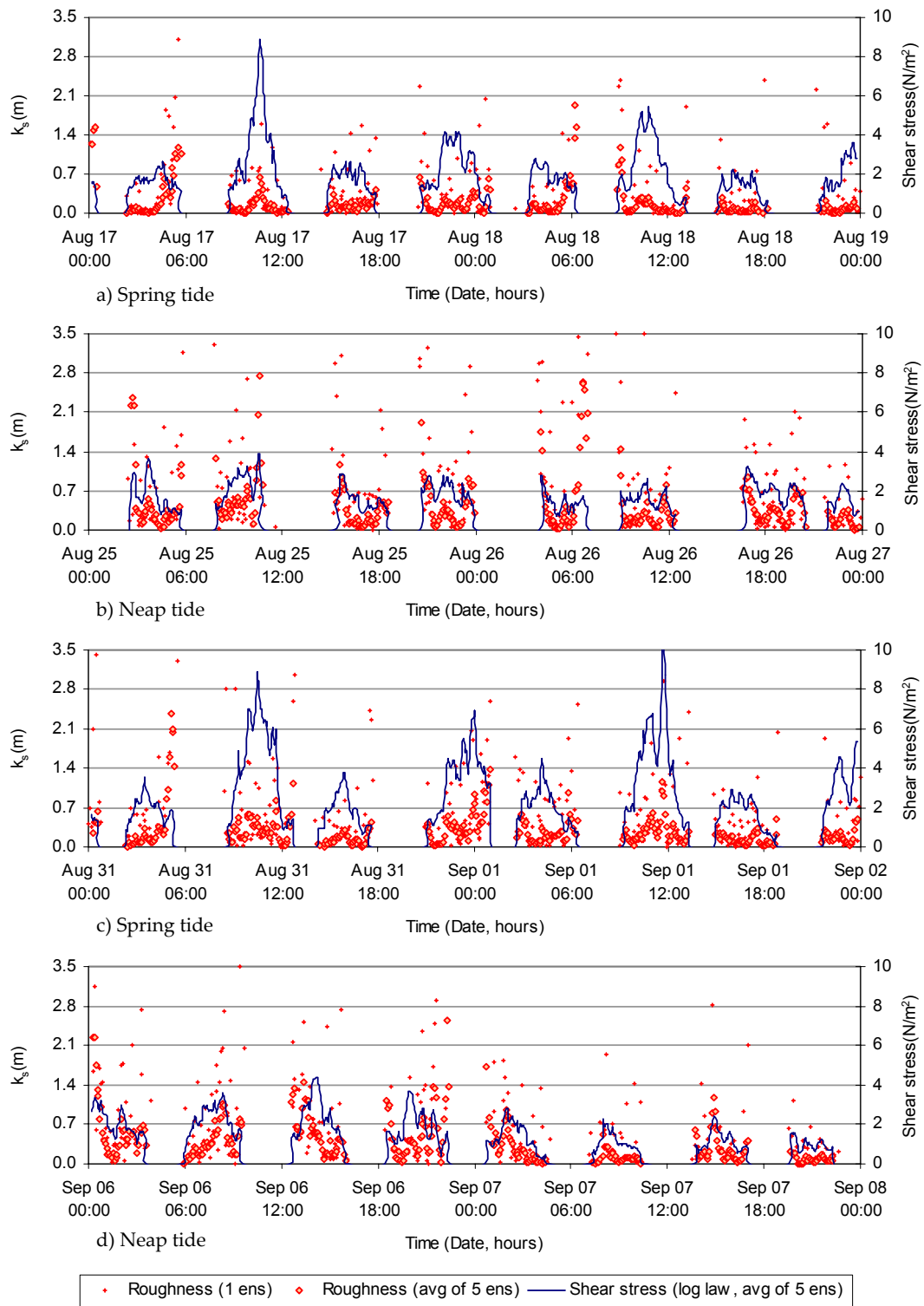


Figure 5.22: Equivalent roughness sizes and shear stresses in the Norderpiep channel. ADCP measurements with 50cm bin size resolution (average of 5 ens covering 20 minutes)

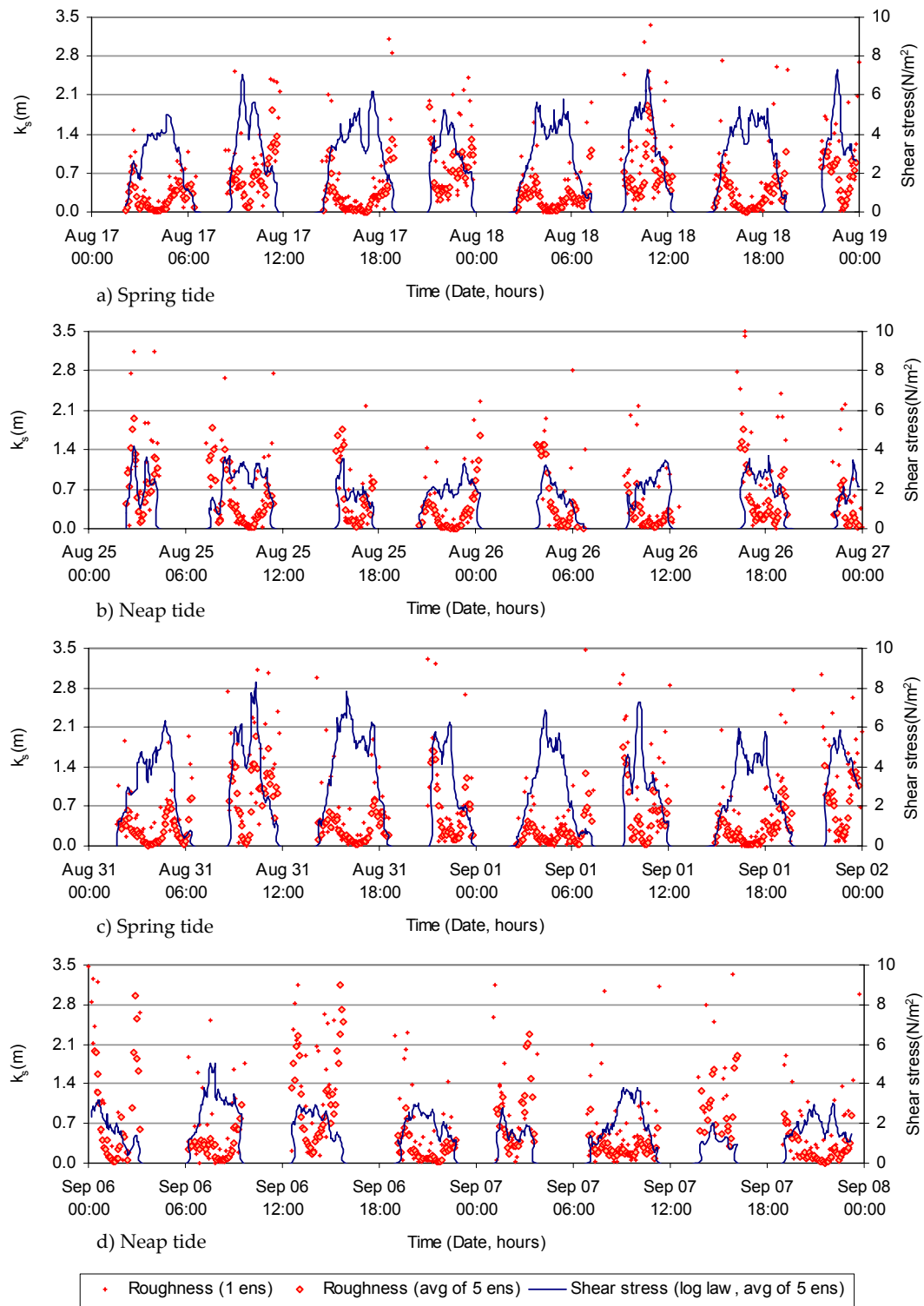


Figure 5.23: Equivalent roughness sizes and shear stresses in the Suederpiep channel. ADCP measurements with 50cm bin size resolution (average of 5 ens covering 20 minutes)

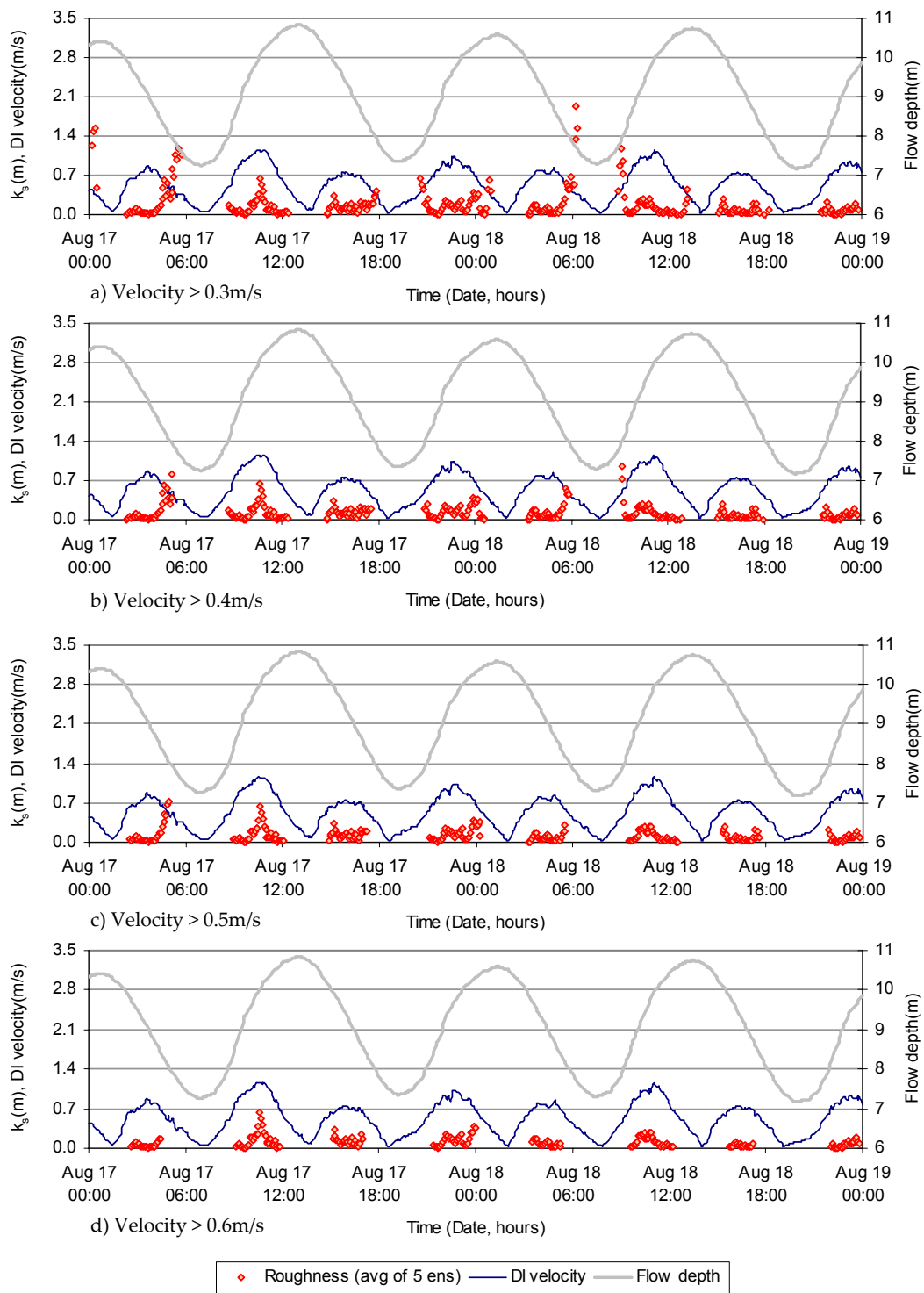


Figure 5.24: Equivalent roughness sizes in the Norderpiep channel.

During spring tide considering various minimum velocities.

ADCP measurements with 50cm bin size resolution (average of 5 ens covering 20 minutes)

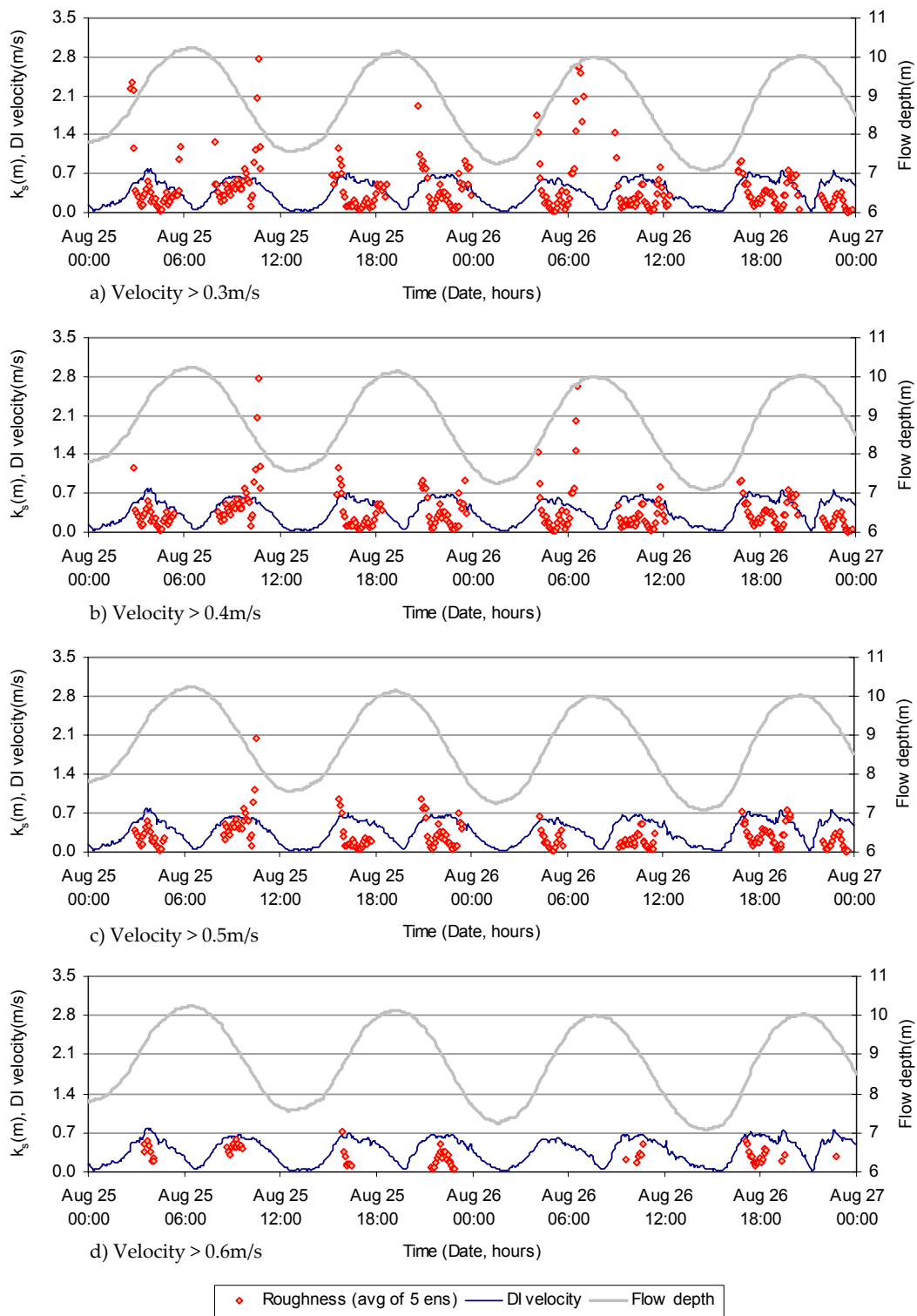


Figure 5.25: Equivalent roughness sizes in the Norderpiep channel.

During neap tide considering various minimum velocities.

ADCP measurements with 50cm bin size resolution (average of 5 ens covering 20 minutes)

5.4 Estimation of equivalent roughness sizes from depth integrated velocities

In this section, equivalent roughness sizes are estimated on the basis of depth integrated velocities. The determination of bed shear stress from the best fit line of velocities in the bottom boundary layer has been explained in the previous section. The bed shear stress is related to the depth integrated velocity (U) as follows:

$$\tau_b = \rho g \left(\frac{U}{C} \right)^2 \quad (5.5)$$

Assuming that the flow is in the rough regime ($u_* k_s / \nu > 70$), the Chezy coefficient C is related to the flow depth h and equivalent roughness k_s :

$$C = 18 \log \left(\frac{12h}{k_s} \right) \quad (5.6)$$

By considering the bed shear stress values obtained from log law fit and depth integrated velocity, equivalent roughness sizes can be determined. In this section, this approach is applied to the ADCP measurements with bin resolution of 15cm and 50cm. ADCP data with bin resolution of 5cm cannot be used because current velocities up to the surface were not recorded.

5.4.1 Measurements with acoustic profiler with 15cm bin size

Figure 5.26 shows the development of bed shear stresses estimated from ADCP data with 15cm bin resolution (Point 5 in Figure 5.12). The averages of 50 and 250 ensembles are computed. The resulting shear stress estimated from depth integrated velocity in conjunction with constant equivalent roughness sizes of 0.01m, 0.1m and 1.0m is shown. The relation between bed shear stress estimated from log law and depth integrated velocity is assessed by using the discrepancy ratio. In this study, a factor of 2, i.e. discrepancy ratios between 0.5 and 2.0 was adopted.

Table 5.2 shows the percentage of data within the factor of 2 between shear stress measured by both approaches. For the average of 50 ensembles, the best agreement is found for the equivalent roughness size of about 0.05m. In other words, on the basis of the present approach, this value gives the best representation of the equivalent roughness sizes in this location for the condition in question. The echo sounder profiles show bedform heights ranging between 0.10m and 0.50m (Table 4.1). In addition, the equivalent roughness size of 0.01m is estimated for average of 250 ensembles.

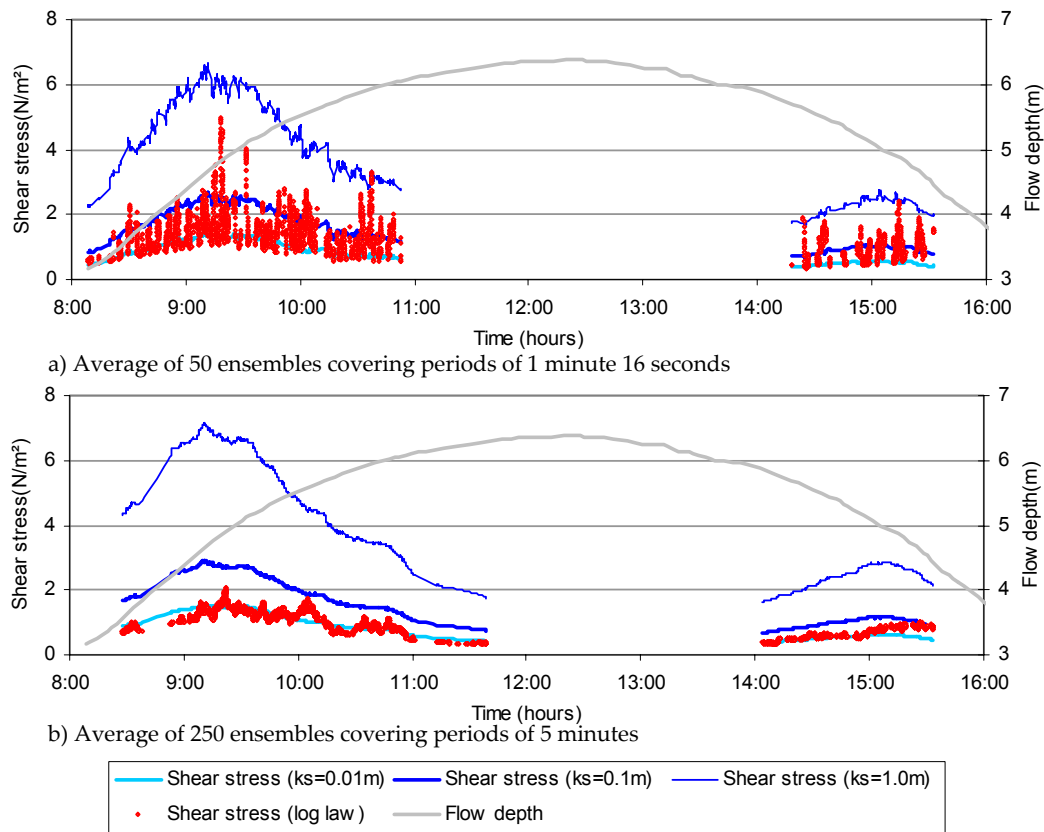


Figure 5.26: Development of bed shear stress on the basis of depth integrated velocities and constant bed roughness. ADCP measurements with 15cm bin resolution

Table 5.2: Percentage of shear stress values within a factor of 2.

ADCP measurements with 15cm bin resolution

$k_s(\text{m})$ to estimate shear stress	Data (%) within $0.50 \leq r_f \leq 2.0$	
	Average of 50 ensembles	Average of 250 ensembles
0.01	78	100
0.05	95	98
0.1	90	72
0.2	70	28
0.3	55	12
0.4	44	5
0.5	35	2
1.0	16	0

Figure 5.27 shows the plots of bed shear stress estimated from depth integrated velocity and log law. The graphs consist of 3508 and 5476 data sets of bed shear stresses for respectively average of 50 and 250 ensembles. Most of shear stresses estimated from depth integrated velocity are within the ratio of 2 to the shear stress

estimated from log law. The data which are beyond the factor of 2 are the results of too low or too high values of shear stress estimated from log law.

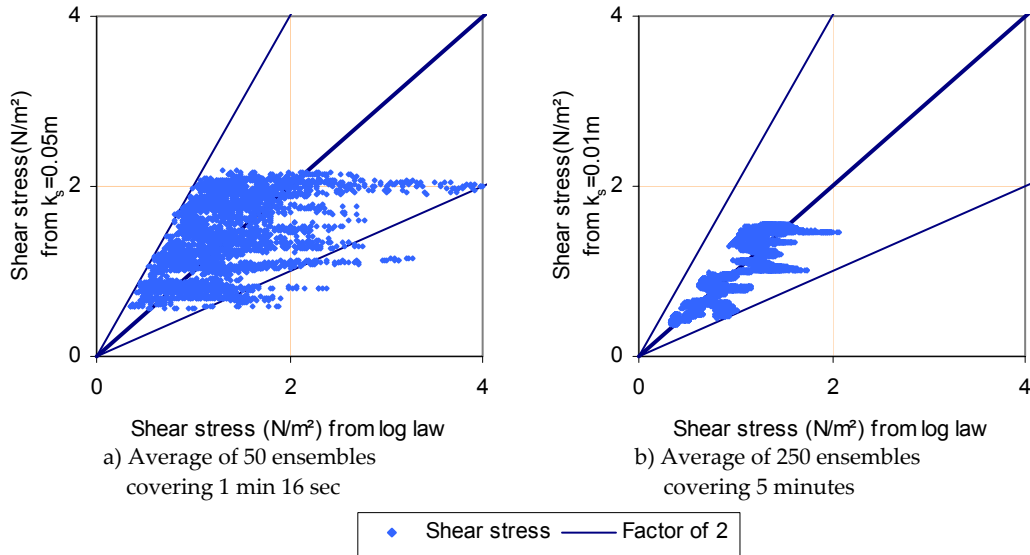


Figure 5.27: Comparison of shear stress obtained from depth integrated velocity and log law. ADCP measurements with resolution of 15cm

5.4.2 Measurements with acoustic profiler with 50cm bin size

The equivalent roughness size is estimated from the depth integrated velocity obtained from ADCP measurements with bin size of 50cm in the Norderpiep and Suederpiep channels (Points 1 and 2 in Figure 5.12). The study focuses on equivalent roughness during spring (August 17-18 and August 31-September 1, 2000) and neap tides (August 25-26 and September 6-7, 2000). Developments of bed shear stresses estimated from log law fit and depth integrated velocity are shown in Figures 5.28 and 5.29 respectively for the locations in the Norderpiep and Suederpiep channels. A wider variation of bed shear stresses is observed by using single ensemble than by considering the average of 5 ensembles. Bed shear stresses estimated from depth integrated velocity by considering constant equivalent roughness sizes of 0.1m and 1.0m are also plotted.

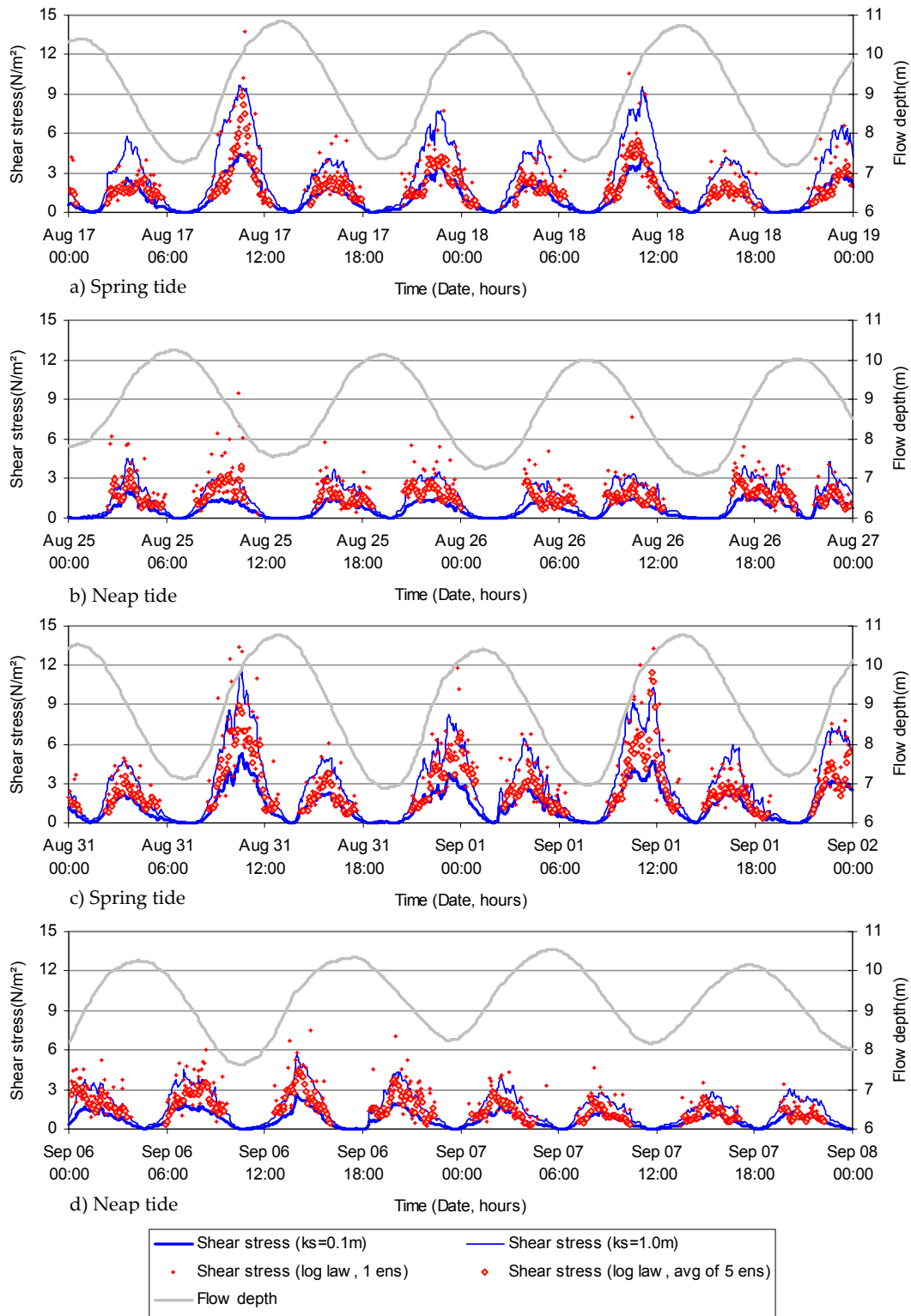


Figure 5.28: Shear stress in the Norderpiep channel.
ADCP measurements with 50cm resolution

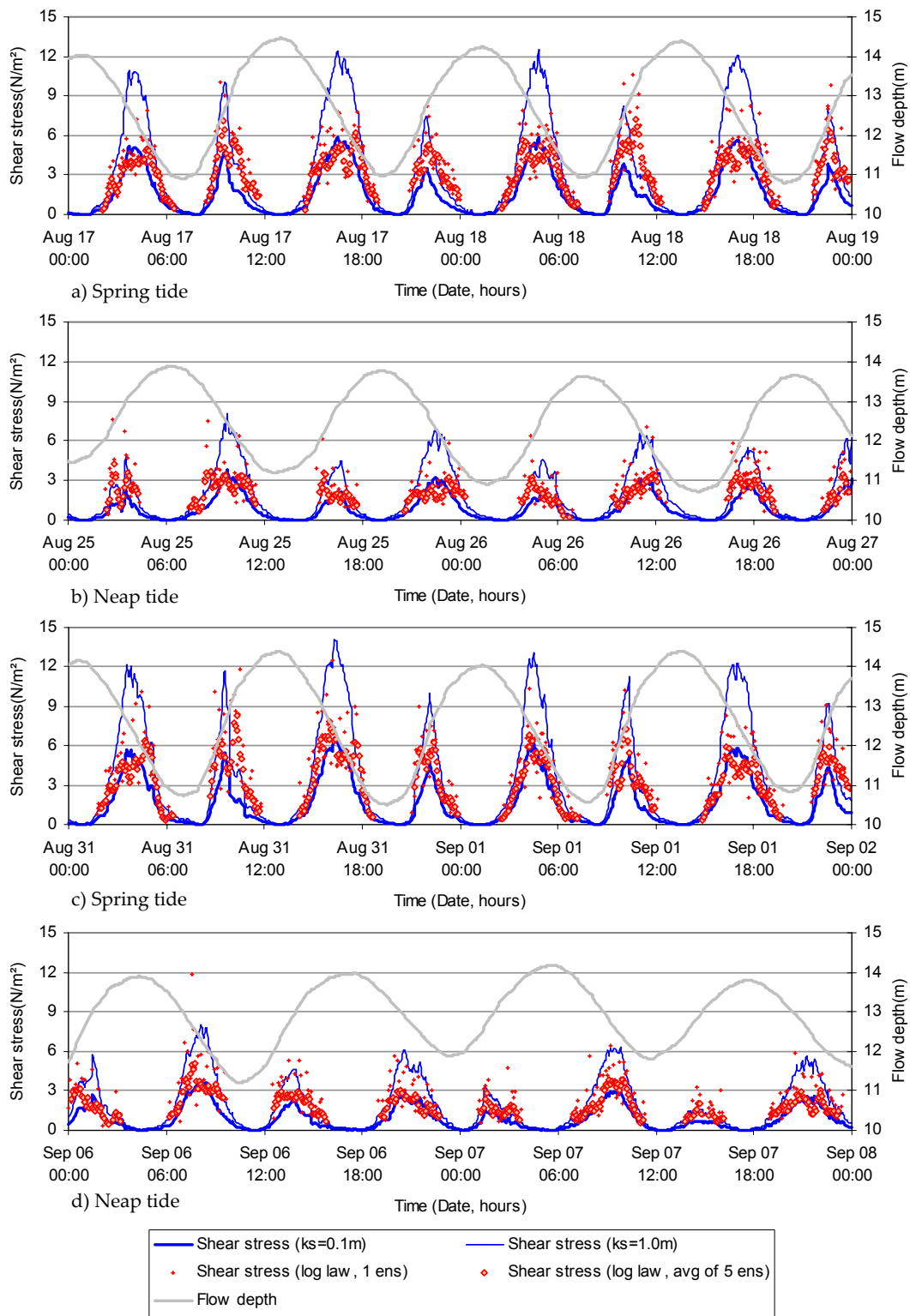


Figure 5.29: Shear stress in the Suederpiep channel.
 ADCP measurements with 50cm resolution

Table 5.3 shows the percentage of data which lies within the factor of 2. The field data are distinguished between spring and neap tides in the Norderpiep and Suederpiep channels. The best estimation of equivalent roughness is found for the highest percentage of data within a factor of 2. In the Norderpiep channel during spring tide, the best agreement of shear stress is obtained by equivalent roughness sizes of 0.2m. On the other hand, equivalent roughness sizes of 0.4m are estimated in the Norderpiep channel during neap tide and in the Suederpiep channel during spring and neap tides. The estimated roughness sizes are higher than the bedform heights observed by echo sounder profiles (Figure 4.4). Relatively flat beds with some outcropping layers up to 0.22m were found in the locations of measurements.

**Table 5.3: Percentage of shear stress values within a factor of 2.
ADCP measurements with 50cm bin resolution**

k.(m) to estimate shear stress	Percentage of values within $0.50 \leq \tau_f \leq 2.0$			
	Norderpiep (spring tide)	Norderpiep (neap tide)	Suederpiep (spring tide)	Suederpiep (neap tide)
0.1	90	77	72	76
0.2	93	90	82	88
0.3	92	94	85	89
0.4	89	95	86	90
0.5	86	93	86	89
1.0	63	80	75	78

Figure 5.30 shows plots of bed shear stresses estimated from log law fit and on the basis of depth integrated velocity. In the Norderpiep channel, 457 and 400 data sets during respectively spring and neap tides are plotted. In the Suederpiep channel, 470 and 317 data sets are used for respectively spring and neap tides. Higher values of shear stresses resulted during spring tide in which high current velocities are observed.

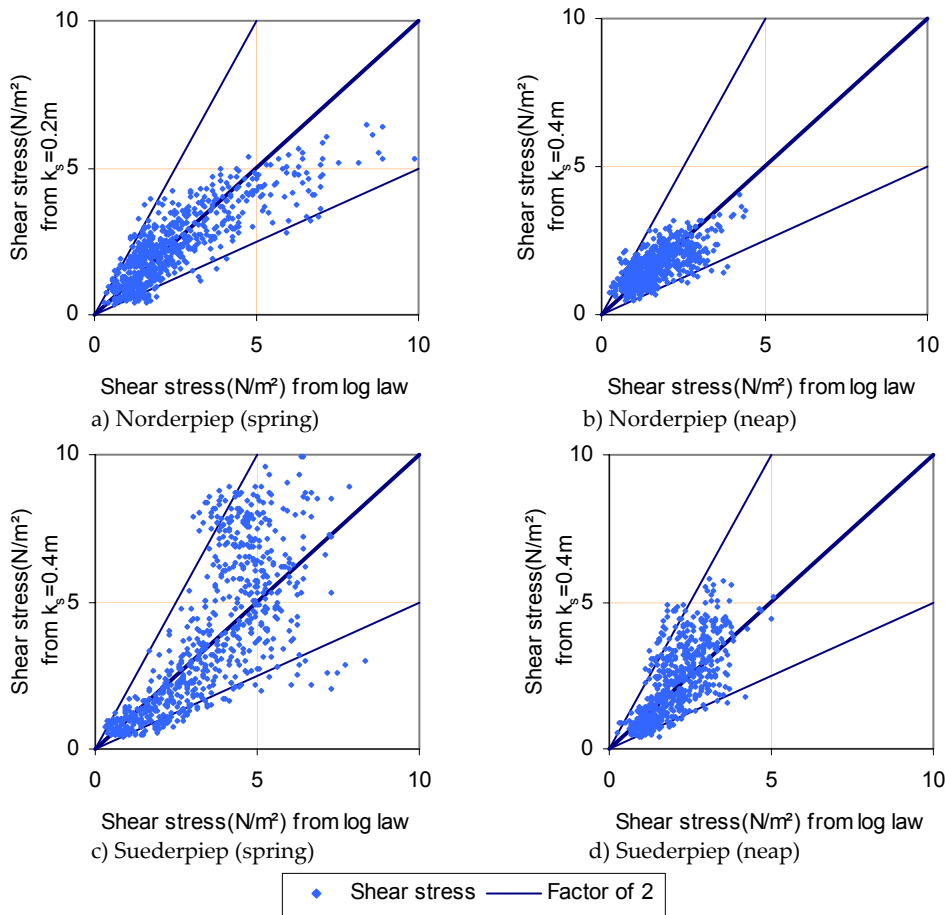


Figure 5.30: Comparison of shear stress obtained from depth integrated velocity and log law. ADCP measurements with 50cm bin resolution

5.5 Verification of the effectiveness of formulas for evaluation of form roughness

To verify the effectiveness of the empirical equations proposed for estimating form roughness from bedform dimensions, the results obtained in the measurements carried out in the inner Piep channel (Point 5 in Figure 5.12) were considered. As already pointed out, simultaneous measurements of bedform dimensions and current velocity using respectively an echo sounder and acoustic profiler were done. Measurements covered about half of the tidal cycle. The current velocity measurements were conducted using an acoustic profiler with 15cm bin size. Figure 5.31 shows shear stresses and equivalent roughness sizes obtained by fitting the log law through the measured velocity profiles. In addition, bedform dimensions obtained from echo sounder profiles are also shown.

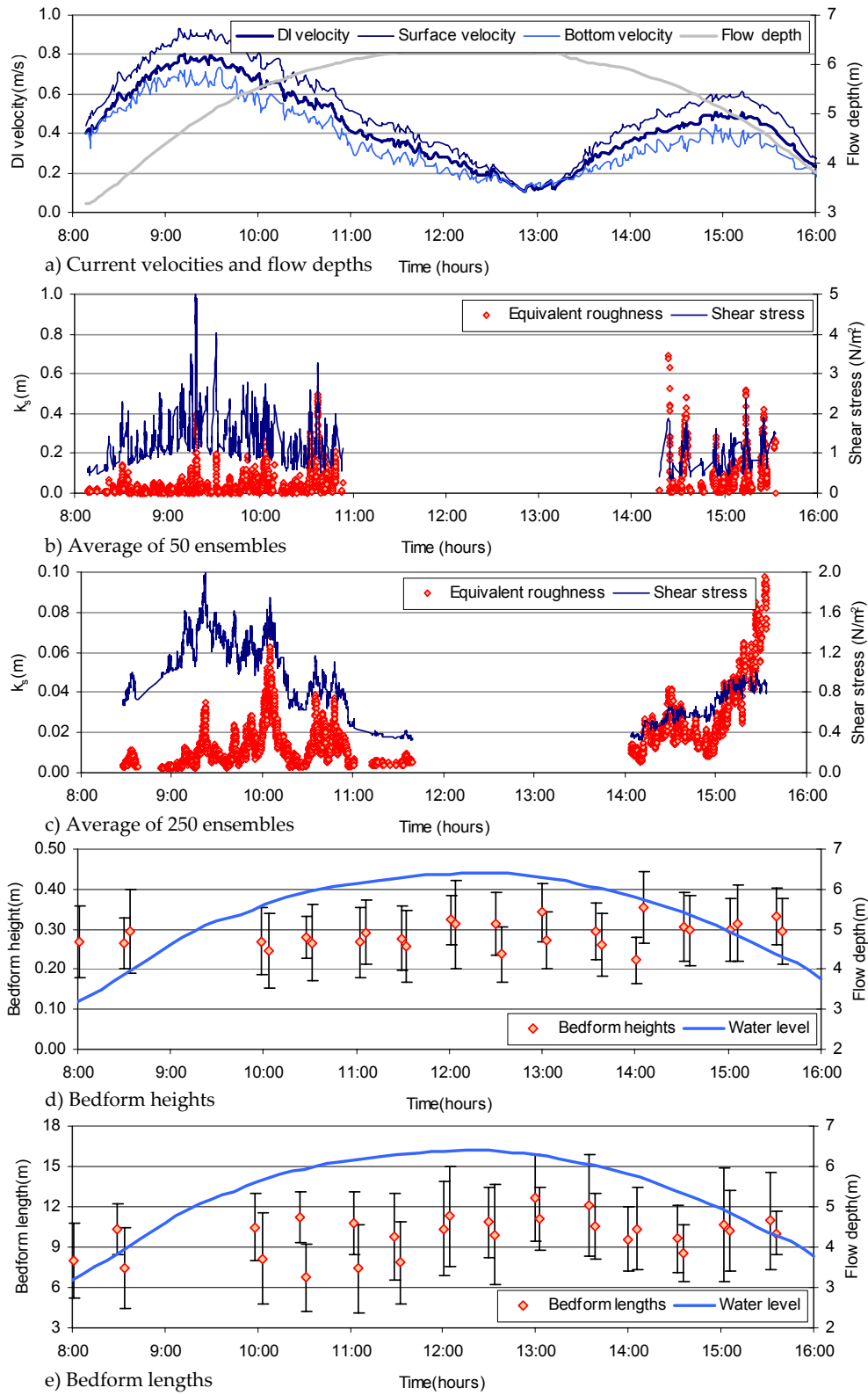


Figure 5.31: Equivalent roughness sizes, shear stresses and bedform dimensions

Thirteen data sets obtained during flood and ebb phases are listed in Table 5.4. Only the data with depth integrated velocity greater than 0.30m/s are considered. Table 5.4 summarizes also equivalent roughness sizes obtained from the log law fit using average of 50 and 250 ensembles.

**Table 5.4: Bedform dimensions and equivalent roughness sizes.
ADCP measurements with 15cm resolution in the inner Piep channel**

Profile	Time	Tidal phase	Depth (m)	DI velocity (m/s)	Δ (m)	λ (m)	k_s (50ens) (m)	k_s (250ens) (m)
10	08:29:24	Flood	3.60	0.61	0.26	10.34	0.03	0.01
11	08:34:06	Flood	3.73	0.56	0.30	7.44	0.03	0.01
12	09:58:26	Flood	5.53	0.66	0.27	10.48	0.06	0.01
13	10:03:14	Flood	5.56	0.66	0.25	8.15	0.06	0.04
14	10:27:20	Flood	5.81	0.60	0.28	11.24	0.05	0.01
15	10:31:31	Flood	5.89	0.57	0.27	6.76	0.11	0.01
16	11:02:03	Flood	6.07	0.51	0.27	10.75	0.06	0.01
29	14:05:38	Ebb	5.82	0.39	0.36	10.38	0.11	0.01
32	14:31:28	Ebb	5.53	0.44	0.31	9.62	0.15	0.03
33	14:35:27	Ebb	5.49	0.45	0.30	8.59	0.17	0.02
34	15:01:36	Ebb	5.05	0.52	0.30	10.64	0.06	0.02
35	15:05:52	Ebb	4.00	0.48	0.31	10.19	0.10	0.03
36	15:31:28	Ebb	4.43	0.45	0.33	10.96	0.17	0.09

As mentioned in Section 4.4, bedforms observed in the study area are identified as megaripples and dunes. These bedforms are characterized with asymmetrical shapes with a rather steep lee side and a gentle stoss side. In addition, the ratios of bedform length to flow depth are between those for megaripples and dunes. Therefore, empirical equations for ripples (Equation 2.26) and dunes (Equation 2.27) proposed by Van Rijn [1993] were considered.

5.5.1 Ripples

The empirical equation (Equation 2.26) relating equivalent roughness sizes and dimensions of ripples was derived using data from flume experiments and measurements in rivers [Mahmood et al., 1984]. It should be noted that Van Rijn used a single term “ripples” covering miniripples and megaripples when defining the form roughness. Figure 5.32 shows the data acquired from flumes and rivers that was considered in the derivation of equation in conjunction with the data obtained in the present study area. The variation of effective form roughness (roughness divided by ripple height) with ripple steepness (height divided by length of ripples) is shown. For the inner Piep data, the ripple steepnesses range from 0.01 to 0.03 and the effec-

tive form roughness resulted less than about 1.0. In addition, the average of bedform dimensions during an entire tidal cycle and the equivalent roughness size of 0.05m acquired from the depth integrated velocity approach is also plotted.

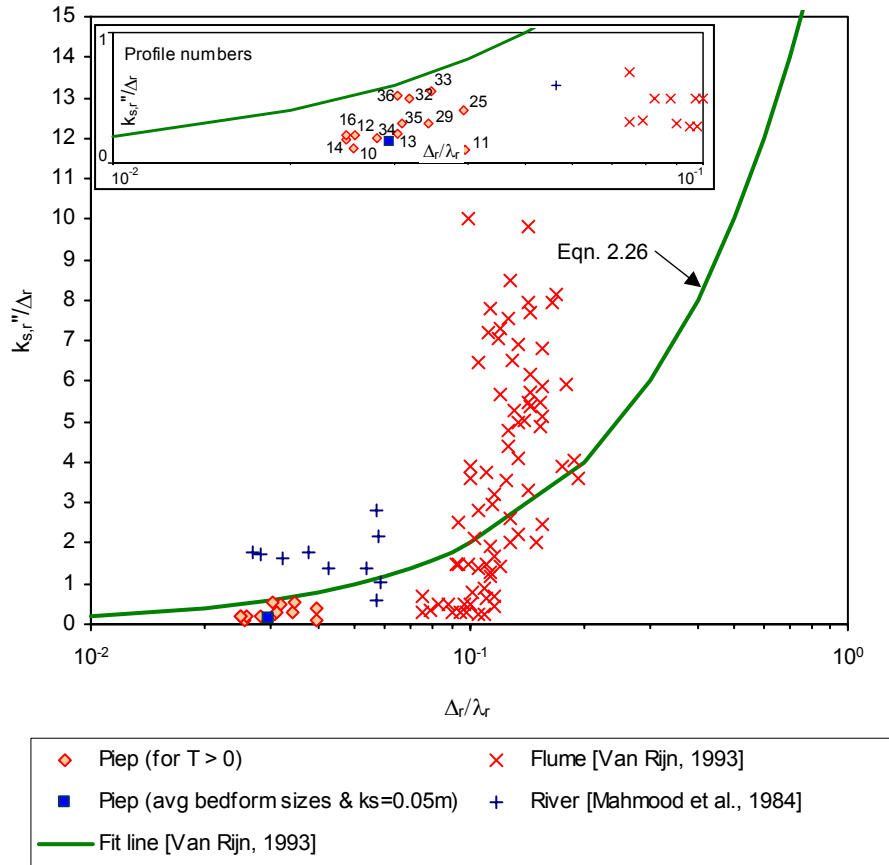


Figure 5.32: Comparison of the form roughness due to ripples from existing and inner Piep channel data

The best fit line for the data collected by Van Rijn [1993] has a coefficient of 20 (Equation 2.26). After considering the inner Piep data, the best fit line with a coefficient of 20 is still applicable suggesting that the equation can be applied to estimate equivalent roughness from dimensions of ripples in the inner Piep channel.

5.5.2 Dunes

For the relation between equivalent roughness and dimensions of dunes, the Equation 2.27 by Van Rijn [1993] is verified. The equation was derived from flume experiments and river measurements. Figure 5.33 plots the data compiled by Van Rijn [1993] and acquired in the inner Piep channel. The average of bedform dimensions during a tidal cycle and the equivalent roughness size of 0.05m acquired from the

depth integrated velocity is also shown. The Piep data are plotted in the range of data obtained from flumes and rivers. The fit line considering data from flumes, rivers and tidal channels is plotted under the fit line by Van Rijn [1993]. The coefficient in the equation resulted slightly smaller, i.e. 0.9 instead of 1.1:

$$k_{s,d}'' = 0.9\gamma_d\Delta_d(1 - e^{-25\Delta_d/\lambda_d}) \tag{5.7}$$

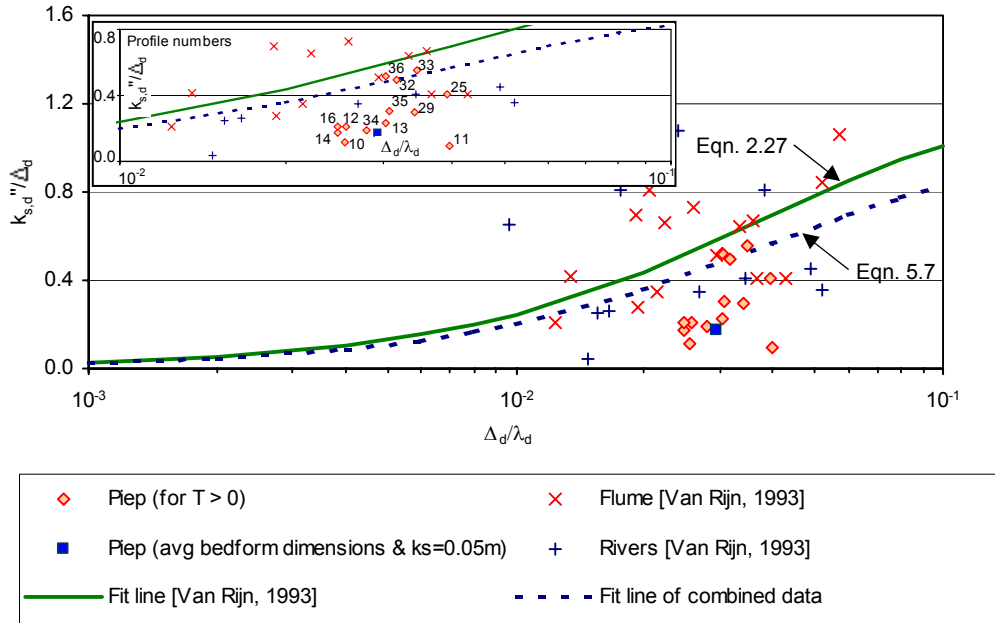


Figure 5.33: Comparison of the form roughness due to dunes obtained from existing and inner Piep channel data

In general, the equations relating equivalent roughness and dimensions of bedforms obtained from flume and river measurements can be used for the conditions in the tidal channels.

5.6 Discussion

In this chapter, the equivalent roughness sizes in tidal channels have been studied. The estimation of equivalent roughness size was conducted on the basis of velocities in the bottom boundary layer and depth integrated velocities. The best fit line was obtained from velocity profiles in the lower 20% of flow depth. The average of ensembles was conducted to minimize errors due to random variations. The time intervals between measured ensembles are significant in determining the number of ensembles. In future measurements, it is recommended the frequency of profile measurements to be less than 5 seconds. Of particular importance are the velocity magni-

tude, the standard deviation of velocity direction and the correlation coefficient of the best fit line to the log law in the near bed region. Only velocity profiles obtained from ADCP measurements with resolution of 5cm, 15cm and 50cm should be considered.

The best fit line of velocities in the bottom boundary layer is employed to estimate the equivalent roughness sizes. The estimated equivalent roughness sizes are up to 0.49m and 0.69m for data of 5cm and 15cm resolution respectively. The estimated values are in the order of observed bedform heights in the investigated locations. However, higher equivalent roughness size up to about 3m is estimated from the measurements with 50cm bin resolution. Relatively flat bed with some outcropping bed layers were in fact observed at the measuring sites. Hence, it is recommended to increase the bin resolution resulting in more point velocity values in the bed boundary layer.

Estimation of equivalent roughness sizes on the basis of depth integrated velocities was also performed. The estimation is obtained from equivalent roughness size which gives the least discrepancy between the computed and measured bed shear stress. For 15cm data sets, the equivalent roughness sizes are estimated between 0.05m and 0.1m. The use of 50cm data results in a slightly higher estimation between 0.2m and 0.4m.

There are, at least, two limitations which should be considered when using current velocities to estimate equivalent roughness sizes. Firstly, the equivalent roughness size cannot be estimated during low and high water levels. These periods are characterized by low velocities and changes in the flow direction between tidal phases. As a result, the standard deviation of velocity direction is high and the correlation coefficient of best fit line is quite low. Secondly, the variations of equivalent roughness are seen. This fluctuation is related to the velocity magnitude which dynamically change during a tidal cycle. These limitations may not reflect the actual change of bedforms. The echo sounder profiles indicate that dimensions of megaripples and dunes stay relatively constant during the entire tidal period even during low and high water levels.

The acquired data on bedform dimensions and equivalent roughness sizes were applied to the proposed equations by Van Rijn [1993] relating equivalent roughness sizes and bedform dimensions. There is a very good agreement between the results of the present study and the equation proposed for ripples. It was found that equivalent roughness sizes estimated on the basis of Van Rijn's equation resulted slightly higher than the ones measured in this study. In order to improve the agreement, the coefficient in the Equation 2.27 was modified slightly.

Chapter 6

Estimation of bedforms and roughness using empirical equations

6.1 Introduction

In this chapter, the empirical equations for definition of bedform types, estimation of bedform dimensions and equivalent roughness sizes presented respectively in sections 4.5, 4.6 and 5.5 are applied to predict the spatial distribution of equivalent roughness sizes in the tidal channels of the Central Dithmarschen Bight. Flow conditions obtained from numerical model simulations are used as inputs to the empirical equations.

6.2 Numerical model setup for the study area

The Delft3D software from Delft Hydraulics in the Netherlands is used to develop the model in the Central Dithmarschen Bight [Delft Hydraulics, 1999]. In this study, the hydrodynamic module known as Delft3D-Flow is employed to generate flow conditions in the area. The 2-D model which is the depth-averaged approach is used. The Central Dithmarschen Bight model was developed and calibrated by Palacio [2002]. Table 6.1 shows the configuration for model simulation.

Flow model simulations were carried out for a period of 16 days (August 11-27, 2000). The simulated period covers a spring (August 17, 2000) and neap (August 24, 2000) tidal cycle. In this section, the model components such as grid, boundary condition and bathymetry are explained.

Table 6.1: Configuration of the Central Dithmarschen Bight model

Components/parameters	Contents/Values
Grid	Curvilinear grid system
Open sea boundary condition	Imposing water levels (Blauort and Buesum)
Bathymetry	Data from year 2000
Time step	0.5 minutes
Eddy viscosity	1 m ² /s
Wind effect	Not included
Wave effect	Not included
Temperature	15 °C
Gravity	9.81 m/s ²
Water density	1026 kg/m ³
Salinity	31 ppt

6.2.1 Model grid

A curvilinear grid system covering an area of about 515 km² in the Central Dithmarschen Bight was used. The grid sizes in the horizontal plane ranges from 60m to 290m.

6.2.2 Open Boundary condition

The open boundaries are defined at the North, South and West boundaries of the model. The open boundaries are divided into several sections as follows: 7 sections in the North, 10 sections in the South and 7 sections in the West boundary. The open boundary condition is defined by imposing time series of measured water levels along the boundaries. The time step of waterlevel records is 10 minutes.

6.2.3 Bathymetry

The bathymetry in tidal channels was obtained from Bundesamt für Seeschifffahrt und Hydrographie (BSH). In the tidal flat areas, the bathymetry was obtained from bathymetrical maps from the Amt für Ländliche Räume (ALR) in Husum. The complete coverage of bathymetry from measurements in 1999 and 2000 was used.

6.3 Spatial distribution of bedforms and roughness

Maps of transport stage parameters, bedform types, bedform dimensions and equivalent roughness sizes were created. This was done for the largest values of transport stage parameters during a neap/spring tidal cycle for which the bedforms are most likely to develop. The periods during high values of transport stage are se-

lected at 17:00 hrs. on August 17, 2000 and at 22:00 hrs. on August 24, 2000 respectively during spring and neap tides.

6.3.1 Transport stage parameters

Figure 6.1 shows maps of transport stage parameters in tidal channels. The transport stage parameter is a function of bed shear stress due to grains and critical shear stress (Equation 2.3).

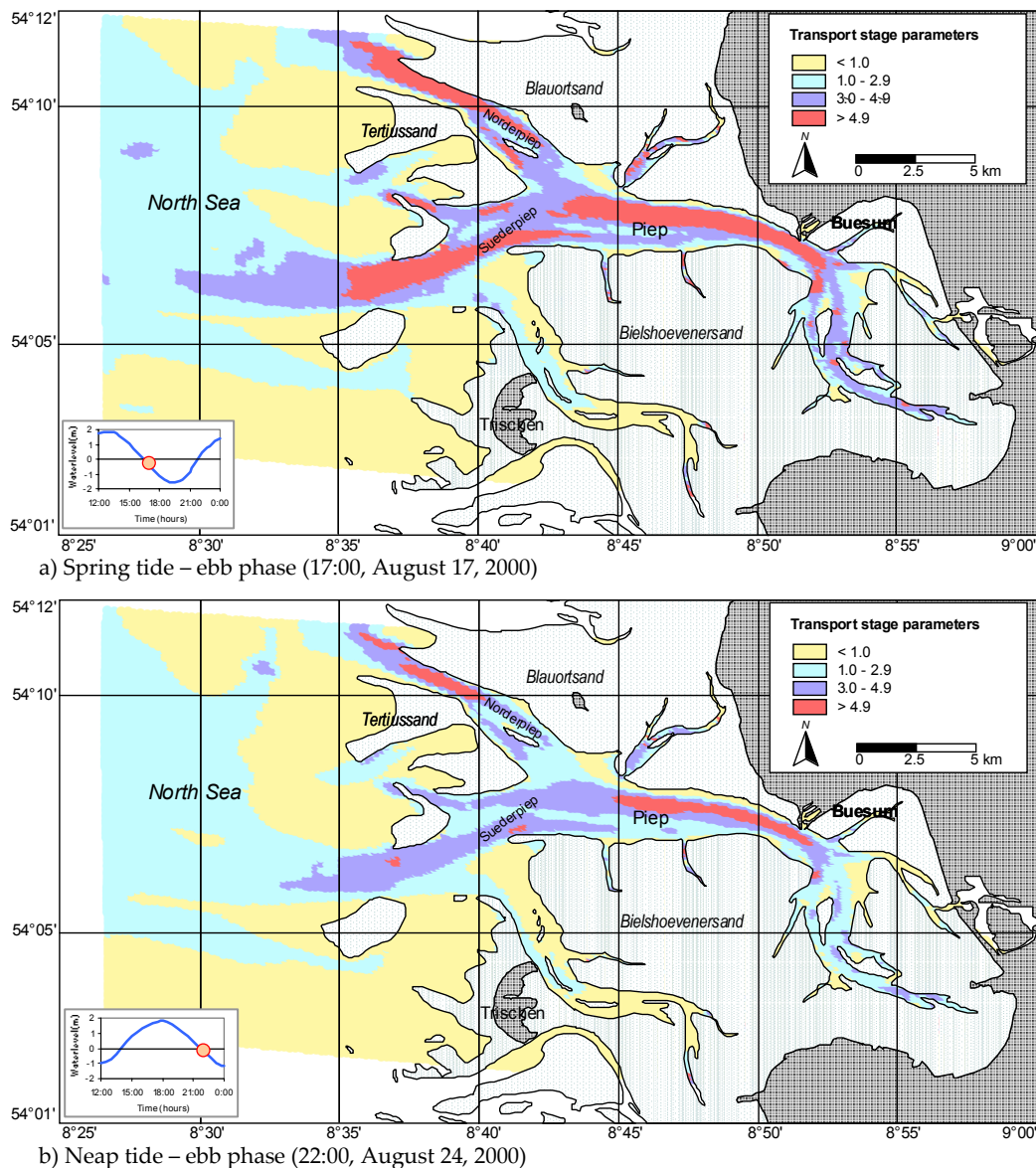


Figure 6.1: Maps of transport stage parameters for maximum current velocity

Higher values of transport stage parameters resulted in the deeper parts of tidal channels in which high current velocities are found. During spring tides, transport stage parameter values reaching up to about 8 are predicted. High transport stage parameters covering large parts of tidal channel in the spring tide are as a result of high current velocities. During neap tides, high values of transport stage are found in small sections in the Norderpiep and Piep channels. The transport stage parameter values resulted up to 7 during neap tides.

6.3.2 Bedform types

For the prediction of bedform types and dimensions as well as equivalent roughness sizes, the availability and type of sediments were taken into consideration. Figure 3.2 shows the availability of sediment layer in tidal channels obtained from field measurements. Bedforms are expected to develop only in areas in which a sediment layer is available. Besides, bed forms are usually absent in areas consisting of consolidated cohesive sediments which are found in the deeper parts of the tidal channels. Another consideration for the prediction of bedforms and equivalent roughness is the type of bottom sediments. Tidal channels covered with sandy sediments and consolidated muds are identified in Figure 3.3. The consolidated fine grained sediments are mostly found in the deeper parts and the flanks of the channels. Bedforms should not be present in areas with consolidated mud.

Figure 6.2 shows the predicted bedform types according to the classification by Van Rijn [1993] (see Table 2.1). The prediction was done considering maximum values of transport stage parameters. Miniripples are predicted in small sections in tidal channels. The bedforms in tidal channels are dominated by megaripples and dunes. During spring tide, megaripples and dunes cover a large part of tidal channels. This prediction is in good agreement with the bedforms observed by side scan sonar measurements (Figure 4.1). The images of side scan sonar indicate the presence of megaripples and dunes in several parts of the Norderpiep and Suederpiep channels.

Figure 6.3 shows a comparison of the observed and predicted bedform types for the spring tide. A good agreement between observation and prediction can be seen in the southern section of Suederpiep channel and the northern section of Norderpiep channel. A discrepancy is found at the junction between Suederpiep channel and Bielshoevener Loch. Miniripples are predicted by empirical equations and numerical modeling, while megaripples are observed by the field measurements. The reason could be that the numerical modeling simulate lower flow velocities and transport stage parameters than measured at the junction of channel resulting in the prediction of miniripples.

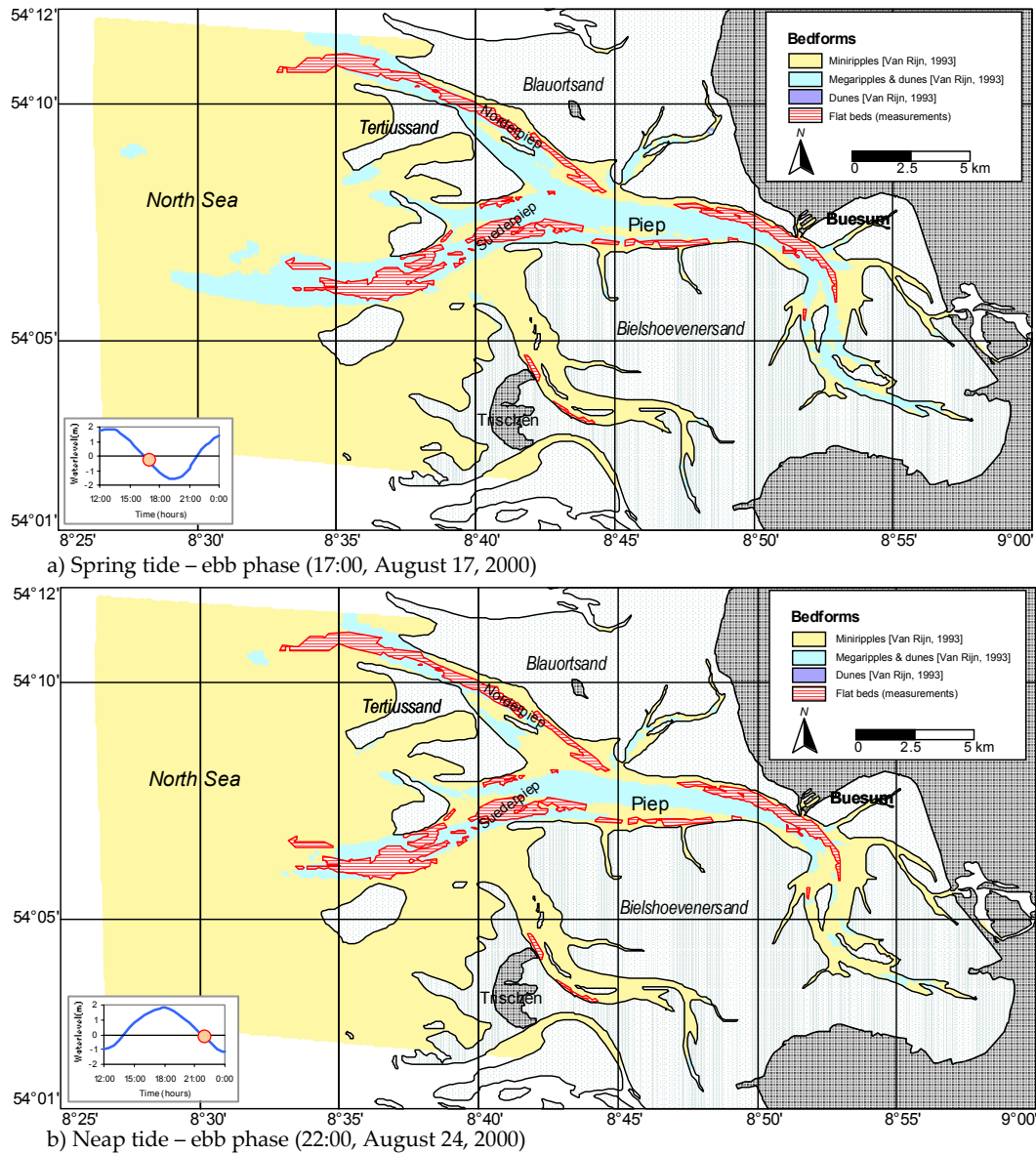


Figure 6.2: Predicted bedform types on the basis of classification by Van Rijn [1993]

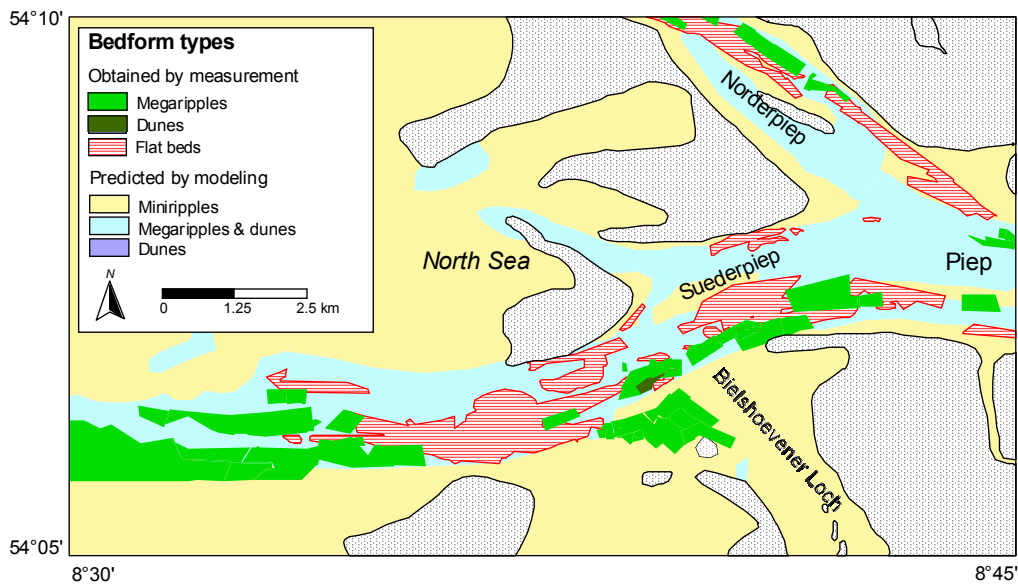


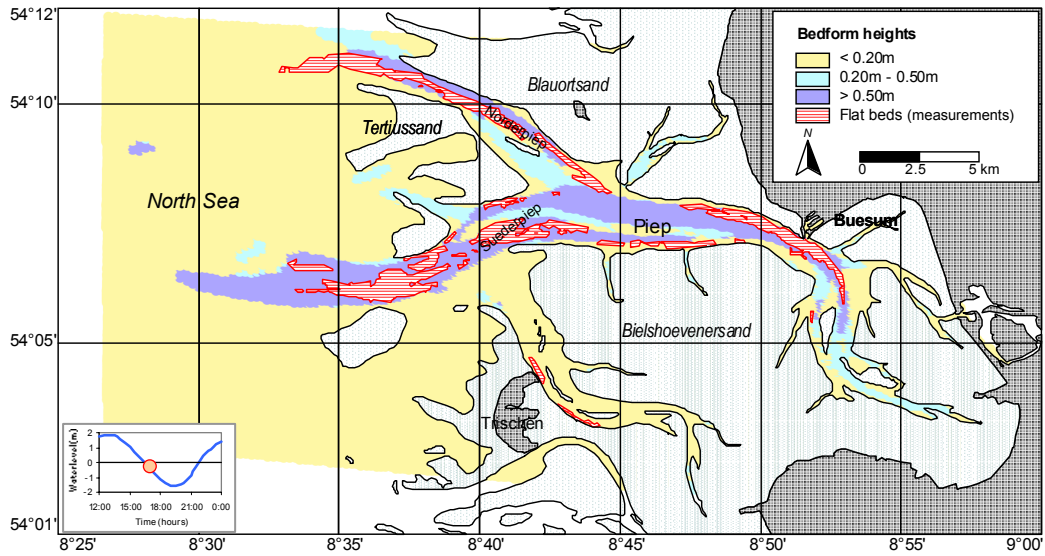
Figure 6.3: Comparison of observed and predicted bedform types

6.3.3 Bedform dimensions

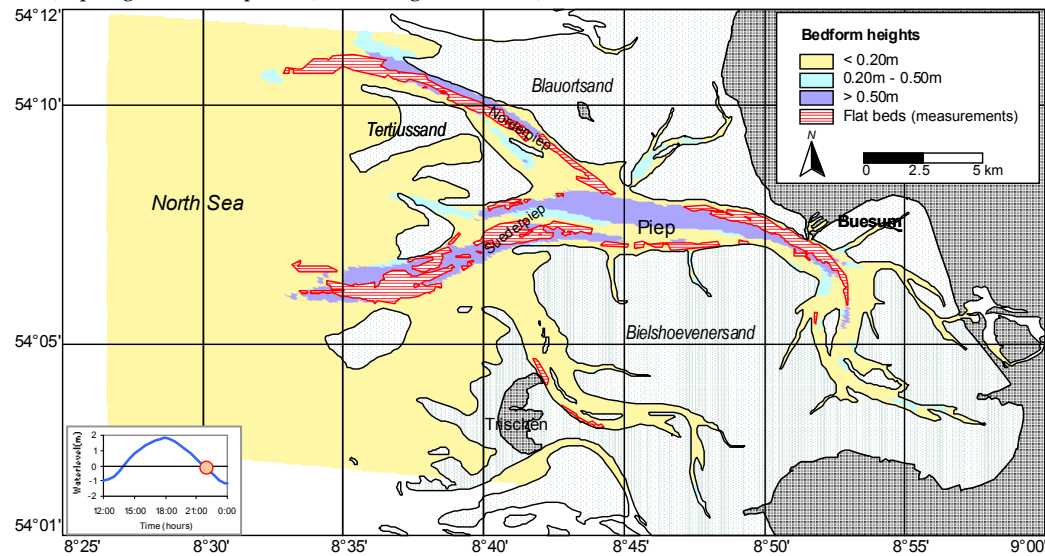
The estimation of bedform heights was carried out using results of the numerical model simulations in conjunction with equations 4.1 and 2.15 respectively for megaripples and dunes. The predicted bedform heights are shown in Figure 6.4. More pronounced distribution of bedform heights greater than 0.50m is found during spring tide. The bedform heights up to 1.1m and 1.2m are estimated respectively during spring and neap tides. In the more shallower areas of the tidal channels the predicted bedform heights are in the order of those obtained from field measurements. Profiles of echo sounder show maximum bedform heights between 0.40m and 0.50m. Higher bedform heights resulted in deeper tidal channels due to the dependency of the bedform heights on the flow depth.

Figure 6.5 shows the predicted bedform lengths in tidal channels during spring and neap tides. The estimation of the bedform lengths followed the results obtained in the measurements, i.e. 1.9 times of flow depths (see Section 4.6.2). Figure 6.6 shows the comparison of bedform lengths observed from side scan sonar images and predicted by empirical equation and numerical simulation. The estimated bedform lengths are in the order of those observed from field measurements in shallow areas. Side scan sonar images indicate that bedform lengths up to 22m are found in tidal channels (Figure 4.1). In the deeper parts of channels, the bedforms lengths exceeding 20m, which are much longer than the observed ones, are estimated. Bedform lengths up to 43m are predicted during spring and neap tides in the Piep channel. This is probably due to the fact that the estimation of the bed form lengths is related

to the water depths only. Other variables and further measurements should be carried out for a more detailed information.



a) Spring tide – ebb phase (17:00, August 17, 2000)



b) Neap tide – ebb phase (22:00, August 24, 2000)

Figure 6.4: Predicted bedform heights for high transport stage parameters

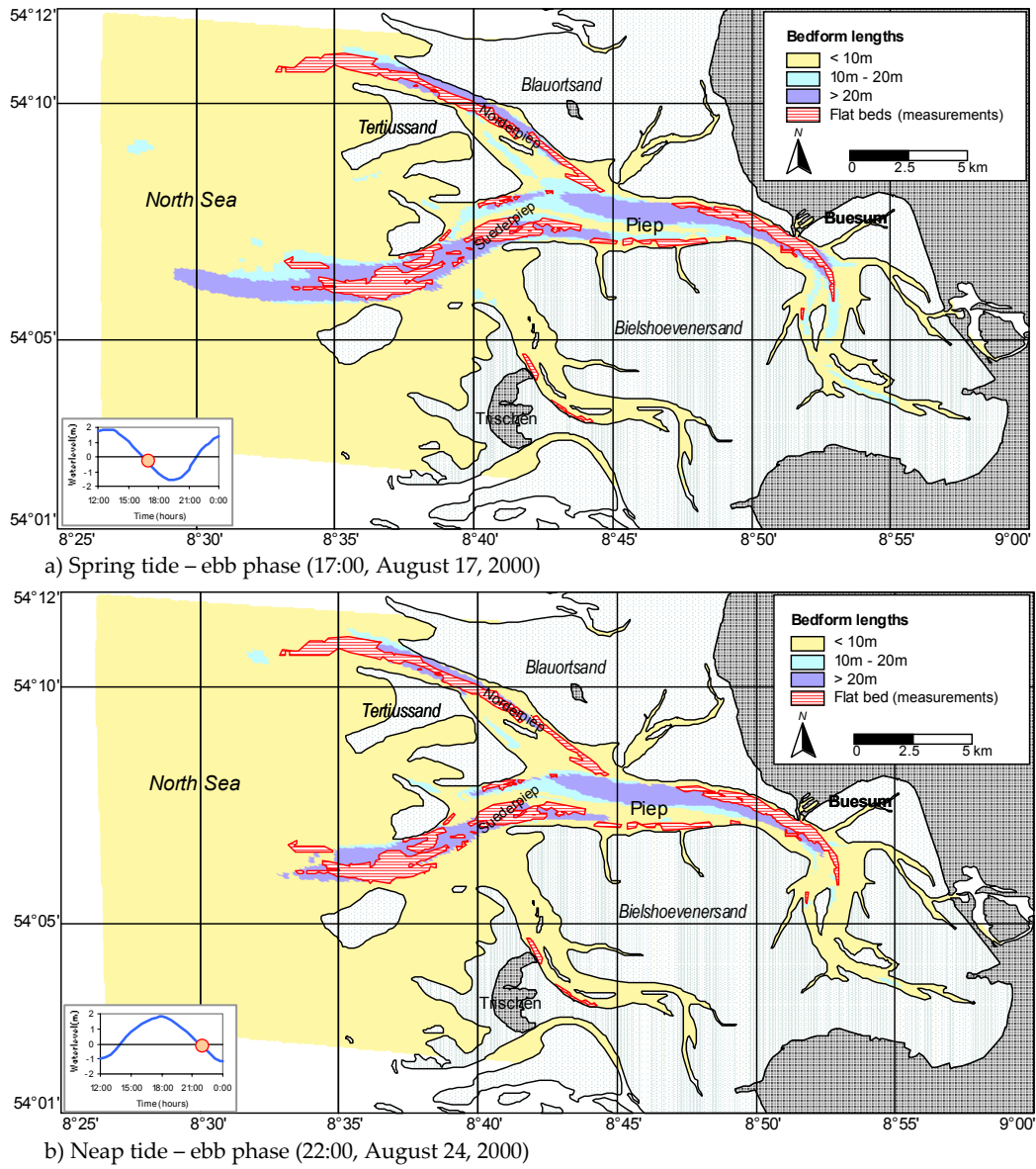


Figure 6.5: Predicted bedform lengths for high transport stage parameters

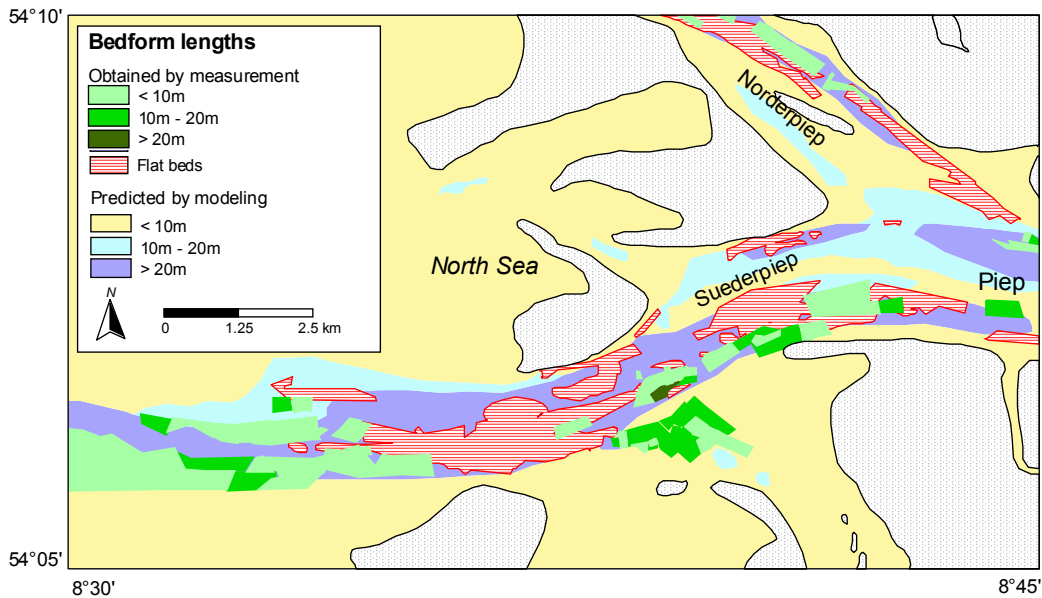


Figure 6.6: Comparison of observed and predicted bedform lengths

6.3.4 Equivalent roughness sizes

Figure 6.7 shows the predicted equivalent roughness sizes during spring and neap tides. The equivalent roughness sizes for ripples and dunes were estimated using respectively equations 2.26 and 5.7. The predicted equivalent roughness sizes in shallow areas are in good agreement with the values of less than 0.50m obtained on the basis of current velocity measurements. These values are also in the order of bedform heights observed in tidal channels. However, equivalent roughnesses up to 0.79m and 0.87m resulted in deeper parts of tidal channels respectively during spring and neap tides. To be noticed that for the estimations carried out for a spring tidal cycle, the equivalent roughness sizes exceeding 0.50m cover a much wider area than for a neap tide.

The distribution of roughness created in the current study is compared with the one used by Palacio [2002]. He found that the roughness map giving a good calibration results was based on the local variability. The map was created by firstly dividing the entire domain into some sub areas. Several roughness schemes varying from smooth to rough conditions were run on each sub area. The roughness scheme which produced best results between computed and measured velocities was selected. Figure 6.8 shows the roughness map using local variability approach. The estimated roughness is very smooth with maximum values of about 0.15m found in the inner Piep channel. Palacio's map also shows equivalent roughness of about 0.06m in the Piep channel and in a short section of the Norderpiep channel. Nearly flat bed is pre-

dicted in the Suederpiep channel. According to echo sounder profiles, the bedform heights in the study area can be as high as 0.50m. The map by Palacio [2002] using approach of local variability may underestimate the equivalent roughness.

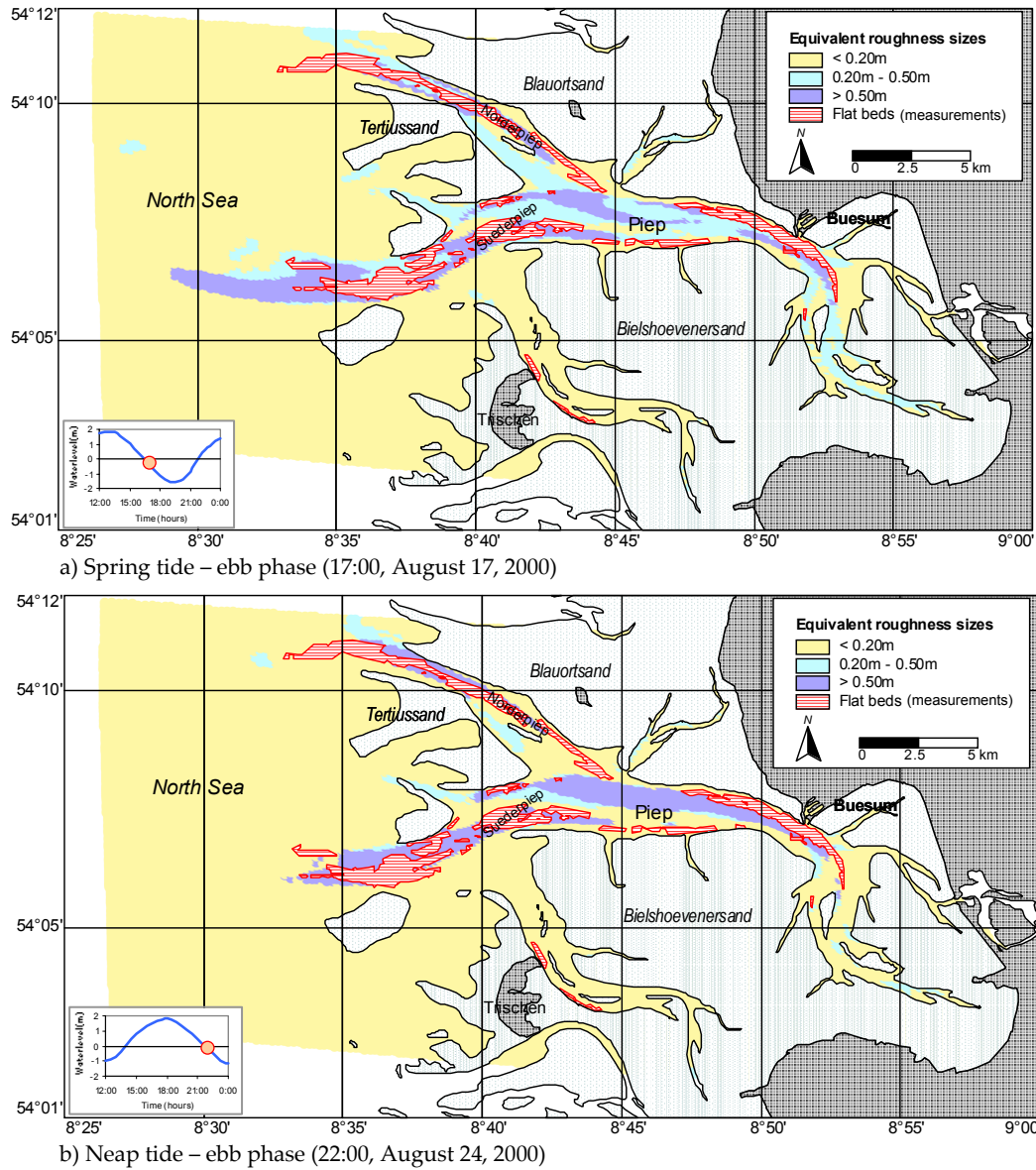


Figure 6.7: Predicted equivalent roughness sizes during high transport stage parameters

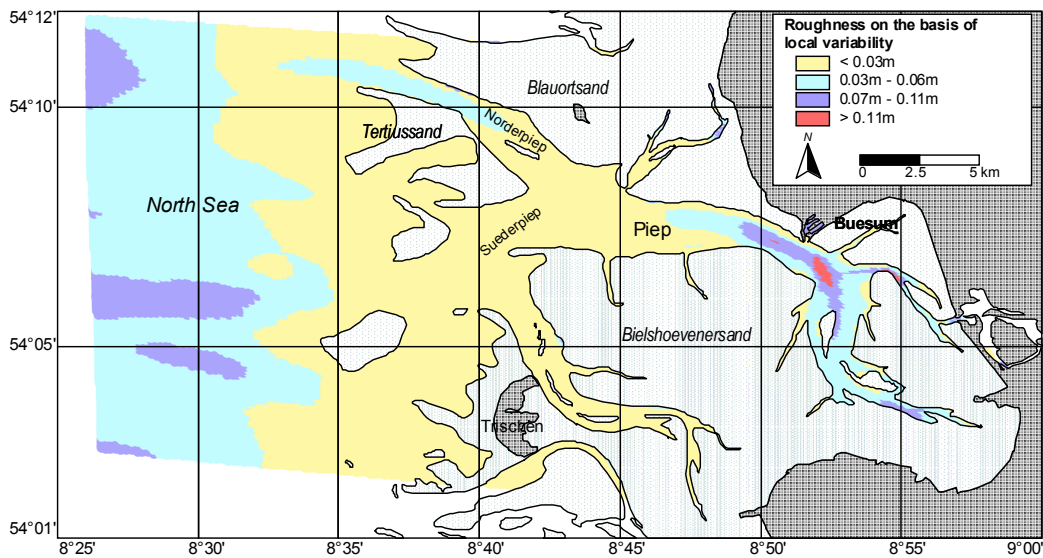


Figure 6.8: Map of equivalent roughness sizes using local variability after Palacio [2002]

6.4 Discussion

Empirical equations for the estimation of bed form types, dimensions and equivalent roughness sizes are applied by using the flow conditions obtained from numerical model simulations. The analysis is performed considering the highest transport stage parameters during spring and neap tides. The availability and type of sediments are considered for mapping the variability of bedforms and equivalent roughness sizes. Bedforms are expected to develop in areas which have sediment layer consisting of fine to medium sands. Megaripples and dunes are predicted in tidal channels. This is relevant to bedforms obtained from images of side scan sonar. Bedform heights and lengths are in general overestimated in deeper channels. Maximum bedform heights of about 1.2m and lengths up to about 43m are predicted while the field measurements of bedforms show maximum bedform heights of 0.5m and lengths of 22m. The reason for high estimation of bedform dimensions is that in the empirical equations the bedform dimensions depend largely on the flow depths. The maps of equivalent roughness sizes using the slightly modified empirical equations provide good predictions in the shallower areas of the tidal channels. Values in the order of 0.5m were predicted. In the deeper parts of the tidal channels, the estimated equivalent roughness sizes are much higher and appear to be unrealistic.

Chapter 7

Conclusions

The bedforms and equivalent roughness sizes in the Central Dithmarschen Bight have been studied. The development and distribution of bedforms have been analyzed. Several methods to estimate the equivalent roughness sizes have been employed. In the followings, the conclusions drawn from the research with respect to the measuring devices and strategy, bedforms and approaches for estimation of bedform dimensions and equivalent roughness sizes in the study area are mentioned.

Field measurements of bedforms and current velocities in tidal channels

The bedforms in tidal channels are measured using side scan sonar and echo sounder. The measurements using side scan sonar covered the entire domain and provided information on bedform lengths only. Echo sounder measurements were done in a few locations in the Norderpiep, Suederpiep and inner Piep channels to determine the heights and lengths of bedforms.

Acoustic profilers with different configurations have been employed to record current velocity profiles. ADCPs which are mounted on the vessel result in less consistent current profiles, while those moored to the bottom platform record well-defined profiles. By mounting it to vessels, the device is subjected to ship instability (pitch, roll and heading) and affected by bottom tracking systems. Less well-defined profiles result in low correlation coefficient of best fit line of the log law near the bottom. This usually leads to high and non-realistic equivalent roughness sizes.

Three points are suggested for proper measurements of bedforms and current velocities in the tidal channel:

1. Simultaneous measurements of bedforms and current velocities are recommended. The effects of flow conditions on the bedforms and vice-versa can be studied. In addition, measured bedforms and flow conditions can be used to de-

- velop bedform classification, and improve existing equations relating flow conditions to bedform dimensions and equivalent roughness sizes.
2. To enable good measurements of bedform dimensions, it is recommended to use echo sounder in conjunction with side scan sonar. Firstly, a vessel mounted echo sounder should be used to record the bedform profiles from which the bedform heights and lengths can be obtained. Secondly, a vessel towed side scan sonar is employed to capture the images of bedforms. From these images, the orientation of bedforms with respect to vessel track can be obtained for accurate determination of bedform lengths.
 3. To provide proper estimations of equivalent roughness sizes, it is suggested to use two acoustic profilers moored to a bottom platform. Both devices should be configured to record velocity profiles over a short period of time (less than 5 seconds). The measurements should be repeated at regular time interval, e.g. every 5 minutes, to cover an entire tidal cycle. The downward looking ADCP is employed to measure current profiles in the bottom boundary layer. A high resolution configuration, e.g. 5cm, should be applied to collect many velocity bins. Another device, with bin sizes between 10cm and 20cm depending on the flow depth, should be used to record velocities up to the free surface enabling the determination of the depth integrated velocity.

Bedform dimensions in tidal channels

According to the results obtained from side scan sonar images and echo sounder profiles, the bedform heights in the study area vary from 0.10m to 0.50m whereas the bedform lengths range from 4m to 22m. According to their shapes and dimensions, the bedforms are classified as megaripples and dunes.

In the inner Piep channel, transect measurements of bedforms covering an entire tidal cycle were carried out. The bedforms with various heights and lengths were obtained in each echo sounder profile. The following conclusions can be drawn on the basis of the measured results:

1. The dimensions of bedforms do not vary significantly between flood and ebb phases, although slightly larger bedform dimensions were found during the ebb phase (bedform heights and lengths respectively up to 0.42m and 19.22m). The larger bedform heights during the ebb phase are probably associated with the deposition of sediments at the bedform crest and the scouring at the troughs. The slightly longer bedforms during the ebb phase are due to sediments deposited on the lee side.
2. The bedforms migrate along the current direction. The measurements show migrations during the flood phase of up to 5m. At this period, the bedforms ad-

vanced along the direction of flood current. During the ebb phase, some profiles show that the bedforms migrate back up to about 2m along the direction of ebb current.

In the deeper parts of the tidal channels, the bedforms are not expected to develop because of the presence of a compacted sea bed consisting of consolidated mud. For example, echo sounder profiles in the Norderpiep and Suederpiep channels show relatively flat beds with outcropping of mud layers with heights up to about 0.22m.

On the basis of sediment properties and flow conditions in tidal channels, several bedform classifications are used to predict the bedforms. Ripples and dunes are mostly predicted by the classifications. The predicted bedforms by these classifications are in agreement with the bedforms observed in the tidal channel. The approach to classify bedforms by Van Rijn [1993] provides reasonable results for the study site since it was developed on the basis of a wider range of conditions. Other existing classifications were derived mainly from flume experiments and measurements in shallow rivers.

Estimation of equivalent roughness sizes from velocity profiles in tidal channels

Equivalent roughness sizes were estimated on the basis of measured current velocity profiles in the logarithmic layer. Velocity profiles in the lower 20% of the flow depth were considered to obtain the best fit line. The average of ensembles was carried out to minimize errors due to random variations in current velocities. The frequency of measurements plays a major role and should be selected carefully. Factors which were found relevant in the selection of valid velocity profiles are:

1. velocity magnitude: only depth integrated velocities exceeding 0.30m/s should be considered,
2. velocity direction: the standard deviation of velocity direction higher than 10°,
3. correlation coefficient of the best fit line to the log law higher than 0.90.

Under some measuring conditions, it was found that the combination of shear stress values obtained from the best fit line and the depth integrated velocity for estimation of the equivalent roughness sizes can be considered in the estimation of a new equivalent roughness size. However, two shortcomings of using current velocity profiles to estimate equivalent roughness sizes should be mentioned:

1. The equivalent roughness sizes are not predicted during low and high water levels. During these periods, low current velocities result in high standard deviation of velocity direction and low correlation coefficient of best fit line.

2. Variations of estimated equivalent roughness sizes are observed. This fluctuation is due to the change of velocity magnitude. Higher equivalent roughness sizes are obtained for lower current velocities and vice-versa.

Empirical equations for estimation of bedform dimensions and equivalent roughness sizes in tidal channels

The results obtained in terms of bedform dimensions and flow conditions were used to check existing equations. To be pointed out that the data used in the derivation of these equations stem mainly from observations in the laboratory. For the conditions in the study area, existing equations for estimation of bedform dimensions and equivalent roughness sizes for ripples and dunes were verified. It should be pointed out that the number of measured bed profiles was limited and restricted to a few locations. To draw more precise conclusions, additional measurements covering various locations should be taken.

The results showed that the proposed equations can be used quite well for the estimation of bedform dimensions in tidal channels. Only minor adjustments are needed to improve the estimation of the height of megaripples. Further, the dune height equation is applicable for the conditions in the tidal channel. The bedform length in the tidal channel is found about 1.9 times of the flow depth. This value is between the formulas for megaripple length ($\lambda_{mer} = 0.5h$) and dune length ($\lambda_d = 7.3h$). For formulas relating equivalent roughness and bedforms dimensions, only minor changes were found to be required.

Prediction of bedform dimensions and equivalent roughness sizes in tidal channels

To develop maps of bedform dimensions and equivalent roughness sizes in the study area, numerical model simulations were carried out in conjunction with empirical equations. Because bedforms in the study area are classified as megaripples and dunes, equations for both bedforms were employed. An existing depth integrated flow model was used to simulate flow depths, velocity magnitudes and shear stresses in the area. The sediment availability and type of sediments obtained as a result of an extensive mapping in the area were taken into account.

In summary, the produced maps show reasonable agreement with conditions found in the field. The prediction of megaripples and dunes in the tidal channels matches with bedforms obtained from images of side scan sonar. In general, the empirical equations are able to predict the bedform dimensions and equivalent rough-

ness sizes in shallow areas in good agreement with observations. In the deeper parts of the tidal channels, the bedform dimensions and equivalent roughness sizes are usually overestimated. Further work is needed to improve the empirical equations.

References

- Aagaard, T. & Masselink, G. (1999). *The Surf Zone*. In Short, A. D., (Editor), *Handbook of Beach and Shoreface Morphodynamics*. John Wiley & Sons Ltd., West Sussex.
- Abegg, F., Ricklefs, K. & Eden, H. (2001). *High Resolution Measurements of Near Bed Sediment Dynamics*. In: *Interim Report 2000 – PROMORPH*. Coastal Research Laboratory, University of Kiel, Kiel, Germany.
- Ackers, P. & White, W. (1973). *Sediment Transport: New Approach and Analysis*. *Journal of the Hydraulics Division*, 99 (HY11):2041-2060.
- Ackers, P. (1964). *Experiments on Small Streams in Alluvium*. *Journal of the Hydraulics Division*, 90(HY4).
- Allen, J. R. L. (1968). *The Nature and Origin of Bedform Hierarchies*. *Sedimentology*, 10:161-182.
- Asp, N. E., Wilkens, J., Ricklefs, K. & Mayerle, R. (2001). *Geology and Morphodynamics of a Tidal Flat Area of the German North Sea Coast and Its Support to a Medium-scale Morphodynamic Modelling*. In: *Proceedings VIII Congresso da ABEQUA*. Mariluz/Imbe, Brazil.
- Athallah, M. (1968). *Prediction of Bedforms in Erodible Channels*. PhD Thesis. Colorado State University, Fort Collins, USA.
- Bagnold, R. A. (1946). *Motion of Waves in Shallow Water, Interaction between Waves and Sand Bottoms*. *Proceedings of the Royal Society of London, Ser. A*, 187:1-18.
- Barton, J. R. & Lin, P. N. (1985). *A Study of the Sediment Transport in Alluvial Streams*. Report 55JRB2. Civil Engineering Department, Colorado College, Fort Collins, USA.
- Bogardi, J. (1974). *Sediment Transport in Alluvial Streams*. Akademiai Kiado, Budapest, Hungary.

- Brown, J., Colling, A., Park, D., Philips, J., Rothery D. & Wright, J. (1991). *Waves, Tides, and Shallow-water Processes*. Bearman, G. (Editor). Pergamon Press, Oxford, UK.
- Brush, L. M., Einstein, H. A., Simons, D. B., Vanoni, V. A. & Kennedy, J. F. (1966). *Nomenclature for Bed Forms in Alluvial Channels*. Journal of the Hydraulics Division, 92(HY3):51-64.
- Cacchione, D. A., Drake, D. E., Kayen, R. W., Sternberg, R. W., Kineke, G. C., & Tate, G. B. (1995). *Measurements in the Bottom Layer on the Amazon Subaqueous Delta*. Marine Geology, 125:235-257.
- Carling, P. A. (1981). *Sediment Transport by Tidal Currents and Waves: Observations from a Sandy Intertidal Zone (Burry Inlet, South Wales)*. In Nio, S. D., Shuettenhelm, R. T. E. & van Weering, Tj. C. E. (Editors), *Holocene Marine Sedimentation in the North Sea Basin. Spec. Pub. of the Int. Assoc. of Sedimentologists 5; Meeting on Holocene marine sedimentation in the North Sea basin*. Blackwell, Oxford, UK.
- Carstens, M. T., Neilson, F. M. & Altinbilek, H. D. (1969). *Bed Forms Generated in Laboratory under an Oscillatory Flow: Analytical and Experimental Study*. Technical Memo, 28. U.S. Army Coastal Engineering Research Center, USA.
- Cheng, R. T., Ling, C. H. & Gartner, J. W. (1999). *Estimates of Bottom Roughness Length and Bottom Shear Stress in South San Francisco Bay California*. Journal of Geophysical Research, 104(C4):7715-7728.
- Delft Hydraulics. (1999). *Delft3D-Flow User Manual Version 3.05*. Delft Hydraulics, Delft, The Netherlands.
- Dittmer, E. (1938). *Schichtaufbau und Entwicklungsgeschichte des Dithmarscher Alluviums*. Westküste, 1.
- Drake, D. E. & Cacchione, D. A. (1989). *Estimates of the Suspended Sediment Reference Concentration (C_s) and Resuspension Coefficient (γ_0) from Near-bed Observations on the California Shelf*. Continental Shelf Research, 9:51-64.
- Ehlers, J. (1988). *The Morphodynamics of the Wadden Sea*. A. A. Balkema, Rotterdam, The Netherlands.
- Garde, R. J. & Ranga Raju, K. G. (1977). *Mechanics of Sediment Transportation and Alluvial Stream Problems*. John Wiley & Sons, Inc., New Delhi, India.

- Gladki, H. (1975). *Discussions of Determination of Sand Bed Roughness for Fixed Beds*. Journal of Hydraulic Research, 13(2):221-222.
- Gordon, L. (1996). *Acoustic Current Doppler Profiler, Principles of Operation, a Practical Primer*. RD Instruments, San Diego, USA, 2nd edition.
- Grant, W. D. & Madsen, O. S. (1982). *Movable Bed Roughness in Unsteady Oscillatory Flow*. Journal of Geophysical Research, 87(C1):469-481.
- Gross, T. F. and Nowell, A. R. M. (1983). *Mean Flow and Turbulence Scaling in a Tidal Boundary Layer*. Continental Shelf Research 2: 109-126.
- Harris, C. K. (2003). *Sediment Transport Processes in Coastal Environments*. http://www.vims.edu/~ckharris/MS698_03/lecturenotes.html (September 12, 2003).
- Harris, C. K. & Wiberg, P. L. (1997). *Approaches to Quantifying Long-term Continental Shelf Sediment Transport with an Example from the Northern California STRESS Mid-shelf Site*. Continental Shelf Research, 17(11):1389-1418.
- Havinga, F. (1992). *Sediment Concentrations and Transport in Case of Irregular Non-breaking Waves with a Current*. Coastal Engineering Department, Delft University of Technology, Delft, The Netherlands.
- Heathershaw, A. D. & Simpson, J. H. (1978). *The Sampling Variability of the Reynolds Stress and Its Relation to Boundary Shear Stress and Drag Coefficient Measurements*. Estuarine and Coastal Marine Science, 6:263-274.
- Jackson, P. S. (1981). *On the Displacement Height in the Logarithmic Velocity Profile*. Journal Fluid Mechanics, 111:15-25.
- Jimenez-Gonzalez, S., Mayerle, R., & Egozcue, J. J. (2003). *On the Accuracy of Acoustic Doppler Current Profilers for In-situ Measurements. A Proposed Approach and Estimations for Measurements in Tidal Channels*. In: Rizoli, J. A., (Editor), *Proceedings of the IEEE 7th Working Conference on Current Measurement Technology*. San Diego, USA.
- Julien, P. Y. (1995). *Erosion and Sedimentation*. Press Syndicate of the University of Cambridge, Cambridge, UK.
- Kamphuis, J. W. (1974). *Determination of Sand Roughness for Fixed Beds*. Journal of Hydraulic Research, 12(2):193-203.

- Lee, T. H. & Hanes D. M. (1996). *Comparison of Field Observations of the Vertical Distribution of Suspended Sand and Its Prediction by Models*. Journal of Geophysical Research, 101:3561-3572.
- Li, M. Z., Wright, L. D. & Amos, C. L. (1996). *Predicting Ripple Roughness and Sand Re-suspension under Combined Flows in a Shoreface Environment*. Marine Geology, 130:139-161.
- Liu, H. K. (1957). *Mechanics of Sediment-ripple Formation*. Journal of the Hydraulics Division, 183(HY2):1-23.
- Lofquist, K. E. B. (1986). *Drag on Naturally Rippled Beds under Oscillatory Flows*. MP-86-13. U.S. Army Corps of Engineers, Coastal Engineering Research Center, USA.
- Lowrance Electronics. (2001). *Sonar Tutorial*. http://www.lowrance.com/tutorials/Printable/sonar_tutorial.asp (June 5, 2003).
- Mahmood, K. Mehrdad, M. H. & Haque, M. I. (1984). *Bed Form Data in ACOP-canals 1979-1980*. Civil Mechanical and Environmental Engineering Department, George Washington University, Washington DC, USA.
- Masselink, G. & Pattiaratchi, C. B. (2000). *Tidal Asymmetry in Sediment Resuspension on a Macrotidal Beach in Northwestern Australia*. Marine Geology, 163(1-4):257-274.
- Mathisen, P. P. (1989). *Experimental Study on the Response of Fine Sediments to Wave Agitation and Associated Wave Attenuation*. Master Thesis, Massachusetts Institute of Technology, Cambridge, USA.
- Mayerle, R. & Palacio, C. (2002). *Assessment of Open Sea Boundary Condition Approaches for Coastal Area Models*. In: Guo, J. J. (Editor), *Proceedings of the 13th IAHR-APD Congress*. World Scientific, Singapore.
- Mayerle, R., Razakafoniaina, T., Palacio C. & Pramono, G. (2002). *Bed Forms and Equivalent Roughness Sizes in Tidal Channels*. In: *Proceedings of International conference on fluvial hydraulics*. Belgium.
- Müller, M. J. (1996). *Handbuch Ausgewählter Klimastationen der Erde: 1272 Stationen*. Forschungsstelle Bodenerosion, Mertesdorf, 5th edition.
- Nap, E. & Van Kampen, A. (1988). *Sediment Transport in Irregular Non-breaking Waves with a Current*. Coastal Engineering Department, Delft University of Technology, Delft, The Netherlands.

- Nielsen, P. (1983). *Analytical Determination of Nearshore Wave Height Variation Due to Refraction Shoaling and Friction*. Coastal Engineering, 7:233-251.
- Nielsen, P. (1986). *Suspended Sediment Concentrations Under Waves*. Coastal Engineering, 10:23-31.
- Nikuradse, J. (1933). *Stroemungsgesetze in Rauhen Rohren*. VDI-Verl., Berlin, Germany.
- Palacio, C. A. (2002). *Metodologia Para la Validacion de Modelos Hidrodinamicos Utilizando Amplia Informacion de Campo: Aplicacion a la Bahia Meldorf en la Costa del Mar del Norte Aleman*. Ph.D. Thesis, Universidad Nacional de Colombia, Medellin, Columbia.
- Raudkivi, A. J. (1988). *The Roughness Height Under Waves*. Journal of Hydraulic Research, 26(5):569-584.
- Razakafoniaina, T. (2001). *Assessment of the Equivalent Bed Roughness Size in Tidal Channels on the Basis of Numerical Model Simulation and Side Scan Sonar Observations*. Master Thesis. Coastal Research Laboratory, University of Kiel, Kiel, Germany.
- RD Instruments. (1999). *General River Profiling – Mode 5 and 8*. In: *Application Note*, FSA-005. RD Instruments, San Diego, USA.
- RD Instruments. (2002). *High Resolution Water Profiling Water Mode 12*. In: *Application Note*, FSA-014. RD Instruments, San Diego, USA.
- RD Instruments. (2003). *Summary of Mode 12's Improved ADCP Advantages*. In: *RDI's Unique Advantages*. RD Instruments, San Diego, USA.
- Reimers, H. C. (2003). *Sedimentverteilung und Benthosverbreitung in den Watten der Dithmarscher Bucht als Indikator für Morphodynamische Veränderungen*. In: GKSS, 2003/18. GKSS Forschungszentrum, Geesthacht, Germany.
- Reineck, H. E. & Singh, I. B. (1980). *Depositional Sedimentary Environments*. Springer-Verlag, Berlin, Germany, 2nd edition.
- Ricklefs, K. (2002). *Investigation Area*. In: *Interim Report 2001 – PROMORPH*. Coastal Research Laboratory, University of Kiel, Kiel, Germany.
- Ricklefs, K. (2004). Personal communication. Research and Technology Center West Coast, University of Kiel, Kiel, Germany.

- Rosengaus, M. (1987). *Experimental Study on Wave Generated Bedforms and Resulting Wave Attenuation*. Ph.D. Thesis. Massachusetts Institute of Technology, Cambridge, USA.
- Schauer, U. (1987). *Determination of Bottom Boundary Layer Parameters at Two Shallow Sea Sites Using the Profile Method*. *Continental Shelf Research*, 7(10):1211-1230.
- Schlichting, H. (1951). *Grenzschicht-Theorie*. Braun, Karlsruhe, Germany.
- Simons, D. B. & Richardson, E. V. (1961). *Forms of Bed Roughness Alluvial Channels*. *Journal of the Hydraulics Division*, 87(HY3):87-105.
- Simons, D. B. & Richardson, E. V. (1966). *Resistance to Flow in Alluvial Channels*. Geological Survey Professional Paper, 422-J.
- Simons, D. B. & Sentürk, F. (1992). *Sediment Transport Technology – Water and Sediment Dynamics*. Water Resources Publication, Colorado, USA.
- Simpson, M. R. (2001). *Discharge Measurements Using a Broad-band Acoustic Doppler Current Profiler*. In: *US Geological Survey - Open-file report 01-1*. USGS, Sacramento, USA.
- Soulsby, R. L. (1983). *The Bottom Boundary Layer of Shelf Seas*. In Johns, B. (Editor) *Physical Oceanography of Coastal and Shelf Seas*. Elsevier, Amsterdam, The Netherlands.
- Soulsby, R. L. (1997). *Dynamics of Marine Sands*. Thomas Telford Publ., London, UK.
- Soulsby, R. L. & Dyer, K. R. (1981). *The Form of the Near-bed Velocity Profile in a Tidally Accelerating Flow*. *Journal of Geophysical Research*, 86(C9):8067-8074.
- Sternberg, R. W. (1968). *Friction Factors in Tidal Channels with Differing Bed Roughness*. *Marine Geology*, 6:243-260.
- Taylor, J. R. (1997). *An Introduction to Error Analysis*. University Science Books, Sausalito, USA, 2nd edition.
- Triton Elics International. (1999). *Isis Sonar – User Manual*. Triton Elics International, Watsonville, USA.
- Van Rijn, L. C. (1982). *Equivalent Roughness of Alluvial Bed*. *Journal of Hydraulic Engineering*, 108(HY10):1215-1218.

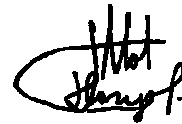
- Van Rijn, L. C. (1984). *Sediment Transport, Part III: Bed Forms and Alluvial Roughness*. Journal of Hydraulic Engineering, 110(12).
- Van Rijn, L. C. (1993). *Principles of Sediment Transport in Rivers, Estuaries and Coastal Seas*. Aqua Publications, Delft, The Netherlands.
- Vanoni, V. A. & Brooks, N. H. (1957). *Laboratory Studies of the Roughness and Suspended Load of Alluvial Streams*. Report E-68. Sedimentation Laboratory, California Institute of Technology, Pasadena, USA.
- Vela-Diez, S. (2001). *Sediment Mapping of the Tidal Flat Channels off Buesum*. Master Thesis. Coastal Research Laboratory, University of Kiel, Germany.
- Vincent, C. E., Hanes, D. M. & Bowen, A. J. (1991). *Acoustic Measurements of Suspended Sand on the Shoreface and the Control of Concentration by Bed Roughness*. Marine Geology, 96:1-18.
- Wiberg, P. L. & Rubin, D. M. (1989). *Bed Roughness Produced by Saltating Sediment*. Journal of Geophysical Research, 94:5011-5016.
- Wieland, P. (1972). *Untersuchung zur Geomorphologischen Entwicklungstendenz des Aussensandes Blauort*. Die Küste, 23:122-149.
- Wikramanayake, P. N. (1993). *Velocity Profiles and Suspended Sediment Transport in Wave-current Flows*. PhD Thesis. Massachusetts Institute of Technology, Cambridge, USA.
- Wilkens, J. (2000). *Initial Morphodynamic Modelling of the Meldorf Bight, Germany*. In: *Corelab Report 01-00*. Coastal Research Laboratory, University of Kiel, Kiel, Germany.
- Williams, J. J. & Rose, C. P. (2001). *Measured and Predicted Rates of Sediment Transport in Storm Conditions*. Marine Geology, 179:121-133.
- Wood, R. G., Black, K. S. & Jago, C. F. (1998). *Measurements and Preliminary Modelling of Current Velocity over an Intertidal Mudflat, Humber Estuary, UK*. In Black, K. S., Paterson, D. M. & Cramp, A. (Editors), *Sedimentary Processes in the Intertidal Zone* 139: 167-175. Geological Society, Special Publications, London, UK.
- Wright, L. D. (1995). *Morphodynamics of Inner Continental Shelves*. CRC Press, Inc., Florida, USA.

-
- Yalin, M. S. (1964). *Geometrical Properties of Sand Waves*. Journal of the Hydraulics Division, 90(HY5):105-119.
- Yalin, M. S. (1972). *Mechanics of Sediment Transport*. Pergamon Press Ltd., Braunschweig, Germany.
- Yalin, M.S. (1985). *On the Determination of Ripple Geometry*. Journal of Hydraulic Engineering, 3(8):1148-1155.

Erklärung

Hiermit erkläre ich, dass die Abhandlung -abgesehen von der Beratung durch meine akademischen Lehrer- nach Inhalt und Form meine eigene Arbeit ist. Diese Arbeit hat an keiner anderen Stelle im Rahmen eines Prüfungsverfahrens vorgelegen. Außerdem erkläre ich, dass diese mein erster Promotionsversuch ist.

Kiel, den 26.5.2004

A handwritten signature in black ink, appearing to read 'Gatot Haryo Pramono', enclosed within a circular scribble.

Gatot Haryo Pramono

Curriculum Vitae

Personal data

Name Gatot Haryo Pramono
Nationality Indonesia
Place, DOB Surabaya, 6 January 1971
Sex Male
Office Bakosurtanal (National Agency for Surveys and Mapping)
Jl. Jakarta-Bogor Km. 46
Cibinong, Bogor 16910
INDONESIA
Phone +62-21-875-9481
Fax +62-21-875-2064
E-mail gatot@bakosurtanal.go.id
gatothp@yahoo.com

Education

May 1999 Master of Applied Science in Geographical Information Systems at University of New South Wales, Sydney, Australia
August 1994 Bachelor of Science in Geography (Environmental Studies) with Honor of Magna Cum Laude at Texas A&M University, College Station, USA.
May 1989 Senior high school at SMAN 2, Surabaya, Indonesia
May 1986 Junior high school at SMPN 12, Surabaya, Indonesia
May 1983 Elementary school at SD PPSP, Surabaya, Indonesia

Working experience

May 1999 Staff at Thematic Database Division of National Coordination Agency for Surveys and Mapping in Indonesia.
September 1994 Staff at System Development Division of National Coordination Agency for Surveys and Mapping in Indonesia.

Project experience

- March 2000* Project director for web development for spatial natural resource data.
- April 2000* Application development for digital map production in Lampung, South Sulawesi, South Kalimantan and Bali.
- December 1999* Development of thematic database and rule-based programming in provinces of NTT and Yogyakarta.
- September 1999* Application for land use change detection in Gorontalo, North Sulawesi.
- August 1998* The Integration of lineage metadata and cartographic modelling: an alternative approach in Geographical Information Systems.
- March 1998* Network analysis in the internet for finding the shortest distance
- January 1997* Application of remote sensing and GIS for locating transmigration area in Sumatra island.
- April 1996* Modelling of dry season in East Java using remote sensing and GIS.
- February 1996* Data fusion of remote sensing in Bali island.
- January 1996* Inventory and mapping of potential wetland in Kalimantan island.
- September 1995* Application of remote sensing and GIS for monitoring of reforestation in Sulawesi island.
- April 1994* Measurement of coastal line changes in Galveston island, Texas.

Hobbies

Jogging, hiking and fishing.